UNIVERSITY OF CALIFORNIA,
IRVINE

Revealing Cell Type Specific Circadian Regulations in the Skin with Single Cell RNA Sequencing and a Circadian Time Predictor Pipeline

DISSERTATION

submitted in partial satisfaction of the requirements
for the degree of

DOCTOR OF PHILOSOPHY

in Mathematical, Computational, and Systems Biology

by

Junyan Duan

Dissertation Committee:
Professor Bogi Andersen, Chair
Professor John Lowengrub
Professor Babak Shahbaba

2024

DEDICATION

To my parents, my husband, and Tautao.

TABLE OF CONTENTS

LIST OF FIGURES

LIST OF TABLES

ACKNOWLEDGMENTS

First and foremost, I would like to thank Dr. Bogi Andersen, for the projects would not have been possible without your amber and invaluable guidance and mentorship. Your passion for science and commitment to rigorous standards have inspired me to approach research with a critical and thoughtful mindset. I would also like to thank my committee members, Dr. John Lowengrub and Dr. Babak Shahbaba, for all the constructive discussions, support, and encouragement.

I would like to thank the members of the Andersen lab, the past and the present, for all the enjoyable collaborations, inspiring discussions, and fun chitchats. I would also like to thank all my friends and collaborators, particularly Michelle, Qiushi, Julie, and Karen, for always being present, cheerful, supportive, and caring.

From the bottom of my heart, I thank my parents for their unwavering support and belief, which have instilled in me the courage, confidence, and resilience to pursue challenges and improvements. To my husband, words cannot express my love and gratitude. Thank you for for sharing my happiness and burden, for being my rock through the ups and downs, and for embracing me with warmth and comfort when things appear to be gloomy and soggy.

To Tautao the very good girl: Thank you for bringing me out for walks and trips to the tide pools, reminding me to appreciate the beauty of nature, and putting a smile on my face with your overloaded cuteness.

The text of Chapter 1 of this dissertation is a reprint of the material as it appears in J. Duan, E. N. Greenberg, S. S. Karri, and B. Andersen. The circadian clock and diseases of the skin. *FEBS Letters*, 595(19):2413–2436, Sept. 2021, used with permission from John Wiley and Sons. The coauthors listed in this publication are Elyse Noelani Greenberg, Satya Swaroop Karri, and Bogi Andersen. The text of Chapter 2 and 3 of this dissertation is an adaption of the material as it appears in J. Duan, M. N. Ngo, S. S. Karri, L. C. Tsoi, J. E. Gudjonsson, B. Shahbaba, J. Lowengrub, and B. Andersen. taufisher predicts circadian time from a single sample of bulk and single-cell pseudobulk transcriptomic data. *Nature Communications*, 15(1), May 2024, used with permission from Springer Nature. The coauthors listed in this publication are Michelle N. Ngo, Satya Swaroop Karri, Lam C. Tsoi, Johann E. Gudjonsson, Babak Shahbaba, John Lowengrub, and Bogi Andersen.

Financial support was provided by an award entitled "Skin Biology Resource-Based Center at UCI - Systems Biology Core" from the Center of Complex Biological Systems funded by NIH/NIAMS P30-AR075047, NSF grant DMS1763272, a grant from the Simons Foundation (594598), National Research Service Award GM136624 from National Institute of General Medical Sciences, and University of California, Irvine.

VITA

Junyan Duan

EDUCATION

Doctor of Philosophy in Mathematical, Computational, and Systems Biology — **2024**
University of California, Irvine — *Irvine, California*

Bachelor of Arts in Mathematics — **2019**
Magna cum laude with Hornors in Major
Bryn Mawr College — *Bryn Mawr, Pennsylvania*

JOURNAL PUBLICATIONS

J. Duan, M. N. Ngo, S. S. Karri, L. C. Tsoi, J. E. Gudjonsson, B. Shahbaba, J. Lowengrub, and B. Andersen. taufisher predicts circadian time from a single sample of bulk and single-cell pseudobulk transcriptomic data. *Nature Communications*, 15(1), May 2024

B. Andersen, J. Duan, and S. S. Karri. How and why the circadian clock regulates proliferation of adult epithelial stem cells. *Stem Cells*, Feburary 2023

J. Duan, C. Grando, S. Liu, A. Chernyavsky, J. K. Chen, B. Andersen, and S. A. Grando. The M3 muscarinic acetylcholine receptor promotes epidermal differentiation. *Journal of Investigative Dermatology*, July 2022

J. Blackwood, M. Malakhov, J. Duan, J. Pellett, I. Phadke, S. Lenhart, C. Sims, and K. Shea. Governance structure affects transboundary disease management under alternative objectives. *BMC Public Health*, 21, October 2021

J. Duan, E. N. Greenberg, S. S. Karri, and B. Andersen. The circadian clock and diseases of the skin. *FEBS Letters*, 595(19):2413–2436, Sept. 2021

J. Duan, M. Malakhov, J. Pellett, I. Phadke, J. Barber, and J. Blackwood. Management efficacy in a metapopulation model of white-nose syndrome. *Natural Resource Modeling*, 34, August 2021

FELLOWSHIPS AND AWARDS

NIH/NIGMS T32 Mathematical and Computational Biology Training Grant **2022–2024**
National Institute of Health/National Institute of General Medical Sciences

NSF-Simons Center for Multiscale Cell Fate Research, Center Fellow **2021–2023**
National Science Foundation

International Societies for Investigative Dermatology Meeting Travel Grant **2023**
The Society for Investigative Dermatology and Leo Foundation

Opportunity Award in the Center for Complex Biological Systems **2020-2022**
University of California, Irvine

Anna Pell Wheeler Prize for Excellence in Mathematics **2019**
Bryn Mawr College

Meritorious Winner – international top 6% **2019**
The Mathematical Contest in Modeling

TEACHING EXPERIENCE

Research Mentor **2024**
Irvine Summer Institute in Biostatistics and Undergraduate Data Science *Irvine, California*

Teaching Assistant **2022-2024**
Foundations in Systems Biology Short Course *Irvine, California*

Peer Mentor **2020-2022**
Mathematical, Computational and Systems Biology Gateway Peer Mentoring Program *Irvine, California*

Teaching Assistant **2021**
The California State Summer School for Mathematics and Science *Irvine, California*

Research Mentor **2021**
MathBioU & Mathematical Experience through Learning Research *Irvine, California*

ABSTRACT OF THE DISSERTATION

Revealing Cell Type Specific Circadian Regulations in the Skin with Single Cell RNA Sequencing and a Circadian Time Predictor Pipeline

By

Junyan Duan

Doctor of Philosophy in Mathematical, Computational, and Systems Biology

University of California, Irvine, 2024

Professor Bogi Andersen, Chair

The circadian clock, a transcription-translation feedback loop responsible for generating robust rhythms that are roughly synchronized to the external 24-hour light-dark cycle, is present in almost all cells in the body. The clock regulates fundamental biological processes, and circadian disruption is associated with the onset and progression of various diseases including diabetes and cancer. Circadian medicine aims to target the circadian clock and optimally time treatment administrations. However, it remains challenging to determine the circadian time of the patient or the tissue of interest. Here, we developed tauFisher, a computational pipeline that can accurately predict the circadian time for a single sample of transcriptomic data. We highlight tauFisher´s performance on datasets collected from various tissues using different assay methods including microarray, bulk RNAseq, and single cell RNAseq, demonstrating that tauFisher is an accessible tool for adapting the existing timestamp-less datasets for circadian studies.

The circadian clock is robust in the skin, an organism's first line of defense against environmental fluctuations and insults. The clock's proper function is essential for maintaining skin homeostasis and optimizing skin's response to stressors. Studying the circadian clock in the skin provides insights into disease development and management. We collected time series of

single cell RNAseq data from mouse skin and discovered different circadian clock properties and differential rhythmic processes in dermal fibroblasts and dermal immune cells. Incorporating tauFisher with bootstrapping, we hypothesize that circadian phase heterogeneity may contribute to the dampened amplitude of the collective core clock in dermal immune cells when compared to dermal fibroblasts. We also found that the clock regulates metabolism and immune responses in the dermal fibroblasts and dermal immune cells respectively. Taken together, our data show that within a single tissue, the circadian clock regulates a highly divergent set of genes in different cell types.

Chapter 1

The circadian clock and diseases of the skin

J, Duan, E. N. Greenberg, S. S. Karri, and B. Andersen. The circadian clock and diseases of the skin. *FEBS Letters*, 595(19):2413–2436, Sept. 2021

1.1 Abstract

Organisms have an evolutionarily conserved internal rhythm that helps them anticipate and adapt to daily changes in the environment. Synchronized to the light-dark cycle with a period of around 24 hours, the timing of the circadian clock is set by light-triggering signals sent from the retina to the suprachiasmatic nucleus. Other inputs, including food intake, exercise, and temperature, also affect clocks in peripheral tissues, including skin. Here, we review the intricate interplay between the core clock network and fundamental physiological processes in skin such as homeostasis, regeneration, immune and stress responses. We illustrate the effect of feeding time on the skin circadian clock and skin function, a previously overlooked

area of research. We then discuss works that relate the circadian clock and its disruption to skin diseases, including skin cancer, sunburn, hair loss, aging, infections, inflammatory skin diseases, and wound healing. Finally, we highlight the promise of circadian medicine for skin disease prevention and management (Figure 1.1).

1.2 Background

As the largest organ of the body, skin provides primary defense against the environment, including toxins, microorganisms, and radiation [204, 223]. It is also a critical part of organismal homeostasis through fat storage and the production of hormones, including vitamin D. Due to its interactions with external stimuli, the skin must be equipped to adapt to its environment.

The circadian clock, an intrinsic autonomous clock that controls the body's divergent functions during day and night, affects the expression of multiple genes that mediate skin stem cell metabolism and proliferation, DNA repair, stimulus response, and immunity. Circadian clock research has elucidated fundamental regulatory mechanisms that contribute to skin cancer, aging, inflammatory and other skin diseases. Emerging clinical research has begun to employ these findings to refine treatment based on the principles of circadian medicine (Figure 1.1). While circadian dermatology is a nascent field, studies conducted on the circadian clock continue to unravel the mysteries of the skin and its complex system of regulation.

Understanding the role of the circadian clock in the skin may provide new insights into the pathogenesis of skin diseases and their treatment. To this end, we review the role of the circadian clock in skin, emphasizing the most recent findings in the field, and discuss the role of circadian clock disruption in skin diseases.

1.3 The circadian clock

From bacteria to plants and animals, all living organisms have intrinsic rhythms that are synchronized with the light-dark cycle with a period of around 24 hours. Controlled by internal biochemical oscillators, the circadian clock is autonomous and maintained at both organismal and cellular levels in the absence of outside stimuli [29, 38]. In this section, we provide a brief overview of the mammalian circadian clock at the organismal and molecular level.

1.3.1 The SCN synchronizes peripheral clocks

In mammals, the circadian clock machinery is present in almost all cells. The suprachiasmatic nucleus (SCN), a small region in the hypothalamus of the brain, acts as the central pacemaker that synchronizes the circadian clocks in peripheral tissues through neuronal and hormonal signals [38, 79].

The primary entrainment signal for the SCN is light. Upon light reception, intrinsically photosensitive retinal ganglion cells (ipRGCs), pivotal components of the retinohypothalamic tract, send signals to set the circadian time in the SCN. In the SCN, a subpopulation of cells produces neurotransmitters such as vasoactive intestinal peptide (VIP) and arginine vasopressin (AVP) to synchronize and stabilize the cellular circadian clocks within the SCN [38, 79, 166]. While the neurons in the SCN are traditionally believed to be the main contributor to circadian rhythm establishment, SCN astrocytes also have the ability to control the circadian rhythm in the SCN [38, 79]. As the robustly autonomous SCN sends signals to peripheral tissues, peripheral clocks are synchronized with respect to the SCN and thus the ambient light-dark cycle (Figure 1.2).

The SCN clock can synchronize peripheral clocks, but it is not necessary for circadian rhythm

maintenance in peripheral organs [104, 169]. Although ablation of the SCN in mice disturbs the circadian rhythms in peripheral tissues, the obliteration of BMAL1 in all tissues except the liver does not completely obliterate circadian rhythms in the liver, irrespective of whether light signals are available [104, 169]. In addition, other signals such as food intake and temperature can set the clock in peripheral tissues independent of the SCN, causing phase shifts in the peripheral clocks relative to the central clock (Figure 1.2) [31].

1.3.2 The molecular clock is a transcription-translation feedback loop

In each cell, the circadian clock is a biochemical oscillator formed with interlocked transcription-translation feedback loops [181]. The primary feedback loop, which is commonly referred to as the core clock gene network, consists of a positive and a negative arm. In the positive arm, transcription factors Brain and Muscle ARNT-Like 1 (BMAL1) and Circadian Locomotor Output Cycles Kaput (CLOCK) form heterodimers, which bind to the enhancer box (E-box) to activate transcription of Period 1, 2, and 3 (*Per*) and Cryptochrome 1 and 2 (*Cry*). PER and CRY drive the negative arm, inhibiting the expression of BMAL1-CLOCK and thus impeding their own transcription. With the levels of PER and CRY decreasing, the BMAL1-CLOCK dimer regains activation until PER and CRY accumulate and deactivate BMAL1-CLOCK again, completing the loop with a period of around 24 hours (Figure 1.3) [181, 150, 39].

In addition to the core clock gene network, a secondary feedback loop reinforces the 24-hour oscillation for *Bmal1* expression. BMAL1-CLOCK activates transcriptions of not only *Per* and *Cry* but also other clock-controlled genes, including RAR-related Orphan Receptors (RORs) and REV-ERBs. While RORs bind to ROR/REV-ERB-response elements (RORE) to activate transcription of *Bmal1*, REV-ERBs bind to the same sites to inhibit *Bmal1*

transcription. With the level of BMAL1 decreasing, transcription of REV-ERBs stalls until transcription of *Bmal1* is reestablished (Figure 1.3) [181, 150, 39].

As simple as the network is, the core clock gene network directly or indirectly modulates the expression of multiple genes and biological processes in all organs, making those processes rhythmic as well. In mice, for example, around 16%, 13%, 12%, and 7% of protein coding genes are rhythmic in the liver, kidney, lung and skin, respectively [220, 72]. While the same clock gene network is omnipresent in cells and the SCN acts as a synchronizer for the entire body, the set of genes that are circadian varies greatly between organs. This is because the circadian machinery regulates different biological processes in different organs to modulate their functions. In addition, there is variability in the amplitudes and the peak times of clock gene expressions between organs, as external signals such as temperature and food intake can selectively entrain peripheral clocks (Fig. 1) [31].

1.4 The circadian clock in the skin

Acting as a protective barrier against toxins and other external stressors, skin is a multi-layer organ harboring various cell types organized into several compartments to fulfill a range of tasks such as water loss prevention, sensation, and hormone synthesis [204, 223]. In humans and mice, the skin comprises three main layers: the epidermis, the dermis, and the hypodermis; each layer has active circadian clocks. With the outside world changing throughout the 24-hour day, a mechanism has evolved to allow the skin to anticipate the environmental shifts and adjust accordingly. Indeed, diurnal rhythms are observed in multiple cell types across all layers of the skin [139].

As in other organs, the SCN synchronizes circadian clocks throughout the skin. This is supported by SCN ablation studies that abolished skin circadian rhythms [183]. More recent

studies have brought to light that epidermal circadian clocks and time-setting mechanisms are independent of the SCN. Selective expression of *Bmal1* only in the epidermis does not disturb the skin diurnal rhythm as long as the mice experience regular light-dark cycles [198], indicating that the epidermal clock does not require the SCN clock or clocks in other tissues. Possible contributors to the maintenance of such diurnality are light sensitive opsin proteins present in various skin cell types (such as melanocytes, keratinocytes, fibroblasts and hair follicle cells) that may be able to entrain the skin circadian clock [174, 30].

1.4.1 The skin is a multi-layer organ with diurnal rhythms in every layer

The outermost layer of the skin is the epidermis (Figure 1.4A). Hosting Merkel cells, melanocytes, T-cells, and Langerhans cells, the epidermis itself is organized into four layers (five on the palm and sole) consisting of keratinocytes at different differentiation stages: *stratum basale*, *stratum spinosum*, *stratum granulosum*, *stratum lucidum* (palm and sole specific) and *stratum corneum* (Figure 1.4B) [204]. The journey of the keratinocytes in the epidermis starts in the *stratum basale*, where the intrinsic circadian clock is required for the diurnal rhythms in proliferation [72] as well as the coordination between cell division and intermediary metabolism [173] in epidermal stem cells. The keratinocyte progeny of stem cells is continuously pushed upwards until arriving in the *stratum corneum* at the top, where the dead keratin-filled cells slough off [204].

Just below the epidermis, separated from it by a basement membrane, is the dermis (Figure 1.4A). The dermis primarily consists of extracellular matrix with collagen fibers synthesized by fibroblasts. It is much thicker than the epidermis and contributes strength and elasticity to the skin [204]. The diverse cellular populations in the dermis include fibroblasts, multiple immune cells such as T cells, mast cells, macrophages, and dendritic cells [204], as well

as dermal white adipocytes (Figure 1.4A). All of these cell types participate in immune responses and wound healing [163]. Despite their spatial proximity, the dermis and the epidermis have distinct circadian behaviors. Computational analysis of data collected from skin biopsies from human forearm, buttock, and cheek revealed that oscillation of clock genes is more robust in the epidermis than in the dermis across all three sites [207]. This may be because the cell types in the dermis are more diverse than in the epidermis, leading to less uniform circadian gene expressions in the dermis.

The hypodermis is the layer just below the dermis (Figure 1.4A); it mainly consists of adipocytes that form the subcutaneous fat, but also contains fibroblasts and macrophages [204, 163]. As an energy reservoir, the adipose tissue has long been studied for its role in metabolic diseases, which are intertwined with the whole-body circadian network. The relationship between the adipose tissue and the circadian clock is reviewed in detail in recent articles [67, 110, 172].

1.4.2 The circadian clock in hair follicles

The hair, one of the defining characteristics of mammals, works together with the epidermis to sense and protect the body from environmental changes. Hair shafts are rooted in hair follicles, which are miniature organs consisting of concentric layers of keratinocytes. They are embedded in the skin, penetrating into the dermis (Figure 1.4A). The infundibulum and isthmus are the two most superficial compartments of hair follicles. They are continuous with the epidermis and their circadian activities are similar to that of the epidermis (Figure 1.4C, D) [139, 162]. The remaining lower compartments of hair follicles, including the anagen-specific bulb, the stem cell-containing bulge, and the mesenchymal-derived dermal papilla, are more dynamic (Figure 1.4C, D). In particular, the dermal papilla and the anagen-specific bulb undergo structural changes as the hair follicles move through the three main stages of

the hair cycle: the growth stage anagen (Figure 1.4C), the regression stage catagen, and the relatively quiescent stage telogen (Figure 1.4D) [139, 162]. Diurnal genes in telogen and anagen skin only partially overlap [72], suggesting that the circadian clock differentially regulates hair follicles at those two stages.

Anagen marks the beginning of hair renewal. During anagen, quiescent bulge stem cells migrate out of the bulge to become proliferating matrix keratinocytes within the anagen bulb. The dermal papilla directs the differentiation of those matrix keratinocytes to form the inner layers of the hair follicle and the hair shaft (Figure 1.4C) [162, 125]. In both the bulge and the anagen bulb of mouse hair follicles, the circadian clock is robustly rhythmic and gates mitotic rhythms by synchronizing the G2/M checkpoint. Due to this synchronization of mitosis, the extension of the hair shafts shows a diurnal pattern, with more growth in the morning than in the evening [140]. *In vivo* studies of the human hair cycle are difficult, but studies indicate that circadian genes are expressed rhythmically in human hair follicles as well [197, 5]. Furthermore, *ex vivo* studies suggest that the circadian clock regulates the human hair cycle, as silencing *BMAL1*, *CLOCK* and *PER1* extends anagen [5]. In addition to hair growth, the circadian clock also controls the pigmentation of the hair during anagen, as melanin production by melanocytes in the human anagen hair matrix increases when the core clock genes *BMAL1* and *PER1* are silenced [78].

Hair follicles cease to grow during catagen and eventually enter the resting stage telogen. During telogen, the hair follicles prepare for the next anagen by forming the secondary hair germ just above the dermal papilla (Figure 1.4D) [125, 8]. Interestingly, in mice, while the hair is not growing during this stage, the amplitude of clock gene expression is significantly higher than during anagen, with the strongest expression in the hair germ. This robust circadian clock in the hair germ regulates stem cell activation as well as anagen initiation [113]. Consistent with this finding, germline *Bmal1* mutation in mice leads to a delay in anagen initiations. Knocking out *Bmal1* specifically in keratinocytes, however, does not

significantly delay anagen initiation [72, 113]. This suggests that *Bmal1* regulates anagen initiation through the central SCN clock or other non-epidermal cell types. In nature, hair cycles for most mammals are seasonal. Given the role of the clock in seasonal cycles, it is tempting to speculate that the circadian clock has a role in seasonal hair growth [71].

Among the bulge stem cells, circadian rhythms are heterogeneous during telogen, with cells expressing higher levels of *Bmal1* being more prone to activation signals. As anagen begins, circadian heterogeneity gradually decreases with most of the stem cells expressing high levels of *Bmal1* [139, 92]. Consistently, overexpression of *Bmal1* by knocking out its repressors *Per1* and *Per2* stimulates proliferation and reduces the number of dormant bulge stem cells [92]. These findings are consistent with a regulatory role of the circadian machinery in the hair cycle and indicate that robust clock output correlates with hair follicle stem cell activation and anagen initiation.

1.4.3 The skin immune system is circadian clock-regulated

In order to fulfill its infection control function, the skin harbors resident innate immune cells distributed throughout the epidermis and dermis (Figure 1.4A) as well as in organized tertiary lymphoid structures [135, 159, 130, 1]. The circadian clock modulates the activation of these cells, possibly to match the likelihood of infections and insults throughout the 24-hour day. By regulating the skin immune response in this way, the circadian clock may decrease the tendency for autoinflammatory and autoimmune skin diseases [75, 11, 108].

Epidermal-resident immune cells include specialized dendritic cells called Langerhans cells, as well as specialized T cells referred to as γ/δ^+ T cells. γ/δ^+ T cells are under clock regulation in that the CLOCK protein directly binds to the promoter of the interleukin 23 receptor (IL-23R) in γ/δ^+ T cells, thereby playing a regulatory role in the development the inflammatory skin disease psoriasis [11]. Langerhans cells appear to be regulated by the

circadian clock as well. For example, when exposed to a viral mimic, imiquimod (IMQ), Langerhans cells highly upregulate anti-viral genes, the expression of which is affected by *Bmal1* deletion [75].

Other immune cells such as macrophages, mast cells, T cells, and dendritic cells reside in the dermis (Figure 1.4A). Macrophages constantly monitor the skin microenvironment and innately respond to pattern-associated molecular patterns and damage-associated molecular patterns produced through infections and inflammation. Other key functions of macrophages, including cytokine production and phagocytosis, are diurnally gated [106, 157]. Mast cells cause allergic responses by releasing histamine, which activates other immune cells to cause allergy-like symptoms such as itching, erythema, and edema. Clock deletion in murine mast cells specifically ablates temporal variations in *IgE*-mediated degranulation and thus passive cutaneous anaphylactic reactions [16, 128], indicating direct regulation by the circadian clock.

Apart from its resident immune cells, the skin recruits adaptive immune cells through chemokine and cytokine release during infections and inflammation. Circadian expression of chemoattractants, and the subsequent rhythmic infiltration of neutrophils and macrophages into the skin, results in diurnal severity of parasitic infection in murine footpad models [101]. Moreover, all rhythms in infection are abolished in clock-deficient macrophages and mice lacking the circadian clock in immune cells [101]. Additionally, the diurnal pattern of T cell recruitment and function parallels nocturnal itching and exaggeration in atopic dermatitis (AD) [210].

1.4.4 Skin microbiome

A diverse community of microorganisms, termed the microbiome, colonizes the human body. Appropriate microbial composition and function is essential for proper host immune and

metabolic activities [112, 192]. Most human studies regarding potential diurnal rhythms in the microbiome have been conducted in the oral cavity [153] or the gut [112, 192, 221, 218], showing that rhythms in the microbiome are primarily driven by food intake. On the skin, taxa abundance, mainly of the phylum *Actinobacteria*, and especially the families *Propionibacteriaceae*, *Micrococcaceae*, *Gordoniaceae* and *Dermacoccaceae*) varies diurnally. This pattern primarily correlates with human activity [201].

1.5 The effect of feeding on the skin circadian clock and skin functions

Although light entrains the SCN clock, additional inputs such as temperature, exercise, and food intake affect the clocks in peripheral tissues [31]. The effects of food intake on circadian clocks in metabolic organs such as liver and fat are extensively studied. In these organs, food intake has major roles in timing of the clock, which is unsurprising given the divergent types of whole-body metabolism required during the day (food intake and activity) and night (fast and rest). In contrast to extensive studies focusing on the liver, the connection between feeding and circadian rhythms in the skin remained unexplored until recently. Below we review some of the findings showing that feeding regulates the skin circadian clock and biology of the skin.

1.5.1 Feeding-induced gene expression changes in skin

In experiments with multiple time-restricted feeding schedules, it is possible to rearrange the transcriptome data into feeding time series covering the beginning of feeding to 8 hours after the beginning of feeding. This allows the study of the effect of feeding on skin independent of time of day. In total, the expression of around 2000 genes changes in response to food

intake, indicating powerful effects of feeding on gene expression in the skin (Figure 1.5, left). The feeding-affected upregulated genes are involved in *lipid biosynthesis* and *protein synthesis*, whereas the downregulated genes are involved in *response to starvation*, *autophagy*, *negative regulation of cell proliferation*, and *response to oxidative stress*. This suggests that the metabolism and cell cycle regulators in the skin respond to feeding. Additionally, the fact that half of the feeding-affected transcripts are diurnal in at least one of the feeding schedules suggests that feeding is a regulator of diurnal gene expression in the skin [195].

1.5.2 Daytime restricted feeding shifts the phase of the circadian clock in the skin

Daytime restricted feeding, as opposed to normal nighttime feeding schedules for mice, shifts the phase and amplitude of the circadian clock in skin (Figure 1.5, middle) [195]. Compared to nighttime feeding groups, daytime-restricted feeding shifts the phase of the core circadian machinery in skin as indicated by *Per2*, *Dbp* and *Per1* mRNA expression patterns. The magnitude and the direction of the shifts depend on the exact feeding time during the day. Additionally, the amplitude of *Per2* mRNA expression decreases with daytime restricted feeding [195]. These changes in the skin circadian clock are different from the changes in the liver, where the phase of the clock is tightly coupled with feeding time, with phase advancements in all daytime-restricted feeding groups. Also, daytime-restricted feeding does not affect the amplitude of the liver clock [195]. These findings demonstrate a strong regulatory effect of feeding time over the skin circadian clock that is different from the effect on the liver clock.

The mechanisms whereby time of feeding shifts the phase and amplitude of the skin circadian clock are unknown. Since feeding regulates the expression of many systemic hormones including insulin, these hormones are potential mediators of the clock phase-shifting effects.

Indeed, application of insulin to mouse whisker hair follicles induces activation of *Per2*, leading to circadian synchronization of hair follicles [40]. Interestingly, application of insulin before the peak of PER2 expression leads to phase advances, while application of insulin after the peak does not [40]. Similar patterns are observed in cultured human hair follicles [94], suggesting that the timing of insulin shifts; therefore, food intake, may disturb the circadian rhythm in human hair follicles. While insulin may be one mediator, the exact mechanisms connecting feeding time to circadian rhythms in the skin remain to be investigated.

1.5.3 Transcriptomic changes in skin are specific to the altered feeding schedules

RNA-seq of the exons, introns, and antisense RNA from the skin of mice under three different restricted feeding schedules shows that while around 2500 to 3000 exons oscillate in each of the schedules, only 147 transcripts are shared in all three groups, including several members of the core clock gene network [195]. Despite the transcriptomic diversity, gene ontology analysis of the diurnal genes indicates *cell death*, *redox regulation*, and *circadian clock* as enriched biological processes for all feeding groups. Significant correlations between the peak expression time of a gene's intron and exon indicated that transcriptional regulation is responsible for the circadian phase shifts induced by restricted feeding. Some cytokinesis genes appear to be the exception to this rule and are regulated post-transcriptionally. Additionally, exons altered by food intake, regardless of the feeding schedule, are mostly related to metabolism, an indicator that feeding plays a role in skin metabolism status [195].

1.5.4 Time-restricted feeding does not affect diurnal rhythms in epidermal stem cell division but influences the sensitivity to UVB-induced DNA damage

Overall, daytime restricted feeding does not alter the structure of the skin with the exception that the dermis is thinner for the daytime-restricted feeding groups compared to the control [195]. Interestingly, although the cell cycle in epidermal stem cells shows a diurnal rhythm that depends on *Bmal1*, the phase of the circadian clock in skin does not control the cell cycle phase: the peak of S phase does not shift in the restricted feeding groups despite the shift in the phase of the clock (Figure 1.5, middle). These experiments suggest that daytime restricted feeding desynchronizes intermediary metabolism and cell division in epidermal stem cells [195].

On the other hand, skin's sensitivity to ultraviolet B (UVB) radiation-induced DNA damage is affected by daytime restricted feeding (Figure 1.5, middle) [195]. More damage is caused by UVB applied during the night than during the day in the skin from the nighttime-feeding group, while more damage is caused during the day for the daytime-restricted feeding group. Furthermore, oscillation of xeroderma pigmentosum group A (*Xpa*), a gene responsible for UVB-induced DNA repair, is dampened and less robust in the restricted feeding groups, suggesting that feeding time affects the diurnal rhythms of genes responsible for UVB protection and DNA damage repair in skin [195].

1.5.5 Time-restricted feeding influences the skin immune response

Expression of interferon-sensitive genes in the skin is also shifted by time-restricted feeding (Figure 1.5, middle) [195], suggesting that feeding time influences the skin immune response. Consistent with this idea, the expression pattern of interferon-sensitive genes in response to

IMQ in the daytime-restricted feeding group is different from the one in the nighttime feeding group. In the daytime-restricted feeding group, interferon-sensitive genes are expressed at higher levels after IMQ application during the night than during the day, which is the opposite of the pattern shown in the nighttime feeding group (Figure 1.5, middle). These findings suggest that time restricted feeding-induced circadian clock alterations affect the skin immune response [75].

1.5.6 The effect of calorie intake on diurnal gene expression and skin function

Besides food intake as such and time of feeding, the amount of calorie intake affects gene expression and function of the skin. Calorie restriction changes the structure of mouse skin by inducing faster hair regrowth after shaving, thicker epidermis, less dermal white adipose tissue, and greater vascular network [65]. Consistently, calorie-restricted mice have more interfollicular and bulge hair follicle stem cells that contribute to epidermal and hair growth. Additionally, calorie restriction alters the metabolism in mouse skin by decreasing oxidative metabolism in the epidermis but increasing it in the dermis [65]. Interestingly, calorie restriction can impede the aging-related reprogramming of clock-controlled genes, suggesting the connections between calorie restriction, circadian controlled genes and skin function (Figure 1.5, right) [171].

On the other hand, high fat diet induces hair thinning and dermal adipose tissue expansion without significantly affecting epidermal thickness [126]. A closer look at the hair follicles in mice taking high fat diet reveals a decrease in hair follicle stem cells in the bulge as well as a fate shift of these stem cells from hair shaft to upper hair follicle components such as sebaceous gland and the epidermis-hair follicle junction zone [126]. On a transcriptomic level, high fat diet induces the expression of around 3000 rhythmic genes enriched for gene

ontology terms such as *fatty acid oxidation*, *responses to oxidative stress* and *mitochondrion organization* [171]. This finding suggests a rewiring of the rhythmic genes to adjust skin metabolism in response to high fat diet (Figure 1.5, right).

Taken together, food intake itself, the time of food intake, and the amount of calorie intake affect the expression of rhythmic genes in the skin, as well as the cellular composition and function of the skin. These findings suggest that feeding has powerful effects on the skin, in part through modulation of the rhythmic transcriptome (Figure 1.5).

1.6 Circadian rhythms and skin diseases

Since the circadian machinery modulates many skin processes, including immunity, cell proliferation, metabolism, and DNA damage repair, it is plausible that circadian dysregulation can contribute to the development and progression of skin diseases.

The connection between circadian dysfunction and skin diseases is being studied both in the laboratory and in clinical settings. In the laboratory, chronic jet lag, prolonged light exposure, and flashlight treatment at night have successfully induced circadian disruption in mice. Additionally, mutation of core clock genes in mice and cultured tissues and cells provide insights into the role of the clock in disease. Human studies mostly focus on epidemiological data collected from shift workers, aiming to delineate the association between shift work-induced circadian disruption and diseases.

In this context, we focus on the role of the circadian clock in various skin diseases, including skin cancer, sunburn, aging, hair loss, inflammatory diseases, infections, and wound healing.

1.6.1 Skin cancer

The two main forms of skin cancers are carcinoma and melanoma. Carcinomas, such as squamous cell and basal cell carcinomas, are derived from keratinocytes. Melanomas, on the other hand, are derived from melanocytes [168]. Although carcinomas are more frequent, melanomas are more deadly by metastasizing through blood [117].

Ultraviolet (UV) radiation, either from the sun or tanning beds, is the major cause of melanomas and carcinomas. UV radiation from the sun can be classified into three types based on wavelength: UVA, UVB, and UVC. UVC is the most damaging of the three, but fortunately the majority of it is absorbed by the ozone layer. On the other hand, most of UVA and a small percentage of UVB still reach the earth. Those two wavelengths are absorbed by skin cells and cause DNA mutations through different mechanisms. UVB directly causes nucleotide changes while UVA raises the level of reactive oxygen species (ROS) that can lead to DNA damage. Additionally, while UVB is a thousand times more carcinogenic than UVA, UVA can penetrate deeper to cause DNA mutations [41, 131].

Epidemiological studies linking work-related circadian disruption to cancer risk have highlighted the role of the circadian clock in several types of cancer, including melanoma [212].

The skin's susceptibility to UV radiation-induced DNA damage is diurnal

Circadian rhythms are robustly present in the skin, an organ that directly experiences variations in UV radiation throughout the day. Indeed, the susceptibility of the skin to UV radiation-induced DNA damage is time-of-day dependent, and this diurnality is controlled by the circadian clock. There are at least two possible mechanisms contributing to the diurnal pattern of DNA damage. The first one relates to the susceptibility of the S phase of the cell cycle to UV-induced DNA damage [72] and the other one to the diurnality in DNA

repair [68, 149].

Exposing the dorsal skin of mice to UVB radiation at different times throughout the day revealed that more DNA damage occurs when the exposure takes place at ZT20 than at ZT8 [72]. Nucleotide excision repair (NER) is ordinarily capable of resolving UV damage, but rate-limiting subunits of the process such as XPA proteins are expressed in a rhythmic pattern due to circadian clock regulation. Because of this rhythmicity, mice that are exposed to UV radiation during dark hours experienced more severe and abundant squamous cell carcinomas compared to mice exposed to UV radiation during light hours [68]. Such time-dependent variation in DNA damage is replaced with a constant high level in $Bmal1^{(-/-)}$ mice, suggesting that the susceptibility to UVB radiation is controlled by the clock [72]. The cell cycle is also diurnal in mouse epidermal cells and controlled by the clock. More cells are in the S phase at night (ZT21) than during the day (ZT9). Similar to the DNA damage, the diurnal variation in the proportion of S phase cells disappeared in single knockout $Bmal1^{(-/-)}$ mice and double knockout $Cry1^{-/-}Cry2^{-/-}$ mice [72, 158]. It is noteworthy that the S phase is more prone to DNA damage, which may contribute to increased susceptibility to UVB radiation at night (ZT20) compared to the day (ZT8) [72].

XPA protein is expressed at high levels during the day and is at low levels at night [68, 149]. P53 protein also accumulates to a higher level in mouse skin exposed to UV radiation at night (ZT21) than at during the day (ZT9). This variation could be explained by changes in the level of MDM2 protein, which stimulates the degradation of P53 protein and shows a diurnal expression pattern. During the night, the levels of both MDM2 and P53 proteins are low, resulting in less degradation of P53. Thus, when mouse skin is exposed to UV radiation at night, the P53 levels rise to a high level with minimum degradation, leading to more P53-dependent responses such as apoptosis. On the other hand, since the expression level of both P53 and MDM2 proteins are already high during the day, UV radiation does not cause much increase in the P53 level because the level of MDM2 is high enough to degrade most

of the P53 proteins. Hence, the P53-dependent responses in mouse skin are less prominent when the radiation occurs during the day instead of at night [69].

The skin is protected from UV radiation by the pigment melanin produced by melanocytes [154]. The core clock component BMAL1 influences melanin production by associating with microphthalmia-associated transcription factor (MITF), the master regulator of melanogenesis. MITF has rhythmic expression levels alongside BMAL1. By overexpressing BMAL1, the resultant melanin from the melanogenesis pathway was correspondingly higher, conferring greater protection against UV radiation for skin cells [155].

For non-UV radiation induced carcinoma, which accounts for about 10% of carcinomas, the loss of *Bmal1* results in decreased development of squamous tumors in mice with an oncogenic background [92]. Compared to the control, mice with *Bmal1* knockout have lower percentages of tumor-initiating cells and increased expressions of tumor suppressors, thus decreasing the severity and abundance of carcinomas.

In sum, the clock affects UV-induced skin cancer initiation by regulating the cell cycle and DNA repair mechanisms in keratinocytes and through regulation of UV-protectant pigment from melanocytes.

The circadian clock regulates skin cancer progression

In addition to controlling susceptibility to UV-induced DNA damage and cancer initiation, the clock is involved in skin cancer progression in at least two ways. On the one hand, cancerous cells possess aberrantly expressed clock genes, resulting in impaired clock function [119]. On the other hand, mutations of core clock genes are associated with melanoma progression [76]. As a result, recent studies have targeted components of the circadian clock to restore tumor cell circadian rhythms in cancer treatment [119].

The clock network is dampened in cancer cells, demonstrating that an oncogenic landscape facilitates clock dysfunction [119]. A comparison of gene expression data from human melanoma and healthy skin samples reveals downregulation of clock genes in melanoma [46]. The upregulation of oncogenes such as *Ras* extends the period of the clock, demonstrating mechanisms in cancer progression that disturb the circadian machinery [144]. Consistently, mice injected with B16-F10 melanoma cells possess severely impaired clock gene regulation within and around the tumor site [47]. Core clock components can be indirectly regulated by proteins of the Melanoma Antigen (MAGE) family that bind to RORs or modify ubiquitination of clock proteins [196, 34]. Similarly, circadian machinery is disrupted in oncogenic keratinocytes; ablation of the tumor suppressor gene *Pten* increases BMAL1 in hair follicle stem cells, highlighting the regulatory influence of tumor suppressors on core clock components [217].

In addition to disrupted circadian clock function in melanoma cells, circadian disruption contributes to other oncogenic mechanisms. Myeloid-specific *Bmal1* knockouts lead to metabolic dysregulation in macrophages, thus promoting immune suppression and melanoma tumor burden [7]. In addition, chronically shifting light schedules alters the immune microenvironment in melanomas by inverting the ratio of M1 and M2 macrophages [3]. Thus, clock dysfunction can lead to tumor-promoting changes in the melanoma microenvironment.

Circadian disruption also promotes cell cycle transitions by upregulating cell cycle genes such as *Ccna2* [3]. Clock proteins like PER can couple with nuclear proteins involved in the cell cycle, enabling circadian control of cell cycle checkpoint genes [105]. Normally, specific components of the clock, such as neuronal PAS domain 2 (NPAS2), also directly limit cellular proliferation by gatekeeping portions of the cell cycle, but mutations in these genes promote cell cycle transitions [66]. Overall, since clock proteins act as critical regulators of cell cycle checkpoint control, disruption of the clock leads to unregulated division and tumor proliferation [97].

Given that clock dysfunction enables tumor proliferation, targeting the clock to improve its function could facilitate cancer management. Inducing circadian rhythmicity in tumor cells by dexamethasone decreases *in vivo* melanoma growth in mice [100]. This response is clock-dependent, as knocking down *Bmal1* in tumors prevents the growth-dampening effect from dexamethasone. Pharmacological studies also targeted components of the circadian clock, nuclear hormone receptors NR1D1 and NR1D2, to stimulate apoptosis in malignant cancer cells [177]. By applying agonists of these receptors, senescent cells like those in melanocytic nevi would undergo cell death, demonstrating that treatments targeting core clock machinery impair melanoma proliferation. In addition to targeting the circadian clock machinery, current cancer treatments can utilize the clock by modulating the time of treatment application. The toxicity of the chemotherapeutic cisplatin towards melanoma cells varies throughout the day, indicating that melanoma treatment is more beneficial in the morning (ZT0) for patients [43].

In sum, the circadian clock plays a role in the initiation and progression of skin cancer. The rhythmicity of the clock regulates DNA-damage repair, thus modulating the susceptibility to UV-induced DNA damage and cancer initiation. Carcinomas and melanomas often possess diminished clock function, promoting cell cycle transitions and cell proliferation. Also, dysregulation of the clock can alter the tumor microenvironment to make it more immunosuppressive. Targeting core clock genes therapeutically to restore clock function may be a promising approach to cancer treatment.

1.6.2 Sunburn

Short-term exposure to excessive UV radiation leads to sunburn. UV radiation-induced DNA damage leads to an inflammatory response characterized by skin redness, swelling, and pain [48]. Consistent with the diurnality in UV-induced DNA damage, the severity of sunburn

symptoms also exhibits a diurnal pattern. While erythema severity saturates at high levels of UV exposure on the dorsal skin of mice, moderate levels of radiation applied during the night (ZT21) caused higher levels of inflammatory cytokines, apoptosis, and worse erythema than during the day (ZT9) [69].

Due to the opposite chronotypes of humans and mice, the diurnal pattern found in mice is speculated to be reversed in humans [72, 41, 69]. Indeed, radiation in the evening (between 7pm to 9pm) caused more serious erythema than in the morning (between 7am to 9am) on human skin, indicating that the human skin is more sensitive to radiation in the evening [132]. Interestingly, P53 protein accumulated more in skin samples collected 24 hours after morning irradiation, which is the same pattern in mice [132]. This could be explained by previous findings wherein UVB-induced accumulation of P53 is not correlated with severity of erythema in human skin [81].

In summary, UV-induced DNA damage directly links to skin carcinogenesis as well as acute inflammatory responses. Furthermore, the effect of UV radiation on skin is time-of-day dependent due to the diurnality of cell cycle and DNA damage repair.

1.6.3 Hair loss

Hair loss, also known as alopecia, is one of the most common skin concerns. While it usually occurs on the scalp, hair loss can affect any hair bearing part of the body. The most common form of alopecia is androgenetic alopecia, which affects both males and females, albeit with a different pattern of hair loss. There is also an aging-associated hair loss that may be independent of androgenetic alopecia. Telogen effluvium is another hair loss disease; it may be triggered by a number of stimuli, including stress, hormones, medications, and illness [73]. In this condition, hair follicles enter the shedding phase in a synchronized manner [189] whereas normally human hair follicles have desynchronized hair cycle stages. Anagen

effluvium on the other hand is caused by cell death in the matrix of growing hair follicles in response to genotoxic stimuli such as ionizing radiation and chemotherapy [143]. Alopecia areata is an autoimmune disease characterized by hair loss. Finally, scarring alopecias are inflammatory conditions that lead to destruction of the hair follicle bulge stem cells and permanent loss of hair follicles [189].

Given the regulatory role of the circadian clock in hair follicles, it stands to reason that clock disruptions could contribute to hair loss, especially aging-related hair loss. Evidence for this, however, is missing from epidemiological studies. The clearest evidence for a role of the circadian clock in hair loss comes from mouse studies showing that the clock gates cell division in growing hair follicles. Thus, γ radiation causes more hair loss when applied to anagen hair follicles at the mitosis peak in the morning than in the evening when mitosis levels drop [140]. Based on this finding in mice, we speculate that radiation in the evening would causes more hair loss than radiation in the morning in humans. Hence, arranging radiotherapy in the morning may be better for managing hair follicle damage during the treatment.

1.6.4 Aging

At an organismal level, aging correlates with circadian rhythm alterations as indicated by features including advanced sleep pattern, flattened body temperature fluctuation, and decreased activity levels during the wake period [84]. Additionally, aged mice cannot adapt to light-dark schedule alterations as well as young adult mice [32]. One explanation for this is related to the impaired functions of retinal cells and the SCN. Since aging reduces the number of ipRGCs, the amount of SCN neurons expressing VIP, and neuron coupling, the circadian rhythm in aged individuals is not as robust as in young adults at the organismal level [18]. While the SCN function is compromised at a tissue level, the clock machinery

evaluated by *Per2* expression in the SCN is as robust as in young adult mice [32]. Similar to the case in the SCN, the molecular clock in mouse peripheral tissues such as kidney, liver, submandibular gland, and epidermis is robust despite the decrease in locomotor activity [179, 171].

In the skin, features of aging include wrinkles and lines, dryness, a thin epidermis, hair loss, loss of elasticity, skin fragility with easy breaking, and slow wound healing. The causes of skin aging are on the one hand intrinsic, strongly correlated with chronological age, and on the other hand extrinsic. Intrinsic aging mechanisms include oxidative damage to DNA and proteins from metabolism-generated ROS, accumulating genetic mutations, stem cell dysfunction, and alterations in hormones. Extrinsic skin aging mechanisms involve primarily UV radiation, but also other insults such as cigarette smoking, and pollution [23].

While the exact mechanism is unknown, clock disruption contributes to intrinsic skin aging as mutations of the core clock genes *Bmal1* and *Clock* in mice lead to premature aging in multiple organs, including the skin [102, 58]. CConversely, aging influences the circadian function, as aging rewires rhythmic genes in the skin [171]. While the circadian machinery is robust in aged epidermal stem cells, other rhythmic genes in the young and aged groups are quite distinct [171]. Thousands of genes are diurnal in young and aged mouse epidermal stem cells, but only 750 genes overlap the two ages, including some genes from the core clock machinery. Additionally, the rhythmic genes present only in the young adult group are mainly related to homeostasis maintenance, while the genes that oscillate only in the aged group are enriched for stress response. This suggests a reprogramming of rhythmic genes in mouse epidermal stem cells as they age while maintaining the core circadian function [171]. Despite premature aging in core clock gene knockout mice [102, 58], the failure to reproduce the transcriptional traits found in physiologically aged epidermal stem cells in *Bmal1* knockout and *Per1/Per2* double knockout mice suggests that the reprogramming of rhythmic genes is due to aging instead of loss of circadian function [171].

A similar observation was made in rat abdominal skin explants. There is no significant overall change in the average value of phase, amplitude and period lengths in rat skin explants as they age, although the phases are significantly more variable in the aged group [151]. However, when looking at the circadian rhythm in fibroblasts derived from these explants collected at different ages, *Per1* expression amplitude attenuates uniformly as the age increases [151]. Along the same line, a microRNA *miR-31* that is upregulated in aged mouse hair follicle stem cells targets at the core clock gene *Clock*, suggesting the potential effects of aging on the clocks in hair follicle stem cells [214]. While the differences in results could be caused by different experimental methods, the question about whether aging affects circadian clocks differently in different cell types warrants further investigation.

As discussed before, the rhythms in the skin regulate cell proliferation in a way to avoid exposing possible genotoxic and radiation stress to the vulnerable S phase [72, 173]. Intriguingly, without affecting the core clock gene network, aging affects the cell cycle timing in mouse epidermal stem cells, which could be an explanation for the transcriptional enrichment of stress response and DNA damage repair in aged cells. While the S phase takes place mostly during the night in young adult epidermal stem cells [72, 171, 173], the peak DNA replication time is shifted to the day for the cells from the aged group [171]. Despite this delay, mitosis is rhythmic and still takes place at ZT20 in the aged group, which is the same as in the young adult group. Such delay may lead to the possible exposure of unwound DNA to oxidative stresses and increase the possibility of cells entering the mitosis with DNA damage [171]. This observation is consistent with some of the skin aging symptoms, as oxidative stress is one of the contributors to interfollicular epidermis stem cell senescence, which could lead to skin wound healing delay, thinning of the epidermis in aged skin, and age-related hair loss [139].

One way to lessen the effect of aging in mouse epidermal stem cells is through calorie restriction. For mice under calorie restriction (70% of the amount taken by the control group), both

physiological and transcriptional traits found in young mice are maintained with rhythmic expressions preserved in genes related to homeostasis maintenance and lower level of oxidized DNA. Also, S phase peaks at ZT12, which is closer to the peaking time in young adult epidermis. Despite a 4-hour phase advancement for the calorie restriction group due to feeding anticipation, other circadian features such as the amplitude and the period length of some of the core clock genes are conserved in the calorie restriction group [171].

Since circadian rhythms in the skin may protect cells from UV-induced DNA damage by regulating cell proliferation [72], circadian reprogramming and cell cycle shifts caused by intrinsic aging may contribute to extrinsic skin aging. Furthermore, clock-related hormone function impairment caused by intrinsic aging can affect skin function and promote extrinsic skin aging. Melatonin is one of the hormones that regulates peripheral clocks and its receptor is present in the skin [170]. Interestingly, melatonin receptor MT1 plays a key role in DNA repair as it activates the P53-dependent DNA damage response [152]. In human skin, MT1 levels drop as we age, leading to increased sensitivity to UV radiation [53]. The receptor MT1 level is drastically lower in cultured dermal fibroblasts from a 67-year old donor when compared with cells from a 19-year donor. Furthermore, after UV radiation, the amount of UV-induced DNA damage and ROS generation is much higher in MT-1 knockdown human fibroblasts, suggesting that aged human dermal fibroblast are more susceptible to UV damage [53].

Much of the connections between skin aging and circadian rhythms remain to be explored. Questions such as whether aging affects the circadian rhythm differently in different cell types, what mechanisms cause the shifts in cell cycle while not affecting the core circadian clock in epidermal stem cells, and what kind of mechanisms contribute to the rescuing effect of calorie restriction on epidermal stem cell aging remain to be answered.

1.6.5 Skin infection

As a first line of protection against outside insults, the skin harbors various defensive strategies, including a physical barrier formed by corneocytes (terminally differentiated keratinocytes), resident innate immune cells, and antimicrobial peptides (AMPs), which are secreted to induce direct antimicrobial effects [159, 130, 51]. The immune system is circadian regulated, possibly to anticipate and prepare for outside insults when they are most likely to occur [139, 160]. The circadian clock regulates immune responses to infections in the respiratory system [178, 164], the liver [37], the digestive system [17], and other body sites [222]. Consistent with these findings, a growing body of animal research supports the hypothesis that immune responses and clinical outcomes of skin infections are influenced by the host's circadian rhythms and time of infection [139, 72, 21, 101].

Bacterial and parasite skin infections

The survival of bacteria on the skin depends on the time of infection. *Staphylococcus aureus* shows maximum survival on mouse skin when applied at ZT22 and minimum survival when applied at ZT16. This may be due to the diurnal expression of certain AMPs in the skin. The expression levels of *Rarres2* (chemerin), *Camp* (cathelicidin CRAMP), and *Defb1* (β-defensins) are diurnal, with the highest expression during the early night when mice are under 12:12 light-dark cycle. However, the rhythms for those genes in mouse skin are lost in constant darkness, although they are maintained in the liver. In contrast, *Defb3* and *Defb14* (β-defensins) aare circadian under both 12:12 light-dark cycles and in constant darkness, with expression peaking during the day [21].

The severity of parasite infections in skin is diurnal as well [101]. Leishmania parasites are transmitted through sandfly bites and use neutrophils and macrophages as host cells. Injection of *Leishmania major* parasite into mice at different times of the day revealed

that inflammation is the mildest when the injection takes place at ZT3, with minimum macrophage recruitment six hours after injection. *In vitro* experiments confirm that the attachment of the parasite to mouse macrophages is circadian and dependent on the circadian machinery, which also regulates the time-dependent release of chemokines and cytokines [101].

Viral skin infections

Skin also has the important task of defending against many viruses, which are biological entities that can only thrive and multiply in a living cell. While there are few studies on circadian regulation of defenses against viral infections of the skin, studies in other organs suggest a role for the circadian clock in regulating this activity. Mice intranasally infected with herpes or influenza viruses during the daytime have greater infection loads and mortality than mice infected at nighttime. This time-of-day dependent difference may be clock controlled as deletion of *Bmal1* exacerbates the infection [61]. In addition, disruption of circadian rhythms by *Bmal1* deletion or altered sleep/wake patterns enhanced acute viral bronchiolitis after Sendai virus and influenza A viral infections [62].

Topical application of the viral mimic IMQ during the day results in greater expression of anti-viral defense response genes compared to application at night. Absence of *Bmal1* results in heightened levels of those same genes [75]. This result suggests that the diurnal gating of sensitivity to viral infection is modulated by circadian clock control of anti-viral factors expressed in the skin. These results have implications for anti-cancer defenses as anti-viral mechanisms limit cancers as well. For example, IMQ is prescribed as an anti-tumor treatment for basal cell carcinomas, as it activates the immune system through type I interferon secretion.

1.6.6 Inflammatory skin diseases

Skin inflammation, which includes redness, heat, itching, sensitivity, and swelling serves to defend against invading pathogens and microbes. While controlled skin inflammation is necessary to regain homeostasis after infection, there are cases in which skin inflammation is triggered by self-peptides or persists following an infection, leading to skin diseases. Inflammatory responses are linked to circadian rhythms [75] and circadian disruption can lead to inflammatory diseases. In mice, for example, chronic jet lag induces ulcerative dermatitis [96]. For humans, psoriasis and AD are two of the most common autoimmune skin diseases. Both of these diseases, which can significantly impair patients' life quality, are linked to circadian rhythms.

Psoriasis is caused in part by the immune system attacking healthy skin cells, resulting in intense inflammation. In humans, disruption of the circadian clock through night shift work is associated with psoriasis [116, 111]. The symptoms of psoriasis also show a diurnal pattern, with more than 70% of patients reporting more severe itch occurring in the evening or at night [64]. With most of the itch occurring at night, AD and psoriasis symptoms compromise sleep quality [184], which in turn disrupts circadian rhythms and increases severity of the disease. This circadian disruption also contributes to the development of metabolic diseases such as obesity [147], which may be causally linked to psoriasis [133].

At a mechanistic level, the inflammatory response in psoriasis is controlled by the circadian machinery [75, 11]. Mutation of *Clock* relieves the induced psoriasis-like symptoms significantly by controlling the transcription of IL-23R in γ/δ^+ T cells while mutation of *Per2*, the inhibitor of *Clock*, promotes IMQ-induced symptoms [11]. Additionally, deletion of *Bmal1* promotes IMQ-induced psoriasis [75]. Conversely, psoriasis inflammation disturbs the circadian clock locally in the skin lesions. In IMQ-induced psoriasis mouse model, the rhythmicity of keratinocyte proliferation is lost, and the expression of core clock genes is dampened [75].

Similar to the case in mice, bulk RNAseq studies using human patients skin samples show that circadian genes such as *CRY2*, *PER3*, *NR1D1* and *RORC* are downregulated in the psoriasis lesion as well as the adjacent normal skin when compared to skin from non-psoriatic individuals [75, 215]. These findings support the intricate connection between psoriasis and the circadian machinery and suggest that the circadian clock is a potential target in psoriasis treatment.

AD is another common inflammatory skin disease characterized by impaired barrier function, eczematous dermatitis, and chronic itching. The causes of AD are not fully understood, but may relate to barrier impairment, dysregulated immune system, and/or dysregulated commensal microbiota. AD symptoms tend to be greater at night and impair sleep quality [211, 35]. There are several mouse models of AD. These typically apply an inflammatory insult (a chemical or hapten) to the skin to activate macrophage cytokine secretion, which in turn provokes release of histamines by mast cells that causes itch; the insult is then re-applied later to induce an adaptive immune response driven by T cells. Disruption in circadian rhythms by forcing mice to run during the day and rest during the night causes loss of rhythmicity in circadian gene expressions and more severe AD symptoms with increased expression of histamine and cytokines, including TNF-α and interleukins (IL-4, IL-10, IL-13). Additionally, more dendritic cells, mast cells and T helper cells are recruited to the skin in mice with the reversed chronotype [82]. Also, hapten induces more inflammation in the skin of mice living in constant light than in the skin of mice living in regular 12:12 light-dark cycle [123]. Implicating the circadian clock on the molecular level, deletion of *Clock* causes more severe delayed-type skin allergic reactions [182]. As the circadian clock regulates the immune responses that contribute to AD symptoms, studying the relationship between the circadian rhythm and AD will yield insights into symptom management.

1.6.7 Wound healing

Skin injuries invoke complex repair mechanisms that require regulation and coordination among cell types throughout the skin. These mechanisms go awry in chronic wounds, a major health problem sometimes caused by metabolic diseases like diabetes and obesity [118]. Several elements of skin wound healing have diurnal features and interact with the core clock machinery.

Wound healing progresses through five steps: hemostasis, inflammation, growth, re-epithelialization, and remodeling. Hemostasis stops the bleeding by forming a hemostatic plug at the injury site [148]. This very first step of wound healing displays diurnal rhythms in humans, with hemostasis being upregulated in the morning and fibrinolysis activation peaking in the afternoon [28]. As discussed earlier, elements of the inflammation step are under circadian control.

The growth stage of skin wound healing displays circadian rhythms. The actin polymeric state, as measured by the ratio of F:G actin produced by fibroblasts, is rhythmic and such rhythm is dependent on the cells' internal circadian machinery [85]. Additionally, the circadian clock affects senescence of myofibroblasts through NONO, a binding partner of PER that regulates cell cycle inhibitors [105]. These findings support the idea that the circadian clock regulates both proliferation and migration of fibroblasts, key functions required for wound healing.

The time-of-day of wounding may affect the length of recovery [85]. Synchronized murine skin fibroblast monolayers scratch-wounded at the peak time of PER2 expression healed almost completely after 60 hours while those wounded at the PER2 trough time were far from closing. This can be explained by the significantly faster initial migration, stronger initial cell adhesion, and greater wound-oriented polarization of the most motile fibroblasts in monolayers wounded at the peak time of PER2 expression. *Ex vivo* wounding experiments

done on 5-day-old murine skin explants harvested during the active phase and the resting phase show similar results, with twice as many fibroblasts invading the wound in the explants collected during the active phase when compared with the sample collected during the resting phase. This observation is reproduced in *in vivo* wounding experiments on adult mouse back skin, suggesting that the invasion of fibroblasts into the wounded area, and thus possibly the recovery of the wound, are dependent on the wounding time in mice [85].

A *post hoc* analysis of the datasets from the Burn Injury Database reveals that burns happening at night took around 60% more time to heal than the burns that took place during the day [85]. While wounds incurred during the active phase of humans and mice take less time to heal [85], the opposite pattern is true in nocturnal hamsters [33]. According to the wound sizes recorded daily, wounds incurred at ZT18 (night) take longer to recover by 50% than wounds incurred at ZT3 (day), even though wounds incurred at both times take the same number of days to heal completely [33].

Re-epithelization may also display circadian rhythms. While there is no *ex vivo* or *in vivo* wounding experiments done so far on human skin, scratch-wounds incurred on human keratinocyte monolayers at the peak time of fibroblast motility healed faster than the monolayers scratch-wounded at the trough time [85]. On the other hand, while the proliferation of mouse epidermal keratinocytes is circadian, with more cells at the S phase at night than during the day [72], the proliferation elevates and loses its rhythmicity when there is inflammation [75].

Circadian disruption delays skin wound healing. Cutaneous wounds in disruptive light-treated hamsters took longer to heal compared to hamsters with normal circadian rhythm, no matter the time of wound occurrence [33]. Similarly, dim light exposure to mice during dark hours before wounding slows down the healing process significantly [193].

Manipulation of the circadian machinery does not always impede wound healing. Partial or complete knock out of *Npas2*, whose protein is a paralog of CLOCK, significantly shortens

the duration of dorsal skin wound healing in mice *in vivo*. *In vitro* experiments using the fibroblasts isolated from *Npas2*$^{-/-}$, *Npas2*$^{+/-}$ and wild type mice uncovered accelerated proliferation of *Npas2*$^{-/-}$, *Npas2*$^{+/-}$ fibroblasts without alternation in the rhythmic expression of most of the core clock genes except *Per2*. Additionally, *Npas2*$^{-/-}$ fibroblasts contract faster than wildtype and *Npas2*$^{+/-}$ fibroblasts. Intriguingly, the expression level of *Acta2* and *Actb*, along with other integrin genes do not differ among the genotypes. Some collagen genes (*Col12a1* and *Col14a1*) are upregulated in cultured *Npas2*$^{-/-}$ and *Npas2*$^{+/-}$ fibroblasts, in agreement with promoted collagen fiber formation observed in those knockout cells [156].

While more extensive studies are necessary to delineate the connection between the circadian clock and skin wound healing, current findings indicate that the time of wounding has an effect on the healing duration [85, 33] and that the circadian machinery plays a role in many wound healing processes [33, 193, 156]. The field remains to be explored, especially the possibility of promoting wound healing via circadian clock manipulation [156].

1.7 The future of circadian medicine for skin health

Circadian medicine and chronotherapy are receiving increasing attention as important components of preventive medicine and patient care [91, 176, 50]. At its core, circadian medicine considers circadian rhythms in pre-clinical research and when developing disease management plans to improve clinical outcomes while minimizing side effects. For example, vaccination in the morning results in greater trained immunity and antibody responses than vaccination in the evening in humans [49, 114, 219]. Additionally, perioperative myocardial injury is more common after on-pump cardiac surgeries in the morning than in the afternoon [124]. In mice, non-steroidal anti-inflammatory drugs better manage pain and promote recovery with less adverse effects on healing after tibia fracture surgery when taken during the active

phase than during the resting phase [6]. Such diurnal variation in treatment efficiency is also observed in other tissues and diseases [91, 176, 50], including cancer [175, 13].

Circadian medicine uses three main approaches: lifestyle adjustments to regulate the internal clock, drugs targeting the clock machinery at a molecular level, and administration of drugs at the time of day that maximizes effectiveness and minimizes side effects (chronotherapy) [158, 176]. Although the skin harbors a robust circadian clock, circadian medicine for skin diseases is a fledging field. Here, we discuss how circadian medicine can benefit skin health.

1.7.1 Managing the internal clock via lifestyle adjustment

Research in model animals and cultured human cells shows how disruptions of circadian rhythms via clock gene manipulations can contribute to the development and progression of various kinds of skin diseases including cancer, sunburns, radiation-induced hair loss, aging, infections, inflammatory diseases, and wounds. Consistent with these experimental studies, epidemiological studies on shift workers show that circadian disruption is associated with increased incidence of metabolic disease [98], cancer [212], and several skin diseases [116, 111, 158]. Therefore, it stands to reason that a healthy lifestyle aimed at maintaining normal circadian rhythms may improve skin health.

Currently, shift work, social jet lag, sleep disorder and excessive light exposure at night are common causes of circadian rhythm disruption in modern society. Shift work is extensively studied as it leads to disruption of the core clock machinery, including the skin [24, 80]. Compared to normal daytime workers, shift workers possess altered circadian rhythms in the skin as indicated by significantly attenuated peak expression level of *Per1* [24]] and altered expression patterns and levels of *Per3*, *Nr1d1* and *Nr1d2* [80] in hair follicles. Shift workers are more prone to skin diseases, including psoriasis, dry skin, itching, dandruff/seborrheic dermatitis, acne, and melanoma [158, 116, 111, 212].

Conversely, skin diseases such as psoriasis and AD can affect the patients' organismal circadian rhythm by disturbing sleep [35, 184, 213], which then adversely feeds back to disease progression. Besides being predisposed to greater disease risk, shift workers may experience worse side effects. In mice, circadian disruption via jet lag or clock gene mutations leads to more severe radiation-induced dermatitis [42]. Because of this, maintaining a normal sleeping pattern and avoiding shift work would be beneficial for minimizing the risk and severity of skin diseases.

As feeding can influence skin circadian rhythms in mice, and thus the immune response, adjusting feeding behavior in terms of both of the feeding time and the caloric intake may be a way to support circadian function in the skin [50, 25]. In mice, time of feeding affects the skin immune response [75]. Additionally, calorie restriction delays the age-associated reprogramming of circadian controlled genes from homeostasis maintenance to stress response [171]. In contrast, high fat diet induces hair loss [126] and rewires the expression of rhythmic genes to favor oxidative metabolism [171]. While well-controlled experimental research in humans on the effect of feeding on skin health is lacking, a recent clinical study focusing on psoriasis patients before and after Ramadan fasting, which happens during daylight time for an entire month, showed alleviation of psoriasis after the fasting [44, 26].

1.7.2 Targeting the clock machinery at a molecular level

Circadian rhythms are often disrupted in diseased tissues. Most often, this takes the form of dampened rhythms due to a loss of synchronization or suppressed circadian gene expression [100, 45, 75, 175]. For example, expression of *Bmal1* is dampened in the skin of IMQ-treated mice [75]. Therefore, it is possible that restoring or enhancing the circadian rhythm can control disease progression. Dexamethasone, for example, activates the circadian clock in B16 melanoma tumors, which decreases cell proliferation and tumor growth [100]. Indeed,

the circadian machinery is a reservoir that may host promising targets for developing skin disease treatments.

For example, without harming normal cells, REV-ERBs agonists SR9009 and SR9011 adversely affect cancer cells derived from tumors, including melanoma [177]. In mice, mutation of *Clock* relieves psoriasis-like symptoms [11] and mutation of CLOCK protein paralog shortens wound healing duration [156]. Additionally, topical application of ROR inverse agonist SR1001 quenches inflammatory response in AD mouse models. For humans, melatonin supplement alleviates AD symptoms [36]. Future studies should explore drugs that target the circadian machinery in skin diseases, including inflammatory and hyperproliferative skin diseases.

1.7.3 Chronotherapy

Circadian rhythms regulate many metabolic enzymes that participate in drug metabolism in the skin [72]. Hence, more clinical studies should be conducted to assess how time of application impacts treatment efficacy and side effects. Experiments done in mice show that maxacalcitol, a vitamin D3 analogue for psoriasis symptom relief, is more effective when applied during the early to middle active phase of mice than during the early to middle resting phase [210]. For AD, application of topical treatment in the evening is proposed to improve symptoms [190].

For cancer, studies from the 1990's describe more effective melanoma tumor shrinkage in mice when interferon was infused during the day as opposed to night [103]. Additionally, radiation chronotherapy in the morning for cancer treatment reduces its damaging effect on skin [167].

It may also be important to consider the time of diagnostic measures. For example, the

time of diagnostic measures is critical for accurate diagnosis in endocrinology, as a number of hormones oscillate in a time-of-day dependent manner [70]. Similarly, it is possible that the time of measurement is important in dermatology, since features such as mitosis [72, 140] trans-epidermal water loss [121], and immune components display diurnal rhythms [195, 75, 21].

1.7.4 Challenges

As promising as circadian medicine is, we face challenges. Most studies are done *in vitro* or *in vivo* using model organisms such as mice, rats and hamsters. Those animals are nocturnal while humans are diurnal, which can lead to difficulty in translating from mice to humans. Also, most pre-clinical intervention studies in mice are carried out during the day, the resting phase of mice. One possible step to reduce the gap between human and model nocturnal animals is to use inverted-light housing, so researchers can still make the measurements during the day while it will be the night for the nocturnal model animals.

Additionally, since circadian medicine works the best when it is correlated with the patient's internal circadian rhythm, health professionals need a feasible method to accurately determine each patient's circadian rhythm before establishing a treatment plan [138]. The most traditional and established way of measuring circadian phase of a patient includes a tedious process of collecting multiple saliva samples throughout the day in a dim room for the dim-light melatonin-onset assay [95, 208, 203]. For clinical applications, several approaches have been proposed to determine a patient's clock phase [120], including body temperature [146], transcript biomarkers in blood [203, 107, 27], cortisol concentration in sweat [188], as well as volatile organic compounds and nitric oxide fraction in breath [202]. The accessibility of skin makes this organ a source to measure rhythms: indeed, transcripts from hair follicles [4], skin biopsies [208] and tape-stripped epidermis [205] can potentially be used for circa-

dian time estimation [138]. However, the question as to which method is the best in terms of accuracy and accessibility remains unanswered. Another challenge to utilizing circadian medicine for skin diseases lies in the complexity of skin. The circadian rhythm in skin may not be as uniform as in other organs [139]. Additionally, two other clocks, hair cycle and natural aging, influence the circadian controlled gene expression, raising questions about whether these variables need to be considered [139, 171].

1.8 Acknowledgements

This work was supported by NIH grants R01 AR056439 and P30AR075047, an NSF grant DMS1763272, a grant from the Simons Foundation (594598), and the Irving Weinstein Foundation (to B. Andersen).

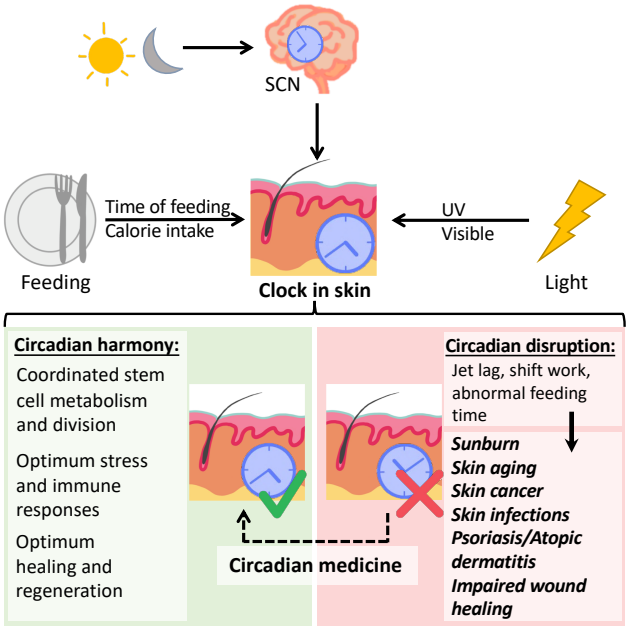

Figure 1.1: **The circadian clock is essential for skin homeostasis.** The mammalian SCN receives time-setting light signals and coordinates the circadian clock in peripheral tissues, including the skin. Other inputs such as feeding and light can directly influence the skin circadian clock, which is essential for proper skin homeostasis. Circadian disruption contributes to skin diseases, which may be managed by circadian medicine via clock restoration in the skin.

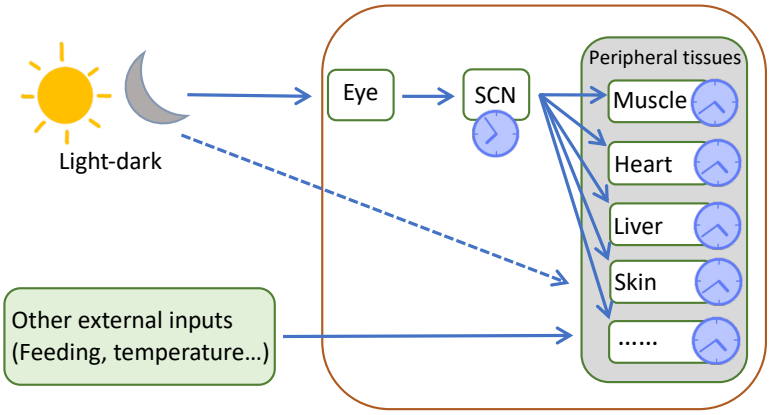

Figure 1.2: **The SCN synchronizes peripheral clocks.** Light sends signals through the retina to set the clock in the SCN, which synchronizes peripheral clocks via neuronal and hormonal signals. As indicated, the phase of peripheral clocks is delayed by a few hours compared to the SCN clock. The SCN, however, is not required for the maintenance of peripheral clocks. It is also possible that light-dark cycles directly regulate clocks in the skin. Additionally, other external inputs such as feeding and temperature entrain peripheral clocks, including in the skin.

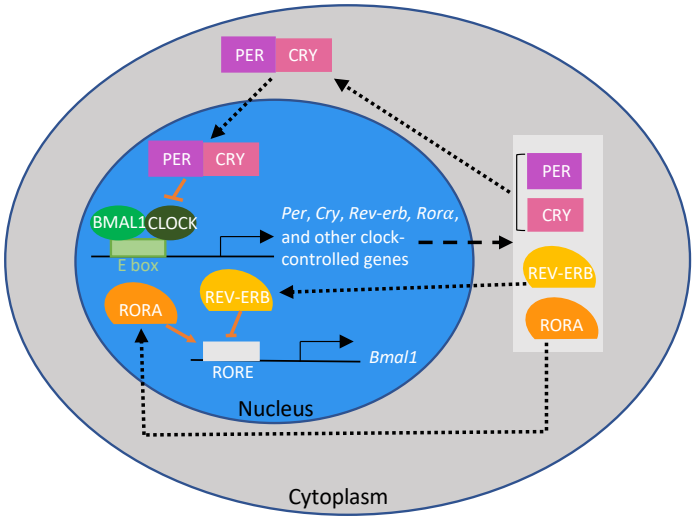

Figure 1.3: **A transcription-translation feedback loop generates circadian rhythms.** The core clock has a positive arm, consisting of BMAL1 and CLOCK, and a negative arm, consisting of PER and CRY, which inhibits the BMAL1-CLOCK heterodimer. RORs, REV-ERBS forms a secondary feedback loop to reinforce the oscillatory expression of *Bmal1*. The clock network directly and indirectly regulates the expression of about 10-20% of genes in each peripheral tissue.

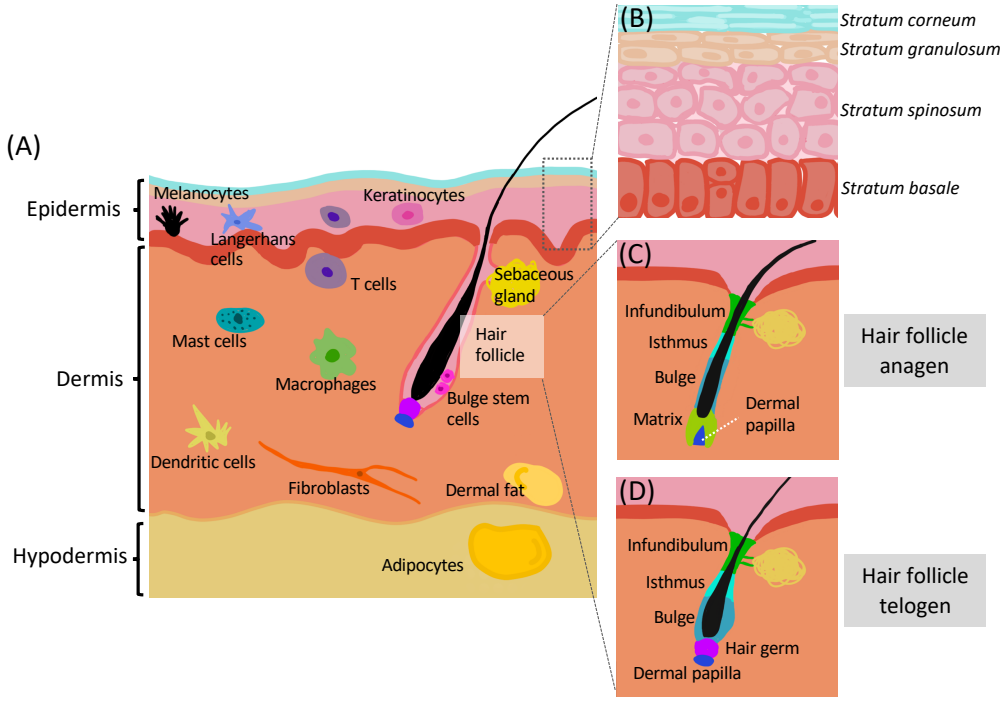

Figure 1.4: **The skin is a multi-layer, compartmentalized organ.** (A) There are three main layers in the skin: epidermis, dermis and hypodermis. Each layer contains multiple cell types. (B) The interfollicular epidermis contains mostly keratinocytes organized into four layers based on differentiation status. The epidermal stem cells reside in the *stratum basale*. (C) The anagen hair follicle. The matrix contains proliferating keratinocytes derived from the secondary hair germ, giving rise to the hair shaft. (D) The telogen hair follicle. The hair follicle bulge contains the slow cycling stem cells. The hair germ contains the progenitor cells for the hair. The dermal papilla is a mesenchymal structure that signals to the hair germ and stem cells.

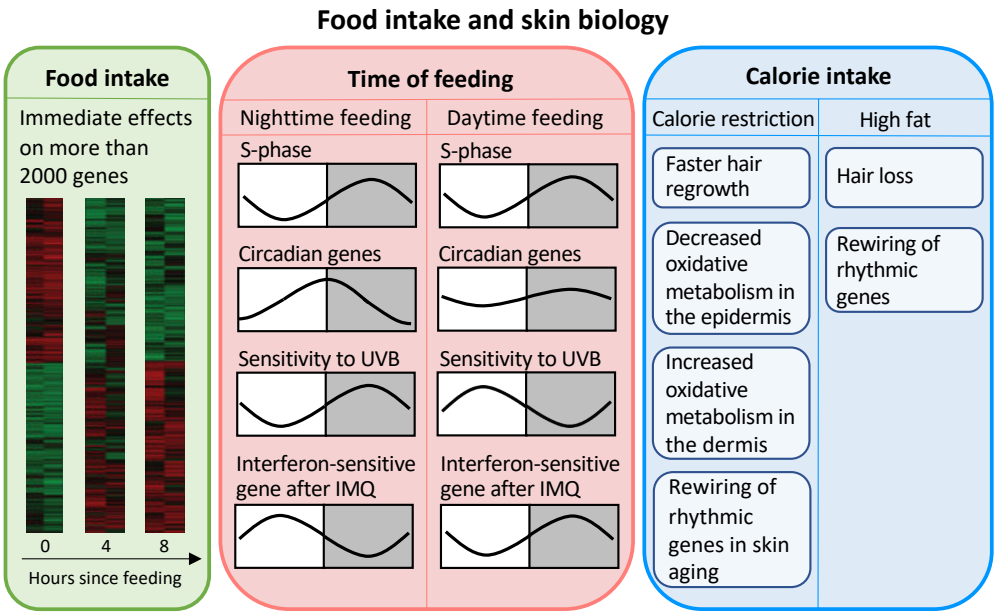

Figure 1.5: **Food intake regulates skin functions.** Left: Food intake immediately changes the expression of more than 2000 genes in the skin. Heat maps show gene expression before, four hours, and eight hours after food intake. Middle: Time of feeding does not affect the diurnal pattern of cell proliferation in the skin. However, daytime feeding shifts and dampens the expression of circadian genes. Daytime feeding also changes the diurnal variation in sensitivity to UVB-induced DNA damage and the IMQ-induced interferon response. Right: Calorie restriction and high fat diet affect metabolism and expression of rhythmic genes, hair follicle stem cell function, and skin aging. IMQ, imiquimod.

Chapter 2

tauFisher predicts circadian time from a single sample of bulk and single-cell pseudobulk transcriptomic data

J. Duan, M. N. Ngo, S. S. Karri, L. C. Tsoi, J. E. Gudjonsson, B. Shahbaba, J. Lowengrub, and B. Andersen. taufisher predicts circadian time from a single sample of bulk and single-cell pseudobulk transcriptomic data. *Nature Communications*, 15(1), May 2024

2.1 Introduction

Organisms have evolved intrinsic circadian clocks that help them anticipate and adjust to environmental changes caused by the 24-hour rotation of the Earth [15, 38]. The mammalian circadian clock is a biochemical oscillator powered by transcription-translation loops consisting of a positive arm and a negative arm [15, 38, 180]. In the positive arm, BMAL1 and CLOCK promote the expression of clock-controlled genes, including the negative arm factors

PER and CRY. PER and CRY inhibit the activating effect of BMAL1-CLOCK, leading to 24-hour oscillations.

In mammals, the suprachiasmatic nucleus (SCN) of the hypothalamus is the central pacemaker that coordinates and synchronizes circadian rhythms in peripheral tissues through neuronal and hormonal signals [31]. Besides signals from the SCN, environmental signals such as temperature [31], feeding [134, 195], and direct light [30] can selectively set peripheral clocks, sometimes causing asynchrony between the central and peripheral clocks. Epidemiological studies of shift workers and chronically jet-lagged individuals show correlations between circadian disruption and cardiovascular diseases [127], mental health disorders [194], metabolic diseases [99, 142, 191], as well as cancer in various organs [119, 165], including skin [76, 212], breast [161, 77], and prostate [52, 200].

The goal of the nascent field of circadian medicine is to consider circadian rhythm and its disruption in patient care. As the rhythm of a patient or diseased tissue is not necessarily synchronized with the external light-dark cycle, an important challenge in circadian medicine is to determine the internal circadian time of the patient or the tissue of focus. Such information can determine optimal time of treatment and identify conditions that might benefit from restoring circadian functions [177, 55]. Current methods of circadian time determination for a patient include the dim-light melatonin-onset assay [95], as well as circadian rhythm inference from body temperature [146], or cortisol levels in biofluids [188].

Additionally, determining the circadian time of a sample is important for research. With the explosion of bulk and single-cell transcriptomics datasets, there is growing effort to integrate and compare such datasets. As about 10% of the transcriptome has diurnal expression patterns, analyzing such datasets without their timestamps may lead to inconsistent observations that are dependent on the time of sample collection. Hence, there is a need to develop method that can determine the circadian time of such datasets.

Several groups have developed methods to infer circadian time of a sample (organism, organ, or tissue) based on transcriptomic data. CYCLOPS [9, 208] uses an autoencoder neural network to infer circadian phases by ordering the data collected from the entire periodic cycle. ZeitZeiger [89] identifies useful features (genes) for prediction, scales the feature expression over time, applies sparse principal component analysis, and predicts according to maximum likelihood estimation. BIO_CLOCK [2] uses supervised deep neural networks with coupled sine and cosine output units. TimeSignatR [27] applies within-subject renormalization and an elastic net predictor, making it generalizable between transcriptomic data from different assay platforms. More recently, a Bayesian variational inference approach called Tempo [14] was designed to predict circadian phase in single cell transcriptomics and it quantifies estimation uncertainty.

Among the methods mentioned above, CYCLOPS, ZeitZeiger, BIO_CLOCK and TimeSignatR can infer circadian time from bulk transcriptomic data and are generalizable for different tissues. But, they have limitations. CYCLOPS outputs the relative ordering, instead of timestamps, of samples, and requires reconstruction to incorporate every new sample as it does not require prior training data. ZeitZeiger frequently runs into linear dependency issues, needs to be retrained before each prediction, and is not generalizable between transcriptomic platforms. BIO_CLOCK does not require re-training for each prediction but is not time-efficient. TimeSignatR performs well if there are two test samples and it achieves its best performance when the two samples are 12 hours apart.

Here, we present tauFisher, a pipeline that can accurately predict circadian time from a single transcriptomic data irrespective of the assay platform. tauFisher improves on previous methods in several ways: (1) it does not require the training data to be a complete time series; (2) the within-sample normalization step allows tauFisher to give an accurate prediction from just one sample; (3) since tauFisher only needs a few features to make accurate predictions, training and testing are computationally efficient; (4) tauFisher is platform agnostic and users

only need to train the predictor once and can use the same predictor to make predictions for external datasets of the same tissue, regardless of the platform; and (5) tauFisher trained on bulk sequencing data is able to accurately predict the circadian time of single-cell RNA sequencing (scRNAseq) pseudobulk data, and it can be used to investigate circadian phase heterogeneity in different cell types.

2.2 Results

2.2.1 Overview of tauFisher

tauFisher is an assay platform-agnostic method that predicts circadian time from a single transcriptomic sample. The training part of the pipeline, which requires a time series of transcriptomic data, consists of five main steps: (1) identifying diurnal genes with a period length of 24 hours, (2) curve fitting using functional data analysis to fill in the missing time points and to decrease noise in the training data, (3) within-sample normalization by calculating and scaling the difference in expression for each pair of predictor genes, (4) linearly transforming the scaled differences using principal component analysis, and (5) fitting a multinomial regression on the first two principal components (Figure 2.1, Methods).

For testing, a transcriptomic sample without a time label is trimmed to include only the predictor genes identified in the training data. After the within-sample normalization step, the test sample is projected to the principal component space and multinomial regression is performed to predict time of the test sample (Figure 2.1, Methods).

2.2.2 tauFisher achieves high accuracy when trained and tested on bulk-level transcriptomic data.

To assess the robustness and accuracy of tauFisher in predicting circadian time from a single sample of transcriptomic data, we applied tauFisher to a diverse set of data collected from different species, tissues and assay platforms (Table 2.1).

For each benchmark dataset, we generated 100 random train and test partitions (without replacement) of the samples. In each partition, we used 80% of the samples for training and 20% for testing. We compared tauFisher to the current state-of-the-art methods: ZeitZeiger [89] and TimeSignatR. [27].

We define a prediction within two hours of the true time to be correct. Using other time ranges to define correctness minimally change the benchmark outcome (Table 2.2).

For eleven out of the twelve benchmarking datasets, tauFisher achieved higher accuracy when using predictor genes found by JTK_Cycle [88] instead of Lomb-Scargle [74]. For six out of the ten transcriptomic datasets collected from mice, tauFisher achieved equal or higher 2-hour accuracy using one test sample than TimeSignatR using two test samples that are 12 hours apart. tauFisher achieved lower but comparable accuracy (difference $< 10\%$) when compared to TimeSignatR in two of the remaining four mouse datasets. For the two human blood datasets, TimeSignatR using two test samples outperformed ZeitZeiger and tauFisher, highlighting the importance and effectiveness of using two test samples to address human variability in circadian phase predictions (Figure 2.2, Table 2.3). ZeitZeiger could not predict the time for several iterations due to linearly dependent basis vectors. Interestingly, whether ZeitZeiger ran into linear dependency issues appeared to be depended on the assay methods, as it ran successfully for most of the microarray data but failed to predict the time for all 100 iterations in the bulk RNAseq datasets collected from mouse kidney, liver, brainstem, and cerebellum (Figure 2.2, Table 2.1).

2.2.3 tauFisher accurately predicts circadian time for cross-platform bulk transcriptomic data.

Since tauFisher gives accurate circadian time prediction for bulk transcriptomic data collected from various platforms, we examined its performance when trained and tested on datasets generated from different platforms. We used rhythmic genes identified by JTK_Cycle in the tauFisher pipeline, since they gave more accurate predictions in the within-platform benchmark.

We trained tauFisher on GSE38622 [72], a microarray dataset collected from mouse dorsal skin every four hours for 48 hours under regular 12:12 light-dark cycle (zeitgeber time [ZT] 2, 6, 10, ...). The test dataset is from GSE83855 [195], a bulk RNAseq dataset collected every four hours for 28 hours under 12:12 light-dark cycle (ZT0, 4, 8, ...) from mouse dorsal skin in a time-restricted feeding study. Since time of feeding influences tissue's circadian clock [195, 55], we only selected the ad libidum control condition for this testing so that the time labels best represent the internal time.

Eighteen genes were selected to be predictor features. Though the training and test datasets are not on the same scale and were collected at different time points, their overall rhythmic patterns agree with each other (Figure 2.3a). For six of the eight tests, tauFisher predicted a circadian time that is within the 2-hour range from the actual time label, giving an accuracy of 0.75 and a RMSE of 4.704 (Figure 2.3b, 2.5b). This example demonstrates tauFisher's ability to predict circadian time across bulk transcriptomics platforms.

After validating tauFisher's performance on cross-platform, bulk-level, transcriptomic datasets collected from healthy/control mouse skin, we also tested it in disturbed systems. In the test groups of the time-restricted feeding study, food was only available to mice from ZT5 to ZT9 or ZT0 to ZT4, whereas mice usually feed during early nights (ZT12-ZT16) [195]. Skin collected from these two time-restricted feeding schedules showed disturbed circadian

patterns with greatly attenuated amplitude and altered peaking times that are not directly correlated with the feeding times [195]. As the system is disturbed, the sample collection time no longer represents the internal circadian time of the tissue as it does in healthy tissue (training data). Consistent with the biological observations, tauFisher trained on control skin microarray data predicted time labels that are away from the test sample collection time, reflecting a disturbed system, and the predictions are not coupled with time-restricted feeding schedules (Figure 2.4a). tauFisher's prediction when trained on control/healthy samples, however, can only tell whether the test system is disturbed or not, and does not provide a measurement of how much the system is disturbed.

We also trained the tested tauFisher within the disturbed systems. Within each of the two time-restricted feeding schedules, we performed leave-one-out cross validation by reserving each sample for testing and using the remaining samples for training. tauFisher produced high accuracy (feeding ZT5-ZT9: accuracy = 0.875; feeding ZT0-ZT4: accuracy = 1) and low RMSE (feeding ZT5-ZT9: RMSE = 2.236; feeding ZT0-ZT4: RMSE = 1.061) for both disturbed systems (Figure 2.4b). The fact that tauFisher trained on samples collected from a disturbed system can add time labels to samples from the same disturbed system suggests that robust correlations between diurnal genes still exist in the disturbed system, and such relationships are different from the ones in the control/healthy individuals.

2.2.4 tauFisher trained on bulk RNAseq data accurately predicts circadian time of scRNAseq samples.

tauFisher's ability to predict circadian time is not limited to cross-platform bulk-level transcriptomic datasets. It can add circadian timestamps to scRNAseq samples as well. In particular, tauFisher only needs to be trained on a time series of bulk-level transcriptomic data, which is more abundant and cheaper to collect than a scRNAseq data time series.

Since most published scRNAseq datasets do not have time labels, the selection of datasets for testing was limited. Here we tested tauFisher on scRNAseq data collected from the mouse SCN [199].

GSE117295 [199] includes twelve single-cell SCN samples collected from circadian time (CT) 14 to 58 every four hours (CT14, 18, 22, ...) under constant darkness, and one light-stimulated SCN sample. Since light immediately induces differential expression of rhythmic genes [199], only the samples from the control experiment were used for the benchmark. For each of the twelve samples, a pseudobulk dataset was generated for testing (Methods). For training, we chose GSE157077 [187], a time series of bulk RNAseq data collected from the mouse SCN every four hours under regular 12:12 light-dark cycle starting at ZT0. Since each time point in the training dataset contains three replicates, instead of averaging them, we concatenated the replicates so that the input training data spans 72 hours.

Twenty genes from the training data passed the feature selection criteria. These genes display robust rhythms in both the training data and the test pseudobulk data (Figure 2.3c). The raw input test data appeared to be noisier as it was not normalized by the total number of reads in each sample. tauFisher does not require the data to be preprocessed before input into the pipeline, as within-sample normalization is an intermediary step.

In ten out of the twelve tests, tauFisher predicted a time that is within 2-hour of the labeled time, resulting a high accuracy of 0.833 and a low RMSE of 1.936 (Figure 2.3d, 2.5a). Although neither TimeSignatR nor ZeitZeiger claims to be able to add time labels to scRNAseq data, we still tested their performance. tauFisher outperformed TimeSignatR and ZeitZeiger in both accuracy and RMSE (Figure 2.3d,e).

In sum, we have demonstrated that tauFisher trained on bulk-level transcriptomic data-can accurately predict circadian time for scRNAseq data, making it particularly useful for expanding the current scRNAseq database for circadian studies by adding time labels to

existing scRNAseq data.

2.3 Discussion

In this study, we developed tauFisher, a computational pipeline that accurately predicts circadian time from a single transcriptomic dataset and is applicable to within-platform and cross-platform training-testing scenarios. Particularly, tauFisher trained on bulk transcriptomic data accurately add circadian timestamps for scRNAseq samples. This method allows investigators to place circadian timestamps on transcriptomic datasets and facilitates the determination of circadian time in the context of circadian medicine.

Most transcriptomic datasets in public genomics repositories lack circadian time labels, which complicates integration with or comparison to other datasets. Adding time labels for existing transcriptomic datasets is important, as the clock modulates the expression of many protein-coding genes; it is necessary to know whether a significant gene is truly differentially regulated by a condition or the expression appears to be different because the samples were collected at different times. Also, computationally adding circadian timestamps to existing transcriptomic datasets collected from various platforms, including from scRNAseq, opens up new possibilities for circadian research and allows investigators to take the full advantage of the shared resource in an efficient and inexpensive way.

Circadian time determination is also a key step in the implementation of circadian medicine. To maximize effectiveness while minimizing side effects of treatments, it is necessary to take into consideration the patient's and relevant tissue's actual circadian time. For example, on-pump cardiac surgeries in the afternoon are less likely to cause perioperative myocardial injury than when conducted in the morning [124] and cancer radiation therapy in the morning causes less skin damage than in the afternoon [167].

There have been several predictors of circadian time based on transcriptomic data [27, 89, 2], but to ensure wide applicability of this approach, an assay platform-agnostic method requiring low number of test samples is desired. tauFisher is preferable as it can accurately determine circadian time from a single sample of transcriptomic data collected from various assay methods including scRNAseq.

Once trained, tauFisher requires a single transcriptomic sample to predict the circadian time. We examined tauFisher's ability to predict circadian time when the training and test data are from the same study, and we benchmarked it against state-of-the-art methods ZeitZeiger [89] and TimeSignatR [27]. tauFisher using one test sample achieved similar accuracy and RMSE for most of the datasets when compared to TimeSignatR that required two test samples that are 12 hours apart. ZeitZeiger failed to run for several of the datasets due to linear dependency issues, and its success was dependent on assay platform (Figure 2.2, Table 2.3). When it did run, ZeitZeiger achieved similar accuracy and RMSE as tauFisher, possibly because both predictors build on principal component analysis, suggesting that the molecular clock is well captured and represented by orthogonal linear combinations of predictor genes.

One of the most powerful features of tauFisher is its ability to accurately predict circadian time when trained and tested on datasets collected from different assay platforms under different experimental settings. tauFisher achieves high accuracy and low RMSE in not only bulk-to-bulk cross-platform predictions, but also bulk-to-scRNAseq predictions. While it is usually assumed that bulk RNAseq data are consistent with pseudobulk data calculated from scRNAseq data, it is necessary to verify this assumption in circadian studies. The experimental settings for bulk and single cell RNA extraction are different in terms of digestion duration and temperature, a factor that can alter the clock [31]. tauFisher's successful bulk-to-pseudobulk predictions assure such consistency. tauFisher outperformed ZeitZeiger and the two-sample TimeSignatR method, and the robustness in performance despite dras-

tically different assay methods and experimental setups suggests that tauFisher captures and extracts the underlying biological correlations in gene expressions while minimizing the effects of the noise and variability introduced by subjects and technology.

Two key steps in tauFisher help achieve this: functional data analysis for training data and within-sample normalization for both training and test data. Functional data analysis for the training data enables tauFisher to remove minor noise, smooth the time expression curves, and generate the expression data between the sampled time points. The within-sample normalization step for both training and test data calculates the difference between each pair of predictor genes at a given time point so that the feature matrix is expanded while some baseline noise is removed. The differences between the genes are then re-scaled to be between 0 and 1 so that the data become unit-less. Doing so in parallel on the training and test datasets brings them individually to the same scale, instead of batch-correcting the train to the scale of the test or the opposite. This allows testing of independent datasets without re-training. We note that this within-sample normalization is different from the within-subject normalization in TimeSignatR[27], which is based on mean expression calculated from multiple samples collected from more than one time point over the circadian cycle.

Despite its unique circadian time prediction ability, tauFisher can be improved in several ways. While tauFisher performs well in terms of both accuracy and RMSE in almost all mouse benchmark datasets, its performance on human blood samples is subpar. Such performance can be attributed to greater human variability in expression patterns of the clock caused by hormones, stress, living style and diet. A recently proposed pipeline called TimeMachine attempted to infer circadian phase from a single human blood sample and reported 2-hour accuracy of 40$\sim$55% [87]. On the other hand, TimeSignatR using two human blood samples 12 hours apart achieved $\sim$ 73% 2-hour accuracy (Figure 2), emphasizing the necessity to address individual variability when predicting circadian phases for human samples and the effectiveness of the two-sample within-subject normalization step. One assump-

tion of tauFisher's within-sample normalization step is that the differences between predictor genes are solely dependent on circadian time, and this step only removes uniform elevation or depression in expression values of clock genes. To further improve tauFisher's flexibility and performance on human data, it is worthwhile to incorporate a within-sample data centering step to address the differences caused by individual variability, while making sure that only one test sample is needed to make a prediction. Additionally, using tauFisher trained on healthy/control data to predict a time for data collected from a circadian-disturbed system only maps the disturbed test onto the timescale of the healthy samples. If one prefers to project a test data onto the timescale of the diseased samples, a time series of transcriptomic data from diseased individuals is required. However, the circadian pattern is dampened in many diseases including cancer [209, 175, 45, 100, 86, 90], making the expression data similar overtime and thus more difficult to distinguish the time points. Although tauFisher showed promise in feeding-disturbed systems in skin (Figure 2.4b), it would be valuable to further validate tauFisher on such datasets as they become available in future studies. Additionally, since uncertainty quantification may be particularly important when testing in disturbed systems, tauFisher can be improved to output confidence scores. Finally, while tauFisher accurately adds timestamps to unlabeled scRNAseq data and can predict circadian time for pseudobulk data generated from a group of cells in scRNAseq data, it cannot overcome the high sequencing dropout rate in scRNAseq and thus cannot predict circadian time at a single cell level. Future work could focus on incorporating an imputation step into tauFisher to infer expression values of predictor genes. This step may not sacrifice computation and time efficiency greatly, as tauFisher only need around 15 genes to make predictions.

In summary, tauFisher's consistent and robust performance in accurately predicting circadian time from a single transcriptomic data makes it a useful addition to the toolbox of circadian medicine and research.

2.4 Methods

2.4.1 tauFisher

tauFisher is a platform-agnostic method that predicts circadian time from a single transcriptomic sample. The method consists of three main steps: (1) identifying a subset of diurnal genes with a period length of 24 hours, (2) calculating and scaling the difference in expression for each pair of predictor genes, and (3) linearly transforming the scaled differences using principal component analysis and fitting a multinomial logistic regression on the first two principal components.

Preprocessing the expression matrix

The first step in tauFisher is to average transcript measurements by genes such that the resulting matrix consists of unique genes. The subsequent training data consist of a gene expression matrix $X \in \mathbb{R}^{N \times P}$ with N unique genes and P samples, and a vector $\boldsymbol{\tau} \in \mathbb{R}^{P}$ of the corresponding time for each sample.

Identification of periodic genes

tauFisher specifies either the Lomb-Scargle [74] or JTK_Cycle [88] method in the `meta2d` function from the R package MetaCycle [206] to determine the periodic genes. It then selects the top ten statistically significant genes with a 24-hour period length. Using different numbers of diurnal genes does affect the prediction outcome. Although choosing the top ten does not guarantee the best performance, it is a safe and reasonable choice across different datasets (Figure 2.5c). These diurnal genes are then combined with the core clock genes that also have a period length of 24 hours to create the set of predictor genes M. The core

clock genes for consideration in tauFisher are: *Bmal1*, *Dbp*, *Nr1d1*, *Nr1d2*, *Per1*, *Per2*, *Per3*, *Cry1*, and *Cry2*.

Data transfromation

Subsetting the averaged expression matrix X on the set of predictor genes M yields averaged gene expression matrix $X' \in \mathbb{R}^{M \times P}$ with M periodic genes and P samples with known time ($\boldsymbol{\tau}$). The matrix X' is then log-transformed element-wise: $X' = \log_2(X' + 1)$.

Functional data analysis

Since experiments have different sampling intervals throughout a circadian cycle, tauFisher uses functional data analysis to represent the discrete time points as continuous functions. This allows tauFisher to evaluate and predict the circadian time of the new samples at any time point and reduces the noise from the training samples.

Briefly, each gene m has a log-transformed measurement at discrete time points $t_1, ..., t_P \in \boldsymbol{\tau}$ that may or may not be equally spaced. These discrete values are converted to a function Z_m with values $Z_m(t)$ for any time t using a Fourier basis expansion:

$$Z_m(t) \approx \sum_{k=1}^{K} c_{mk}\phi_k(t) \tag{2.1}$$

where $\phi_k(t)$ is the k-th basis function for $k = 1, ..., K$, and $\forall t \in \boldsymbol{\tau}$. c_{mk} is the corresponding coefficient. The Fourier basis is defined by $\phi_0(t) = 1$, $\phi_{2r-1}(t) = \sin(r\omega t)$, and $\phi_{2r}(t) = \cos(r\omega t)$ with the parameter ω determining the period $2\pi/\omega$. Since the log-transformed data matrix X' is non-negative, a positive constraint is imposed such that the positive smoothing function is defined as the exponential of an unconstrained function: $Y_m(t) = e^{Z_m(t)}$. The smoothing function also contains a roughness penalty to prevent overfitting. In practice,

tauFisher sets the number of basis functions to $K = 5$, as it produces curves that are the most sinusoidal. Users can specify a different number of basis functions.

Although functional data analysis represents the discrete time points as continuous functions for each gene, tauFisher predicts circadian time at a user-defined time interval. By default, the time intervals are set to be one hour. The fitted functions $Y_m(t)$ are evaluated at the user-defined time interval to create the smoothed expression matrix $Y \in \mathbb{R}^{M \times T}$, where T is the number of evaluated time points, and $\boldsymbol{\tau}_F \in \mathbb{R}^T$ is the new set of time points. If the time course of the samples spans less than 24 hours, then the fitted curves are evaluated hourly from $[0, 23]$ such that $T = 24$ to ensure all 24 hours are evaluated. If the time course duration of the samples spans greater than 24 hours, then fitted curves are evaluated from $[\min(\boldsymbol{\tau}), \max(\boldsymbol{\tau})]$ such that $T = \max(\boldsymbol{\tau}) - \min(\boldsymbol{\tau}) + 1$.

Calculating and scaling of the differences between each pair of genes

For each time point, tauFisher generates all possible pairings of the selected predictor genes. It then calculates the differences between the two genes' functional data analysis-smoothed expression (stored in matrix Y). The resulting matrix retains differences between Gene A and Gene B (Gene A - Gene B) as well as between Gene B and Gene A (Gene B - Gene A). Then within each time point, the differences calculated from the gene pairs are scaled to be between 0 and 1 using the `rescale` function in R package scales. This way, 0 represents the minimum difference value and 1 represents the maximum. The formula is (value - min)/(max-min). As examples, we provided the resulting matrices for the training data (Supplementary Data 5) and the test data (Supplementary Data 6) when tauFisher was trained on GSE38622 and tested on GSE83855.

The multinomial regression model

The differences matrix is projected onto a lower dimensional space via principal component analysis, and the first two principal components become covariates x_{i1} and x_{i2} for observation i in the multinomial regressor:

$$\log\left[\frac{P(\boldsymbol{\tau}_{Fi}=t|x_{i1},x_{i2})}{P(\boldsymbol{\tau}_{Fi}=0|x_{i1},x_{i2})}\right]=\beta_{t0}+\beta_{t1}x_{i1}+\beta_{t2}x_{i2} \tag{2.2}$$

All time points $t_1,...,t_T \in \boldsymbol{\tau}_F$ are converted to be $[0,23]$, since time 0 is equal to time 24. Time zero, $\boldsymbol{\tau}_F = 0$, is set as the reference level in the model. The fitted multinomial regression model is then used to predict the circadian time of the new samples. We note that since time can be ordinal (accounting for the order) or continuous between $[0,24)$, we also tried other models such as an ordinal regression. However, these models were not as robust as the multinomial regression model and failed to run on the entire set of time points.

2.4.2 Calculating prediction error

To evaluate the performance of tauFisher, we need to calculate how close the predicted time is to the true time. Since the outcome is cyclic and ranges from $[0,23]$, we applied the following conversion to calculate the true difference D from the difference d between the predicted time and true time:

$$D=\begin{cases} d-24, & \text{if } d>12 \\ d+24, & \text{if } d<-12 \end{cases} \tag{2.3}$$

2.4.3 Datasets and analysis

Preprocessing for benchmark

For GSE56931, we filtered out the time points related to the 38-hour continuous wakefulness and subsequent recovery sleep from the dataset provided in the TimeSignatR [27] package, to only include the 24-hour normal baseline time points. For GSE38622, expression matrix was normalized as described [72]. For GSE157077, we used the transcriptomes of the mice who were fed normal chow through an entire circadian cycle (24 hours). We concatenated the three replicates of 24 hours to create one set of samples over 72 hours. For GSE54650, the raw CEL files for the kidney and liver were imported using the function `read.celfiles` in R package oligo. Each raw data matrix was then normalized with Robust Multiarray Average (RMA) using the function `rma`. To map the GPL6246 platform ID_REF to Ensembl transcript IDs, we used the transcript cluster ID and gene assignments listed in the table provided at https://www.ncbi.nlm.nih.gov/geo/query/acc.cgi?acc=GPL6246. For each transcript cluster ID, we removed all gene assignments unless they were Ensembl transcript IDs or started with Gm. If a transcript cluster ID was mapped to more than one gene, then we replicated that row by the number of genes (e.g., transcript reference ID 10344614 is assigned to three Ensembl transcript IDs so that row in the normalized dataset was replicated three times). The expression for each transcript cluster ID was then divided by the number of genes assigned (e.g., since transcript reference ID 10344614 has three gene assignments, the values for all three rows in the normalized dataset were divided by three). Transcript cluster IDs that were not assigned to any genes were removed from the normalized dataset. To convert the Ensembl transcript IDs to gene names, we use R package biomaRt [59, 60]. If biomaRt did not find a gene name, then we kept the original Ensembl transcript ID. For GSE54651, we converted the Ensembl gene IDs to gene names using R package biomaRt [59, 60]. If biomaRt did not find a gene name, then we kept the original Ensembl gene ID.

For each time point in GSE117295 , we summed the counts of each gene in all the cells without any pre-processing to create a pseudobulk dataset. In the case where the same gene occurs multiple times in the data, we took the mean of those entries. The resulting pseudobulk data at each time point is a single row vector in which each entry represents the expression value of a unique gene. The light-stimulated group is not considered in this paper.

2.5 Data Availability

All published datasets used in this paper can be accessed through their respective GEO accession codes. The time series of microarray data collected from mouse kidney, liver, brainstem and cerebellum are available under GSE54650 [220]. The time series of bulk RNAseq data collected from mouse kidney, liver, brainstem and cerebellum are available under GSE54651 [220]. The time series of microarray data collected from mouse skin are available under GSE38622 [72]. The time series of bulk RNAseq data from mouse SCN are available under GSE157077 [187]. The time series of scRNAseq data from mouse SCN are available under GSE117295 [199]. The bulk RNAseq data collected from mouse skin in control and time-restricted feeding conditions are available under GSE83855 [195]. Although the datasets in [12] and [27] are both accessible through their GEO accession codes GSE56931 and GSE113883 respectively, this paper used the versions provided in the TimeSignatR package [27]: `https://github.com/braunr/TimeSignatR`.

2.6 Code Availability

tauFisher is available as an R package at https://github.com/micnngo/tauFisher [129]. The two methods we compared tauFisher against are also available as R packages: TimeSig-

natR at `https://github.com/braunr/TimeSignatR` and ZeitZeiger at `https://github.com/hugheylab/zeitzeiger`.

2.7 Acknowledgements

This project is supported by an award entitled "Skin Biology Resource-Based Center at UCI - Systems Biology Core" from the Center of Complex Biological Systems funded by NIH/-NIAMS P30-AR075047 (J.D. and M.N.); National Institute of Health grants R01AR056439 and P30AR075047 (B.A.); NSF grant DMS1763272 and a grant from the Simons Foundation (594598) (J.D., M.N., J.L. and B.A.); National Institute of General Medical Sciences, National Research Service Award GM136624 (J.D.); NSF grant DMS1936833 (M.N. and B.S.); the California Institute for Regenerative Medicine Training Program Award EDUC4-12822 (S.S.K.); and Chan Zuckerberg Initiative grant DAF2022-239946 (B.A., J.G., and L.C.T.).

Data	Year	GEO	Species	Tissue	Platform	Sampling Frequency	Time Course Duration
Zhang R *et al.* [220]	2014	GSE54650	*Mus musculus*	Kidney	Affymetrix Mouse Gene 1.0 ST Array	2h	48h
Zhang R *et al.* [220]	2014	GSE54650	*Mus musculus*	Liver	Affymetrix Mouse Gene 1.0 ST Array	2h	48h
Zhang R *et al.* [220]	2014	GSE54650	*Mus musculus*	Brainstem	Affymetrix Mouse Gene 1.0 ST Array	2h	48h
Zhang R *et al.* [220]	2014	GSE54650	*Mus musculus*	Cerebellum	Affymetrix Mouse Gene 1.0 ST Array	2h	48h
Zhang R *et al.* [220]	2014	GSE54651	*Mus musculus*	Kidney	Illumina HiSeq 2000	6h	48h
Zhang R *et al.* [220]	2014	GSE54651	*Mus musculus*	Liver	Illumina HiSeq 2000	6h	48h
Zhang R *et al.* [220]	2014	GSE54651	*Mus musculus*	Brainstem	Illumina HiSeq 2000	6h	48h
Zhang R *et al.* [220]	2014	GSE54651	*Mus musculus*	Cerebellum	Illumina HiSeq 2000	6h	48h
Arnardottir ES *et al.* [12]	2014	GSE56931	*Homo sapiens*	Blood	Custom Affymetrix Microarray	4h	72h
Braun R *et al.* [27]	2018	GSE113883	*Homo sapiens*	Blood	Illumina NextSeq 500	2h	28h
Geyfman M *et al.* [72]	2012	GSE38622	*Mus musculus*	Skin	Affymetrix Mouse Gene 1.0 ST Array	4h	48h
Tognini P *et al.* [187]	2020	GSE157077	*Mus musculus*	SCN	Illumina HiSeq 4000	4h	24h

Table 2.1: Datasets from different species, tissues and assay platforms were used to benchmark tauFisher's ability to predict circadian time.

Data	Metric	ZeitZeiger	TimeSignatR w/ 2-sample	tauFisher w/ Lomb-Scargle	tauFisher w/ JTK_Cycle
[220][2,4]	Accuracy (within 3 hr)	0.996 ± 0.028	**1.000 ± 0.000**	0.996 ± 0.028	**1.000 ± 0.000**
	Accuracy (within 2 hr)	0.986 ± 0.051	**1.000 ± 0.000**	0.966 ± 0.086	**1.000 ± 0.000**
	Accuracy (within 1 hr)	0.728 ± 0.179	0.904 ± 0.154	0.880 ± 0.158	**0.916 ± 0.128**
	Accuracy (exact)	0.004 ± 0.028	0.000 ± 0.000	**0.370 ± 0.219**	0.358 ± 0.209
[220][1,2,5]	Accuracy (within 3 hr)	NA	0.875 ± 0.279	0.720 ± 0.416	**0.945 ± 0.200**
	Accuracy (within 2 hr)	NA	0.620 ± 0.409	0.695 ± 0.414	**0.945 ± 0.200**
	Accuracy (within 1 hr)	NA	0.195 ± 0.333	0.565 ± 0.453	**0.815 ± 0.346**
	Accuracy (exact)	NA	0.000 ± 0.000	0.250 ± 0.314	**0.375 ± 0.344**
[220][3,4]	Accuracy (within 3 hr)	0.964 ± 0.100	**1.000 ± 0.000**	0.936 ± 0.133	0.986 ± 0.059
	Accuracy (within 2 hr)	0.868 ± 0.156	**0.988 ± 0.048**	0.880 ± 0.161	0.932 ± 0.103
	Accuracy (within 1 hr)	0.626 ± 0.225	0.844 ± 0.172	0.764 ± 0.196	**0.850 ± 0.162**
	Accuracy (exact)	0.002 ± 0.020	0.000 ± 0.000	**0.312 ± 0.189**	0.308 ± 0.219
[220][1,3,5]	Accuracy (within 3 hr)	NA	0.840 ± 0.340	0.840 ± 0.332	**0.970 ± 0.171**
	Accuracy (within 2 hr)	NA	0.565 ± 0.406	0.765 ± 0.344	**0.910 ± 0.269**
	Accuracy (within 1 hr)	NA	0.275 ± 0.385	0.585 ± 0.427	**0.735 ± 0.313**
	Accuracy (exact)	NA	0.000 ± 0.000	0.155 ± 0.263	**0.335 ± 0.326**
[220][6,4]	Accuracy (within 3 hr)	0.984 ± 0.061	**1.000 ± 0.000**	0.834 ± 0.166	0.922 ± 0.130
	Accuracy (within 2 hr)	0.924 ± 0.130	**0.998 ± 0.020**	0.790 ± 0.183	0.896 ± 0.141
	Accuracy (within 1 hr)	0.558 ± 0.219	**0.872 ± 0.152**	0.612 ± 0.218	0.682 ± 0.211
	Accuracy (exact)	0.002 ± 0.020	0.000 ± 0.000	0.240 ± 0.203	**0.242 ± 0.191**
[220][5,6]	Accuracy (within 3 hr)	NA	0.525 ± 0.457	0.420 ± 0.323	**0.595 ± 0.360**
	Accuracy (within 2 hr)	NA	0.280 ± 0.410	0.365 ± 0.347	**0.565 ± 0.353**
	Accuracy (within 1 hr)	NA	0.140 ± 0.257	0.300 ± 0.284	**0.410 ± 0.358**
	Accuracy (exact)	NA	0.000 ± 0.000	0.110 ± 0.208	**0.115 ± 0.211**
[220][4,7]	Accuracy (within 3 hr)	0.932 ± 0.121	**1.000 ± 0.000**	0.824 ± 0.183	0.904 ± 0.146
	Accuracy (within 2 hr)	0.786 ± 0.200	**0.990 ± 0.044**	0.760 ± 0.201	0.842 ± 0.166
	Accuracy (within 1 hr)	0.504 ± 0.226	**0.794 ± 0.192**	0.566 ± 0.222	0.608 ± 0.224
	Accuracy (exact)	0.004 ± 0.028	0.000 ± 0.000	**0.266 ± 0.182**	0.246 ± 0.203
[220][5,7]	Accuracy (within 3 hr)	NA	0.570 ± 0.444	0.360 ± 0.302	**0.810 ± 0.316**
	Accuracy (within 2 hr)	NA	0.305 ± 0.340	0.300 ± 0.293	**0.660 ± 0.382**
	Accuracy (within 1 hr)	NA	0.185 ± 0.272	0.185 ± 0.243	**0.430 ± 0.302**
	Accuracy (exact)	NA	0.000 ± 0.000	0.03 ± 0.119	**0.15 ± 0.241**
[12][4]	Accuracy (within 3 hr)	0.548 ± 0.105	**0.869 ± 0.095**	0.567 ± 0.132	0.563 ± 0.117
	Accuracy (within 2 hr)	0.400 ± 0.108	**0.720 ± 0.135**	0.414 ± 0.123	0.471 ± 0.126
	Accuracy (within 1 hr)	0.218 ± 0.097	**0.428 ± 0.142**	0.254 ± 0.108	0.299 ± 0.103
	Accuracy (exact)	0.006 ± 0.023	0.000 ± 0.000	0.086 ± 0.087	**0.103 ± 0.067**
[27][5]	Accuracy (within 3 hr)	0.601 ± 0.105	**0.914 ± 0.061**	0.407 ± 0.083	0.462 ± 0.114
	Accuracy (within 2 hr)	0.446 ± 0.111	**0.750 ± 0.095**	0.306 ± 0.074	0.370 ± 0.104
	Accuracy (within 1 hr)	0.213 ± 0.091	**0.452 ± 0.089**	0.197 ± 0.072	0.235 ± 0.082
	Accuracy (exact)	0.000 ± 0.000	0.000 ± 0.000	0.063 ± 0.033	**0.078 ± 0.045**
[72][4]	Accuracy (within 3 hr)	0.563 ± 0.350	**0.867 ± 0.171**	0.783 ± 0.248	0.750 ± 0.286
	Accuracy (within 2 hr)	0.460 ± 0.344	0.690 ± 0.269	**0.740 ± 0.258**	0.670 ± 0.330
	Accuracy (within 1 hr)	0.307 ± 0.275	0.427 ± 0.289	**0.590 ± 0.280**	0.543 ± 0.295
	Accuracy (exact)	0.010 ± 0.057	0.000 ± 0.000	**0.257 ± 0.263**	0.227 ± 0.241
[187][5]	Accuracy (within 3 hr)	0.108 ± 0.298	**0.932 ± 0.181**	0.610 ± 0.237	0.705 ± 0.237
	Accuracy (within 2 hr)	0.075 ± 0.218	**0.818 ± 0.251**	0.545 ± 0.239	0.635 ± 0.237
	Accuracy (within 1 hr)	0.040 ± 0.150	**0.542 ± 0.256**	0.412 ± 0.257	0.468 ± 0.253
	Accuracy (exact)	0.000 ± 0.000	0.000 ± 0.000	**0.190 ± 0.195**	0.182 ± 0.181

Table 2.2: **tauFisher performs well when different definitions of accuracy is used.** Benchmark results (mean ± standard deviation) when we used 80% of the data set for training and the remaining 20% for testing. Accuracy was calculated when different definitions of correctness were used. When a pipeline failed to predict for part of the 100 iterations, accuracy for the failed iteration is set to 0. [1] If ZeitZeiger [89] was unable to do a 3-fold cross validation, we ran ZeitZeiger without any cross validation and set `sumabsv` = 1 and `nSpc` = 3; [2] kidney; [3] liver; [4] microarray; [5] bulk RNAseq; [6] brainstem; [7] cerebellum.

Table 2.3: **tauFisher accurately adds time stamps to bulk transcriptomic data collected from various organs.** Benchmark results (mean ± standard deviation) when we use 80% of the data set for training and the remaining 20% for testing. When a pipeline failed to predict for part of the 100 iterations, accuracy and RMSE for the failed iteration are set to 0 and 12 respectively. [1] If ZeitZeiger [89] was unable to do a 3-fold cross validation, we ran ZeitZeiger without any cross validation and set `sumabsv` = 1 and `nSpc` = 3; [2] kidney; [3] liver; [4] microarray; [5] bulk RNAseq; [6] brainstem; [7] cerebellum.

Data	Metric	ZeitZeiger	TimeSignatR	tauFisher	
			w/ 2-sample	w/ Lomb-Scargle	w/ JTK_Cycle
[220][2,4]	Accuracy	0.986 ± 0.051	**1.000 ± 0.000**	0.966 ± 0.086	**1.000 ± 0.000**
	RMSE	0.849 ± 0.244	**0.568 ± 0.195**	1.021 ± 0.406	0.911 ± 0.256
	# NA	0	0	0	0
[220][1,2,5]	Accuracy	`NA`	0.620 ± 0.409	0.695 ± 0.414	**0.945 ± 0.200**
	RMSE	`NA`	2.035 ± 1.766	2.965 ± 3.117	**1.076 ± 0.981**
	# NA	100	0	0	0
[220][3,4]	Accuracy	0.868 ± 0.156	**0.988 ± 0.048**	0.880 ± 0.161	0.932 ± 0.103
	RMSE	1.391 ± 1.124	**0.689 ± 0.240**	1.797 ± 1.479	1.182 ± 0.451
	# NA	0	0	0	0
[220][1,3,5]	Accuracy	`NA`	0.565 ± 0.406	0.765 ± 0.344	**0.910 ± 0.269**
	RMSE	`NA`	2.262 ± 1.836	2.269 ± 2.356	**1.203 ± 0.825**
	# NA	100	0	0	0
[220][4,6]	Accuracy	0.924 ± 0.130	**0.998 ± 0.020**	0.790 ± 0.183	0.896 ± 0.141
	RMSE	1.148 ± 0.450	**0.633 ± 0.248**	2.603 ± 1.540	1.709 ± 0.994
	# NA	0	0	0	0
[220][5,6]	Accuracy	`NA`	0.280 ± 0.410	0.365 ± 0.347	**0.565 ± 0.353**
	RMSE	`NA`	3.586 ± 2.588	5.763 ± 2.645	**3.468 ± 1.882**
	# NA	100	0	0	0
[220][4,7]	Accuracy	0.786 ± 0.200	**0.990 ± 0.044**	0.760 ± 0.201	0.842 ± 0.166
	RMSE	1.526 ± 0.653	**0.751 ± 0.253**	2.683 ± 1.623	2.063 ± 1.262
	# NA	0	0	0	0
[220][5,7]	Accuracy	`NA`	0.305 ± 0.340	0.300 ± 0.293	**0.660 ± 0.382**
	RMSE	`NA`	3.255 ± 1.913	5.921 ± 2.656	**2.386 ± 1.405**
	# NA	100	0	0	0
[12][4]	Accuracy	0.400 ± 0.108	**0.720 ± 0.135**	0.414 ± 0.123	0.471 ± 0.126
	RMSE	4.609 ± 0.802	**2.598 ± 1.220**	4.998 ± 0.848	5.087 ± 0.845
	# NA	0	0	0	0
[27][5]	Accuracy	0.446 ± 0.111	**0.750 ± 0.095**	0.306 ± 0.074	0.370 ± 0.104
	RMSE	4.095 ± 0.806	**1.806 ± 0.367**	5.959 ± 0.547	5.481 ± 0.660
	# NA	0	0	1	1
[72][4]	Accuracy	0.46 ± 0.344	0.690 ± 0.269	**0.74 ± 0.258**	0.67 ± 0.330
	RMSE	4.558 ± 3.640	**1.822 ± 0.820**	2.488 ± 1.662	2.707 ± 1.976
	# NA	15	0	0	0
[187][5]	Accuracy	0.075 ± 0.218	**0.818 ± 0.251**	0.545 ± 0.239	0.635 ± 0.237
	RMSE	10.784 ± 3.317	**1.439 ± 1.101**	3.722 ± 1.880	2.969 ± 1.477
	# NA	88	0	0	0

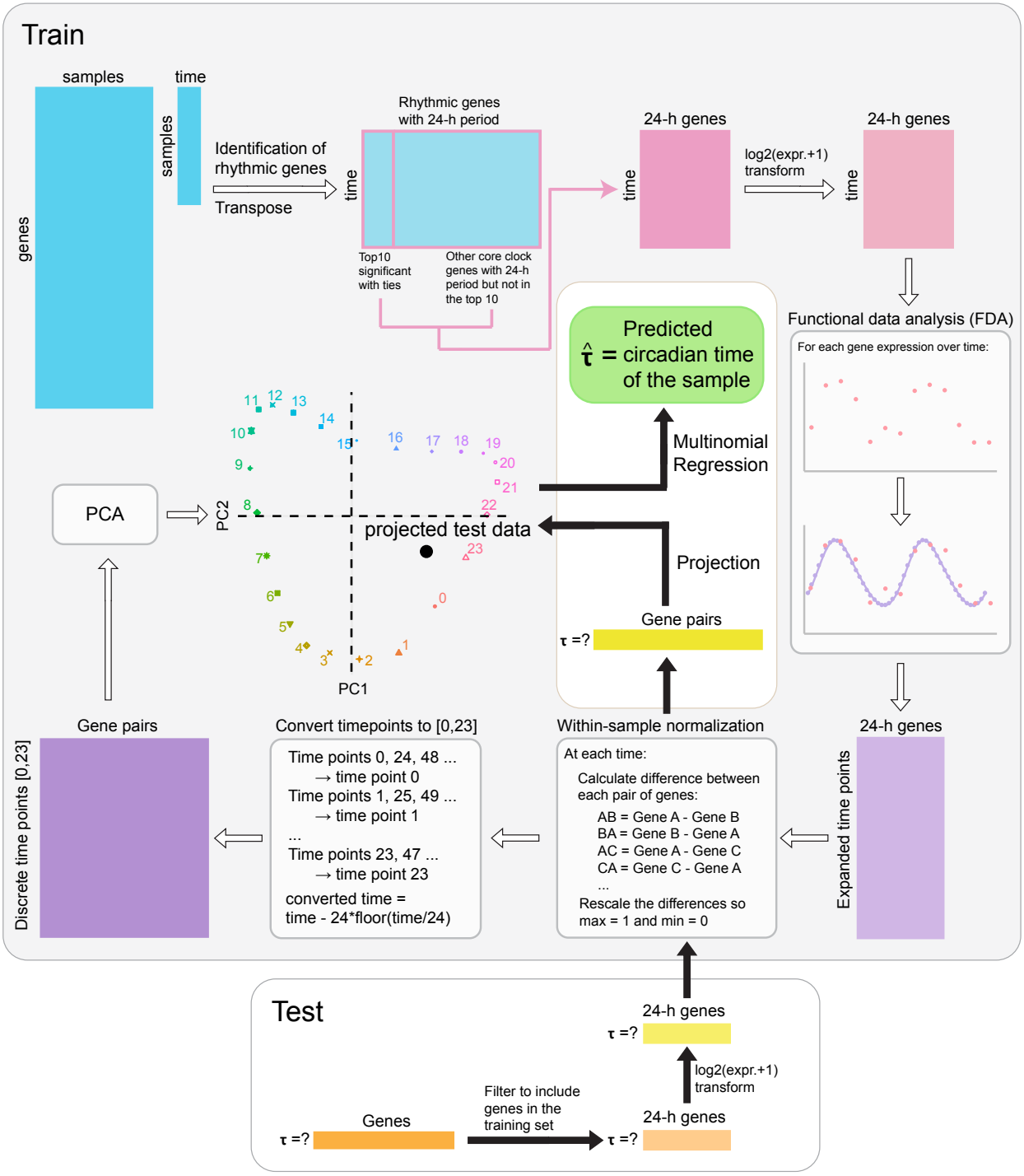

Figure 2.1: **The tauFisher pipeline involves multiple steps.** Key steps of the tauFisher pipeline include identification of rhythmic genes using MetaCycle, functional data analysis, within-sample normalization, linear transformation, and multinomial regression.

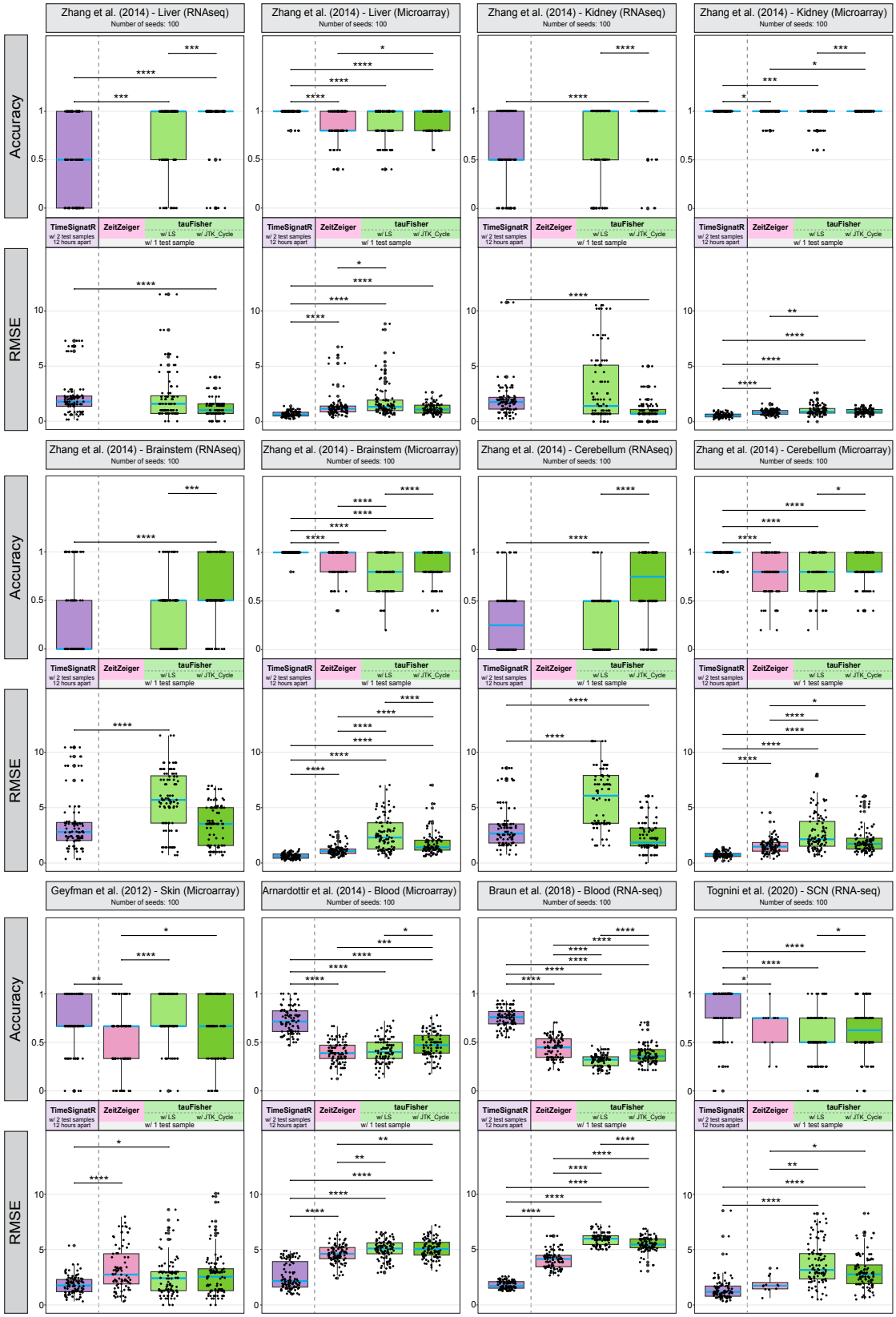

Figure 2.2: Legend on the next page.

Figure 2.2: **tauFisher requires only one test sample and performs well in both accuracy and RMSE for transcriptomic data collected from various organs and assay platforms.** Blue line inside each box indicates the median. Bounds of box represent the first and third quartiles. The upper and lower whiskers extend to the largest and smallest value within 1.5 times the inter-quartile range respectively. NAs excluded from the plot. RMSE: root mean square error. $*$: p-value ≤ 0.05, p-value ≤ 0.01, $***$: p-value ≤ 0.001, $****$: p-value ≤ 0.0001. P-values are determined using Wilcoxon rank-sum test and adjusted using Bonferroni correction. For each dataset, n = 100 randomly generated training-testing partitions.

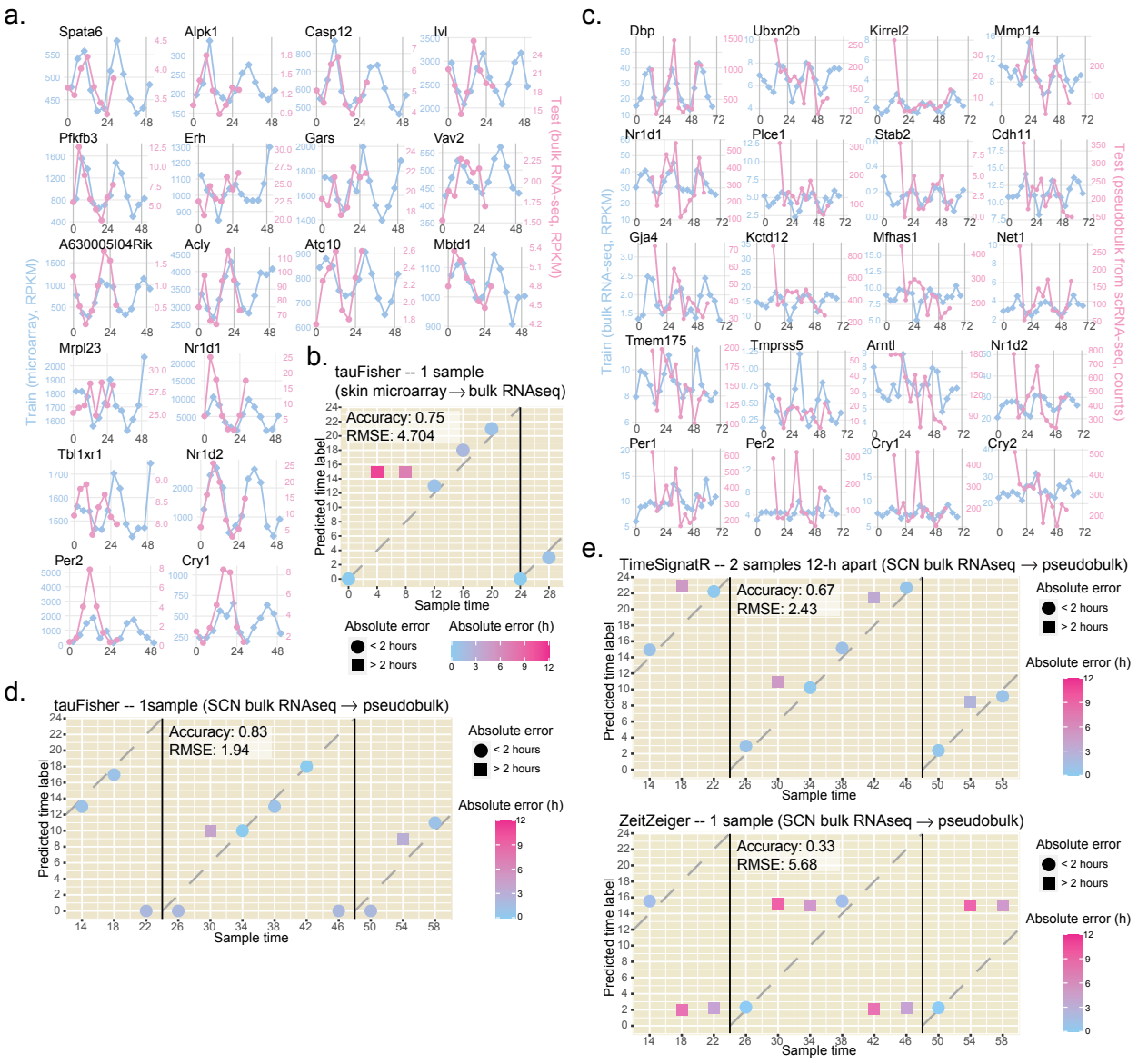

Figure 2.3: **tauFisher accurately predicts circadian time when the training and test data are from different assay methods. a-b** tauFisher trained on mouse skin microarray data can predict circadian time for skin bulk RNAseq data. **a** Overlay of the predictor gene expression in GSE38622 (training) and GSE83855 (test). **b** Prediction outcomes from tauFisher. **c-d** tauFisher trained on mouse SCN bulk RNAseq data can predict circadian time of pseudobulk data generated from mouse SCN scRNAseq data. **c** Overlay of the predictor gene expression in GSE157077 (training) and GSE117295 (test). **d** Prediction outcomes from tauFisher. **e** Prediction outcomes from TimeSignatR and ZeitZeiger when trained on mouse SCN bulk RNAseq and tested on mouse SCN scRNAseq pseudobulk. **b, d, e** The dashed lines mark where predictions equal truth. RMSE: root mean square error.

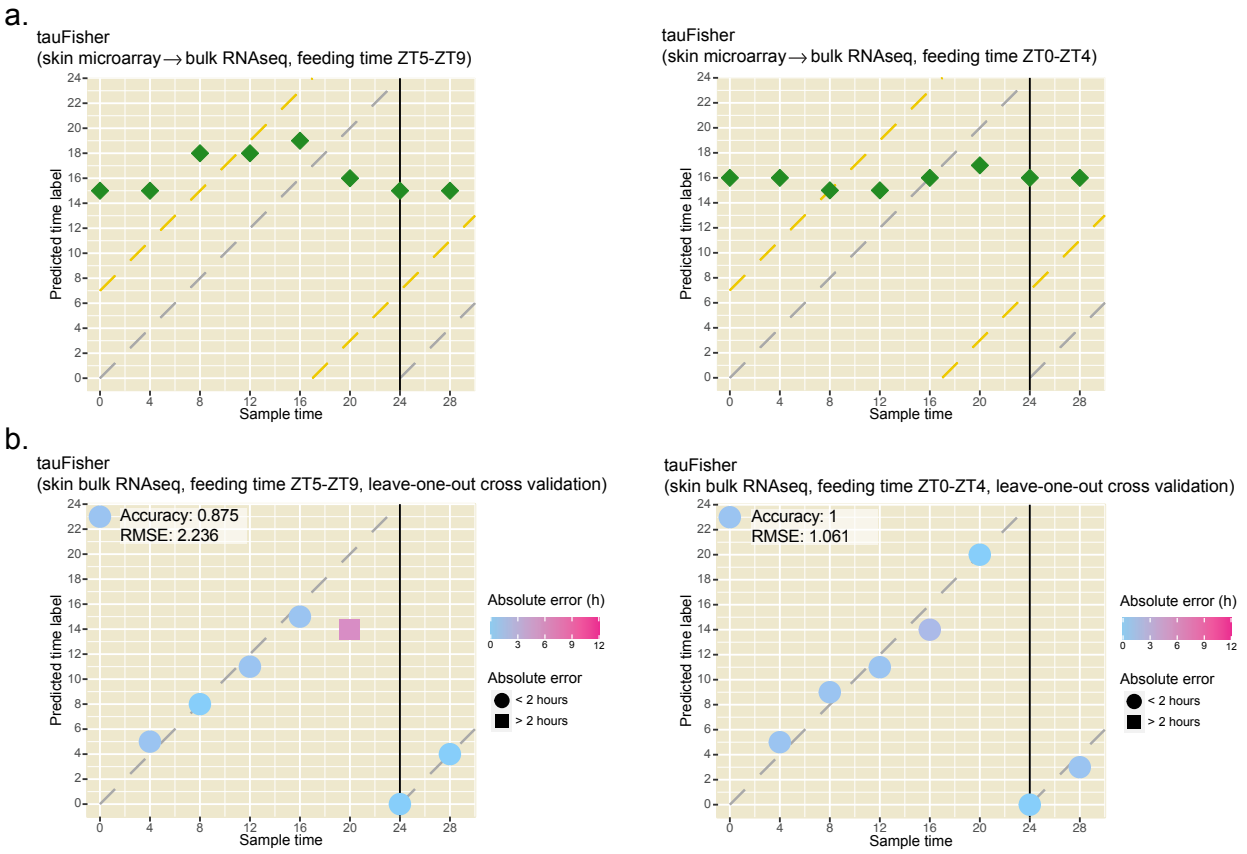

Figure 2.4: **tauFisher's performance in systems with disturbed circadian rhythms.** **a** tauFisher trained on a control/healthy diurnal system predicts time labels that are away from the sample collection time of the tested disturbed systems. tauFisher was trained on skin microarray data collected from control/healthy mice (GSE38622) and tested on skin bulk RNAseq (GSE83855) collected from mice experienced time-restricted feeding schedules. Food was available between ZT5-ZT9 or ZT0-ZT4, while mice usually feed during early night (ZT12-ZT16). Grey dashed lines mark where predicted time labels equal sample collection time. Yellow dashed lines mark where predictions equal the internal circadian time if the internal circadian time is phase-shifted according to the feeding schedule, which is not true [195]. **b** tauFisher trained on data collected from a disturbed system can predict time labels of samples collected from the same system. Using skin bulk RNAseq (GSE83855) collected from mice experienced the two time-restricted feeding schedules mentioned above, we performed leave-one-out cross validation. Each sample in each of the two feeding schedules was reserved for testing while tauFisher trained on the remaining samples. Grey dashed lines mark where predicted time labels equal sample collection time.

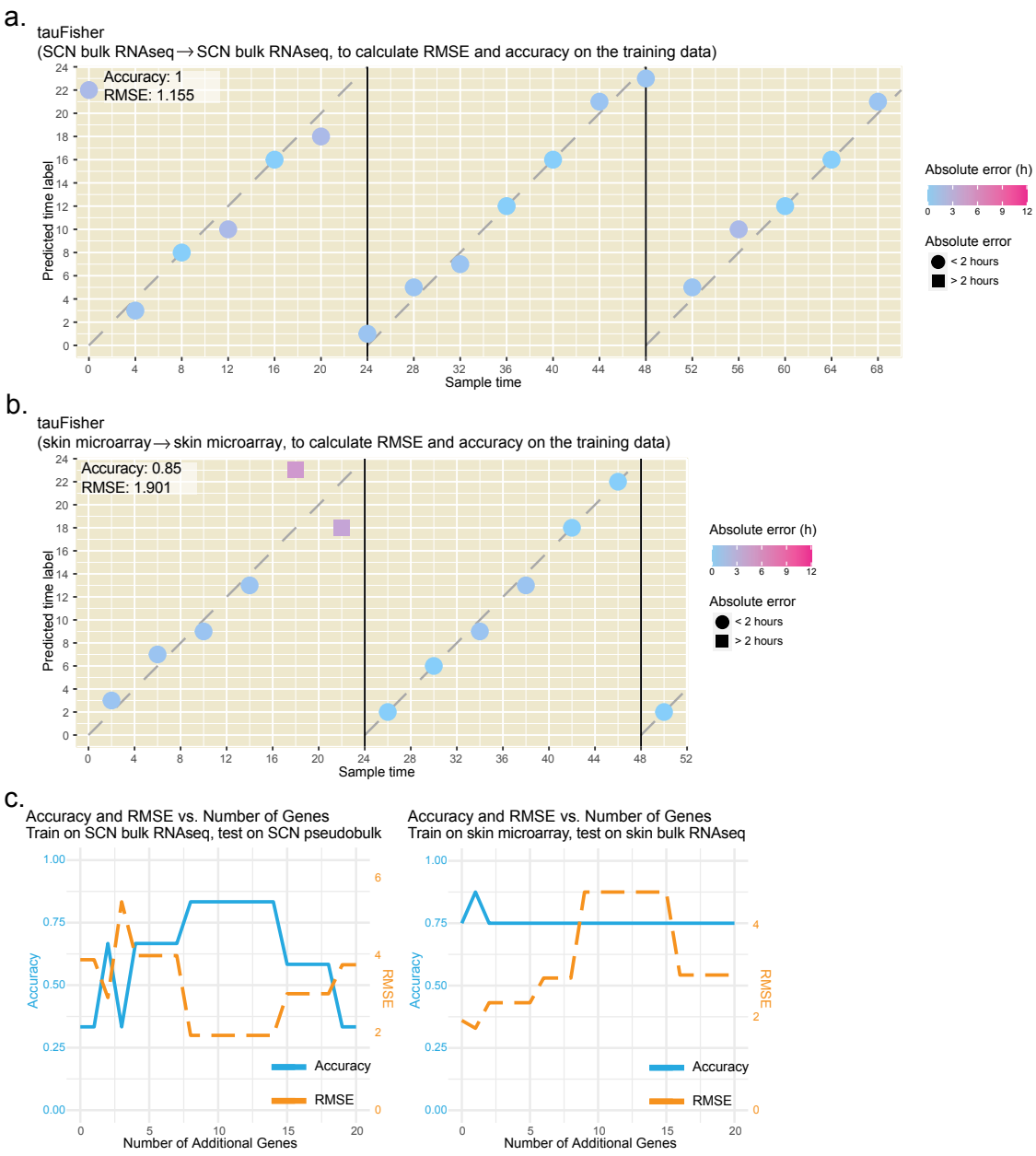

Figure 2.5: **tauFisher's performance within the training data and its sensitivity to the number of genes used in the pipeline. a** Prediction results when tauFisher was trained on mouse SCN bulk RNAseq (GSE157077) and tested on the same data. **b** Prediction results when tauFisher was trained on mouse skin microarray (GSE38622) and tested on the same data. **a-b** Grey dashed lines mark where predictions equal sample collection time. **c** tauFisher's performance is sensitive to the number of additional predictor genes used in the pipeline. We performed a sensitivity analysis and calculated accuracy and RMSE when we chose different numbers of diurnal genes in addition to the core clock genes with 24-hour period length. Although including 10 additional genes does not guarantee the best performance, it is a reasonable choice across different datasets.

Chapter 3

Uncovering cell type specific circadian regulations in mouse dermis with single cell RNAseq

J. Duan, M. N. Ngo, S. S. Karri, L. C. Tsoi, J. E. Gudjonsson, B. Shahbaba, J. Lowengrub, and B. Andersen. taufisher predicts circadian time from a single sample of bulk and single-cell pseudobulk transcriptomic data. *Nature Communications*, 15(1), May 2024

3.1 Introduction

Located just beneath the epidermis and above the hypodermis, the dermis provides strength and elasticity to the skin. Skin organelles such as hair follicles, sweat glands, and sebaceous glands are embedded in the dermis, all of which require proper interaction with the dermis for their functions. The dermis itself contains a diverse population of cells, with the most abundant being the fibroblasts, which produce collagen and other connective fibers. In

addition to fibroblasts, the dermis also contains immune cells such as macrophages, T cells, mast cells, and dendritic cells, which play active roles in immune responses [145, 204].

The circadian clock is robustly present in all three layers of the skin. In the dermis specifically, the circadian clock regulates the infiltration of dendritic cells [83] as well as the proliferation, migration, and actin production of dermal fibroblasts [156, 105]. Due such circadian regulations, wounds incurred on mice at different times of the day heal at different rates and circadian disruptions result alternations in the wound healing [105, 156, 216].

To study the circadian clock in the dermis, we we performed scRNAseq on adult wild type C57BL/6J mouse dorsal dermis every four hours for 72 hours under 12:12 light-dark cycle. We found that most of the rhythmic processes are metabolism-related in dermal fibroblasts, whereas almost all rhythmic processes are related to immune responses in dermal immune cells. Additionally, we found that the amplitude of the collective rhythm is dampened in dermal immune cells compared to dermal fibroblasts. Incorporating bootstrapping and tauFisher, a computational pipeline that predicts circadian time labels for transcriptomics datasets, revealed that circadian phase heterogeneity contributes to the dampened collective rhythm as well as fewer rhythmic genes found in dermal immune cells.

3.2 Results

3.2.1 tauFisher trained on microarray data accurately predicts circadian time of scRNAseq samples.

We first tested tauFisher's performance on the collected scRNAseq data to validate its performance for peripheral tissues. The pseudobulk matrices for the 18 samples were computed directly from the unprocessed data. We trained tauFisher on GSE38622 [72], a time series

of skin microarray data. Because two of the rhythmic genes, *A630005I04Rik* and *Ivl*, are not present in the pseudobulk data, only 16 features were selected in the tauFisher pipeline in this test (Figure 3.1a).

Although the input test data, the unnormalized pseudobulk data, appears to be noisy, tauFisher successfully predicts circadian times for the 18 samples thanks to the within-sample normalization step in the tauFisher pipeline. In 14 out of the 18 tests, tauFisher predicted circadian time within 2 hours of the labeled time, giving a high accuracy of 0.778 and a low RMSE of 2.198 (Figure 3.1b).

We have demonstrated that tauFisher trained on microarray data, can accurately predict circadian time for scRNAseq data as well.

3.2.2 Collective circadian rhythms are dampened in dermal immune cells compared to dermal fibroblasts.

Due to the frequency of sequencing dropouts of clock genes in scRNAseq data, investigating the circadian clock within each cell is not yet achievable. To overcome this limitation, previous studies have used pseudobulk approaches to investigate the clock in scRNAseq data [199].

To validate the pseudobulk approach for studying the circadian clock in mouse dermis, we normalized the pseudobulk scRNAseq data, and compared it with the published microarray data GSE38622 from mouse whole skin [72]. Overlay of the expression of nine core clock genes, *Arntl*, *Dbp*, *Per1*, *Per2*, *Per3*, *Nr1d1*, *Nr1d2*, *Cry1* and *Cry2*, reveals perfect consistency between the microarray data and the scRNAseq pseudobulk data (Figure 3.2a), indicating that circadian clock gene expression in the dermis is captured in the pseudobulk data generated from scRNAseq data.

To study the circadian clock at a cell-type level in the skin, we integrated all samples and performed scRNAseq analysis to identify cell types. In total, 16,866 cells passed the quality control, with around 950 cells per sample and around 2,800 cells per ZT. Four major cell types, fibroblasts (N = 12,649), immune cells (N = 3,353), muscle cells (N = 722) and endothelial cells (N = 142) were identified using canonical marker genes (Figure 3.2b). Due to low cell counts for muscle and endothelial cells (N<20) in some samples, we could not generate a reliable time series of pseudobulk data for these two cell types. Thus, we focus on the circadian clock in dermal fibroblasts and immune cells in this study.

In general at the single cell level, the expression ranges of the core clock genes are similar in the two cell types, and the measurements of the clock genes in fibroblasts are more variable (Figure 3.3). To compare the core clock in fibroblasts and immune cells, we computed and normalized the pseudobulk data for each of the two cell types in each sample. Both fibroblasts and immune cells possess robust circadian clock at the pseudobulk level. While the overall rhythms in the two cells types are consistent with each other, with core clock gene expressions peaking and troughing around the same time, the amplitudes of the oscillations are reduced in the immune cells compared to fibroblasts, indicating a dampened collective clock in immune cells (Figure 3.2c). Whether this observation indicates less synchronous clocks in immune cells than in fibroblasts, or weaker clock function in each individual immune cell, is not known.

3.2.3 Dermal fibroblasts and immune cells harbor different rhythmic pathways and processes.

To study diurnal genes and pathways in dermal fibroblasts and immune cells, we used JTK_Cycle to identify rhythmic genes from the normalized pseudobulk data. We identified 1,946 and 432 rhythmic genes in fibroblasts and immune cells, respectively (Figure

3.4a). The fewer rhythmic genes in immune cells is not caused by the lower cell count of immune cells, as randomly down-sampling the fibroblasts to the number of immune cells produced similar results. Only 79 genes were rhythmic in both cell types, with most of them related to the core clock network and metabolism.

Gene Ontology analysis revealed that rhythmic processes in fibroblasts and immune cells are different. Shared terms reflect basic cell integrity maintenance and function, including nucleocytoplasmic transport, regulations of cellular amide metabolic process, regulation of protein stability, and rhythmic process (Figure 3.4b). For fibroblasts, additional metabolism processes and migration are significantly enriched in the rhythmic genes (Figure 3.4b, red). For immune cells, the rhythmic genes enrich for immune responses including defense response to virus, regulation of T-helper 2 cell differentiation, and response to interferon-beta (Figure 3.4b, blue).

We selected some of the rhythmic genes in fibroblasts (Figure 3.4c) and immune cells (Figure 3.4d) and compared their expression patterns in the two cell types. For fibroblasts, we highlight genes related to glucose metabolism (*Pkm*), glycosylation (*Gal3st4*, *Plpp3*), oxidative phosphorylation (*Ndufs8*), collagen regulations (*Loxl2*, *Tgfb1*), amino acid metabolism (*Ivd*), sterol synthesis (*Scp2*, *Por*), and cell adhesion and migration (*Elmo2*, *Antxr1*), suggesting circadian regulation of the above processes at a molecular level (Figure 3.4c). Interestingly, while some genes are only significantly rhythmic in fibroblasts because they are not expressed in immune cells (e.g. *Loxl2*), some are expressed at similar or higher levels in immune cells, but are not significantly rhythmic in the latter (e.g. *Ndufs8*, *Scp2*), indicating cell-type specific circadian regulations.

In the immune cells, genes related to inflammatory and immune response (*Cdk19*, *Cd84*), post-translational modification (*Sumo1*), extracellular matrix regulation (*Mmp9*), transcription regulation (*Med16*), electrochemical gradient maintenance (*Atp1b1*), and intercellular communication (*Stxbp6*) are rhythmic (Figure 3.4d). We note that *Sumo1* is rhythmic in

both fibroblasts and immune cells, but the expression peaks 4-hour later in immune cells than in fibroblasts.

Interestingly, the expression of *Il18r1* is significantly rhythmic with a high amplitude in fibroblasts (p-value = 2.21×10^{-7}), but not in immune cells (p-value = 0.7104) (Figure 3.4c). The level of IL18, the ligand that binds to IL18R1, was found to be rhythmic in mouse peripheral blood [109]. Here, *Il18*, is significantly rhythmic in neither fibroblasts (p-value = 0.3097) nor immune cells (p-value = 0.0925) (Figure 3.4d). But, it is possible that the insignificance of the p-value for immune cells is caused by noise introduced by summing the expression of all types of immune cells while it is mostly expressed in the myeloid cells.

To further explore the rhythmic pathways in dermal fibroblasts and immune cells, we divided the list of rhythmic genes into four groups based on their peaking time (Methods): day (ZT3 - ZT9), evening (ZT9 - ZT15), night (ZT15 - ZT21), and morning (ZT21 - ZT3 of the next day). The rhythmic genes are roughly evenly split: in fibroblasts, 426 peak during the day, 554 peak in the evening, 545 peak at night, and 421 peak in the morning; in immune cells, 129 peak during the day, 111 peak in the evening, 87 peak at night, and 105 peak in the morning. We then performed Gene Ontology analysis on the quarter-day rhythmic gene lists to identify the biological processes that are upregulated at different times of the day. We highlight some of the terms related to metabolism, signaling, cell proliferation and apoptosis, gene regulation, and immune regulation (Figure 3.4e).

During evening and night, when mice wake up, start feeding, and become active, processes such as generation of precursor metabolites and energy, cellular respiration, mitochondrial respiratory chain complex I assembly are upregulated in fibroblasts (Figure 3.4e). Meanwhile, glycolytic processes are upregulated in fibroblasts, which is consistent with the finding that glycolysis is preferred at night in epidermal stem cells [173]. Additionally, similar to epidermal stem cells, more dermal fibroblasts may be in the S-phase of the cell cycle during the evening and night, as DNA biosynthetic process is enriched during this time. Various signal-

ing pathways are also enriched during this time, including prostaglandin metabolic process and regulation of apoptotic signaling pathway. Gene-regulatory mechanisms such as histone modification and mRNA splicing are upregulated during the evening and night in fibroblasts. Fibroblast migration peaks at night, which is consistent with previous findings that mouse wounds heal fastest during the active phase [85]. Immune regulation is also circadian regulated in fibroblasts, as terms including regulation of inflammatory response are enriched during this time. Compared to dermal fibroblasts during the evening and night, fewer terms related to metabolism, signaling, and gene regulation are enriched in dermal immune cells (Figure 3.4e). But, almost all immune regulation terms such as defense response to virus and interferon-beta production are upregulated in dermal immune cells during the evening and night, potentially contributing to shorter healing duration for wounds occurring during mice's active phase as well [85]. Additionally, such findings in mice imply that circadian regulation of immune response may be related to the more severe symptoms of inflammatory skin diseases, such as psoriasis, in the evening and at night [63, 55].

In the morning and during the day, mice sleep and have lower food intake. Consistently, rhythmic genes peaking during this time in fibroblasts enrich for lipid catabolic process, glucose metabolic process, lipid storage, and response to starvation. Interestingly, extracellular matrix organization and cell-matrix adhesion peak during the day, possibly preparing for fibroblast migration, which peaks in the evening (Figure 3.4e). For immune cells, rhythmic genes peaking during the morning and day generate fewer terms than the ones peaking during the evening and night, especially in the immune regulation category (Figure 3.4e). Interestingly, rhythmic genes the mouse dermal fibroblasts significantly enrich for genes linked to SNPs associated with systemic sclerosis [115], an inflammatory disease with increased collagen production by fibroblasts. Rhythmic genes in mouse dermal immune cells significantly enrich for SNPs associated with not only systemic sclerosis, but also vitiligo [93], a disease characterized by immune-mediated depigmentation of the skin (Figure 3.4f).

In sum, we found that more genes are collectively rhythmic in fibroblasts than in immune cells, while only a few rhythmic genes are shared. Additionally, more metabolism processes are diurnally regulated in fibroblasts, with respiration peaking during the evening and night, and response to starvation and lipid storage peaking during the morning and day. On the other hand, immune regulation is almost exclusively upregulated by rhythmic genes that peak during the evening and night in immune cells. Importantly, rhythmic genes found in both fibroblasts and immune cells significantly enrich for Genomewide Association Studies (GWAS) SNPs associated with human skin immune-mediated conditions, pointing to a potential link between the skin circadian clock and autoimmune diseases of the skin.

3.2.4 tauFisher determines that circadian phases are more heterogeneous in dermal immune cells than in fibroblasts.

Analysis of the pseudobulk data from dermal fibroblasts and immune cells reveals dampened amplitudes of the core clock genes (Figure 3.2c) in the immune cells and finds fewer rhythmic genes in immune cells than in fibroblasts (Figure 3.4a). This observation could mean that each individual immune cell harbors weaker circadian clock, and/or the immune cells have more heterogeneous phases, so collectively they display a dampened clock. Note that variations of mean expression in single cells (vertical shifts of expression curves) do not cause dampened amplitudes at the pseudobulk level (Figure 3.5c, d), so this scenario is not considered in the following analysis.

To investigate the cause behind the dampened clock in dermal immune cells, we executed a bootstrapping approach that incorporates tauFisher for its ability to predict circadian time for transcriptomic data at different scales (Figure 3.6a). Since the heterogeneity of a set of heterogeneous clocks should be captured at any given time point, we performed the analysis within each time point. The workflow involves the following steps: (1) trimming the

scRNAseq data so that the expression matrix only includes the predictor genes identified in the training data and the cells labeled to be the interested cell types; (2) randomly sampling the same number of cells for each cell type to remove potential bias caused by different cell numbers, and summing the transcript counts in the pulled cells for each gene to create a pseudobulk dataset; (3) repeating the random sampling process (step 2) with replacement many times to create pseudobulk replicates for each cell type; and (4) predicting circadian time labels for the pseudobulk replicates using tauFisher. The idea is that if the cells harbor synchronous clocks, the pseudobulk replicates calculated from different rounds of sampling will be similar. In this case, the distribution of predicted time labels will be more concentrated. On the other hand, if the cells harbor heterogeneous clocks, the pseudobulk replicates calculated from the cells in different rounds of sampling will differ depending on which cells are pulled. The distribution of the prediction outcome in this case will be wider. Since the prediction outcomes are circular data, we then perform Rao's Tests for Homogeneity and Wallraff Test of Angular Distances to compare the mean and the dispersion around the mean.

To ensure that the pipeline works as expected, we generated simulated single-cell circadian gene expression datasets to represent a group of synchronized but dampened clocks (Figure 3.5a), and a group of out-of-phase but robust clocks (Figure 3.5b). As expected, the prediction outcome for the out-of-phase clocks has a significantly greater dispersion around the mean, indicating a more heterogeneous mixture of phases (Figure 3.5e, f).

We then applied the pipeline to the collected scRNA-seq data, focusing on the fibroblasts and immune cells. At each time point, we randomly selected n cells for each cell type, with n equal to 20% of the cell count of the cell type with the smaller population (immune cells in this dataset). Then, we used the exact same procedure to generate 500 pseudobulk replicates for the two cell types at each time point. tauFisher then predicts the circadian time for each pseudobulk replicate, yielding 500 predicted timestamps for each of the two cell types. We

compared the distribution of the 500 predicted time labels of the two cell types at each time point.

In general, the prediction means are centered at different times for fibroblasts and immune cells (Figure 3.6b), but around the predicted time for the whole-sample pseudobulk data (Figure 3.1g). Whether one cell type's circadian clock is ahead of the other is inconclusive (Figure 3.6c). Additionally, the distributions of the prediction outcome for immune cells are mostly multimodal and not as centered as the prediction distribution for fibroblasts (Figure 3.6b). Indeed, the standard deviation of the prediction distribution is significantly greater for immune cells for five out of the six ZTs (Figure 3.6c). This means that the bootstrapping pulled from a more heterogeneous population when sampling the immune cells, and thus implying that the clock phases are more heterogeneous in immune cells than in fibroblasts.

In sum, we were able to use tauFisher to obtain insights into the circadian heterogeneity for different cell types by predicting the circadian time for random samples from each of the cell types. We hypothesize that the circadian clock is more heterogeneous in dermal immune cells than in dermal fibroblasts, and such heterogeneity may be the reason behind the dampened core clock and fewer rhythmic genes we found in immune cells based on collective, cell-type level, gene expression data. Such a result is not unexpected, as the fibroblasts (Figure 3.7a, b) may be more homogeneous in their biological function than the immune cells, which contain dendritic cells as well as different types of macrophages and lymphocytes (Figure 3.7d, e) that serve different immune functions. Unfortunately, we did not capture enough cells for each specific fibroblast and immune cell types in the scRNAseq experiment to generate reliable pseudobulk data that is required for further circadian analysis (Figure 3.7c, f).

3.3 Discussion

In addition to testing tauFisher on published datasets, we also collected a time series of scRNAseq from mouse dermis. Consistent with previous findings [141, 55], the circadian rhythm is robustly present in the dermis and the oscillatory patterns of the core clock genes agree with published data [72]. Comparing the rhythmic genes in fibroblasts and immune cells, we found that only a few rhythmic genes are shared by the two cell types and many pathways and processes are rhythmically regulated in a cell type-specific manner. Shared diurnally regulated terms includes basic cellular functions and the rhythmic genes in fibroblasts have greater enrichment for metabolism related terms, whereas the rhythmic genes in immune cells have greater enrichment for immune responses.

Combining tauFisher with other methods can guide the application of circadian medicine by providing additional insights and explanation of clinically observed circadian dysfunction. Dampened clock gene expression has been observed in psoriasis-affected skin [75, 215], as well as in various types of cancer [209, 175, 45, 100, 86, 90]. There is also evidence that restoring dampened circadian oscillations in diseased tissues can be effective in reducing cancer cell proliferation and tumor growth [100, 90].

There are two possible behind-the-scene causes of dampened circadian rhythms at a bulk level: first, the circadian rhythm is dampened in every cell, but the cells are synchronous to each other (Figure 3.5a); second, the clock is normally functioning in every cell, but the cells are out of phase relative to each other (Figure 3.5b). Understanding which of the two scenarios is responsible for a dampened bulk-level clock gene expression is particularly important because in one case, it would be optimal to stimulate the clock to restore the circadian clock in the diseased tissue, while in the other case, synchronizing the clock is more suitable.

Here, we observed that the collective circadian rhythm in dermal immune cells is dampened

compared to fibroblasts. We incorporated tauFisher with bootstrapping to investigate the cause behind the dampened collective circadian rhythm in dermal immune cells. tauFisher's prediction outcome suggests that the circadian phases in dermal immune cells are more heterogeneous than those in dermal fibroblasts, and this heterogeneity may contribute to the dampened rhythm in immune cells at a collective level. Due to technological constrains, our claim on differences in phase heterogeneity between dermal fibroblasts and immune cells relies on the computational analysis of the mouse skin scRNAseq and the simulated single-cell data.

The advantages tauFisher brings goes beyond accurately adding timestamps when incorporated with other methods. For example, combining tauFisher with a batch-effect correction method may facilitate a cleaner integration and help minimize the effect of the circadian clock in transcriptomic data analysis. This approach harbors great potential as many efforts are going into integrating datasets from different studies to create meta databases such as in the Human Cell Atlas.

3.4 Methods

3.4.1 scRNAseq experiments

Mouse strains and husbandry

The experiment is approved by the Institutional Animal Care and Use Committee (IACUC) at University of California, Irvine under AUP-22-003. Wild type male C57BL/6 mice were housed under 12:12 light-dark cycle for two weeks prior to and during the time of experiment. To collect telogen skin, mice were about 54 days old by the time of sample collection.

Sample collection and sequencing

Immediately after sacrificing a mouse with CO_2, hair on dorsal skin was removed with an electric razor and Nair Hair Removal cream. After the dorsal skin was isolated from the body, fat and remaining blood vessels were scrapped away with a scalpel blade. A circular piece of skin was obtained with a 12mm biopsy punch, and minced into tiny pieces. The minced skin was then digested with 2mL of a solution consisting of 0.27% Collagenase IV (Sigma, C5138), 10mM HEPES (Fisher Scientific, BP310-100), 1mM Sodium Pyruvate (Fisher Scientific, BP356-100), and 5U/mL DNase I (Thermo Scientific, EN0521) at 37 °C for 1.5 hours. The suspension was then filtered with a $70\mu m$ and a $40\mu m$ cell strainers to obtain single cells. SYTOX blue viability dye (1:1000; Invitrogen, S34857) was added to the cell suspension and live cells were sorted out using FACS at the UCI Stem Cell Research Center.

Samples were collected every four hours for three days to generate in total 18 samples, providing three biological replicates per circadian time point. The Chromium Single Cell 3' v3 (10x Genomics) libraries were prepared and sequenced by University of California Irvine Genomic High Throughput Facility with Illumina NovaSeq6000.

Statistics and reproducibility

No statistical method was used to predetermine sample size. We chose to collect three biological replicates per circadian time point because previous circadian gene expression experiments showed that n = 3 allowed robust detection of circadian genes [72, 195, 199, 220]. A random mouse was selected to sacrifice for each sample collection. No dataset was excluded from the analyses. During the collection and analysis of the scRNAseq data collected from mouse dermal skin, the investigators were not blinded to the time labels.

3.4.2 Datasets and analysis

For each time point in GSE223109 (collected in this study), we summed the counts of each gene in all the cells without any pre-processing to create a pseudobulk dataset. In the case where the same gene occurs multiple times in the data, we took the mean of those entries. The resulting pseudobulk data at each time point is a single row vector in which each entry represents the expression value of a unique gene. The light-stimulated group is not considered in this paper.

scRNAseq data analysis for dermal skin

We used CellRanger version 3.1.0 with MM10 reference to process the raw sequencing output. The downstream analysis was done in Seurat V3 according to the vignette.

Cells with 850-7800 features and less than 13% of mitochondrial genes were kept. The SCTransform function was performed on each sample and 3250 integration features were selected using SelectIntegrationFeatures for each sample. Principal component analysis was then done on the integrated dataset and the Louvian algorithm was used to generate the clusters. Cluster identities were then determined in combination of marker genes found in the current clustering outcome and feature plots of canonical marker genes.

Pseudobulk data analysis for dermal skin

Pseudobulk data was calculated by summing the number of reads for each gene from all cells in a group. Normalized pseudobulk was calculated as transcript counts divided by total number of reads times 10,000. `meta2d` from the MetaCycle package was used on the pseudobulk data generated from the scRNAseq data collected from dermal skin to identify rhythmic genes. Genes with JTK_pvalue<0.05 were determined to be significantly rhythmic.

We used the meta2d_phase column to split the rhythmic genes into four groups based on their peaking time.

Gene Ontology analysis was performed using clusterProfiler in R with p-value < 0.05 as the significance cutoff.

3.4.3 Enrichment for GWAS SNPs

For rhythmic genes with JTK_pvalue<0.01 in the dermal fibroblasts or immune cells, we used the hypergeometric test to assess their enrichment among genes that are within 200kb of the GWAS signals of different skin immune-mediated conditions [137, 136, 122, 115, 93, 20, 19]. We used the transcripts expressed in the cells as the background gene list in the enrichment analysis. Significance cutoffs are false discovery rate$\leq$0.05 and observed-to-expected ratio$\geq$2.

3.4.4 scRNAseq circadian gene expression simulations

In Results, we demonstrated that tauFisher can be used to investigate circadian phase heterogeneity using simulated scRNAseq circadian gene expression data. We simulated three groups of data to represent three scenarios: (1) a group of synchronized but dampened clock genes, (2) a group of normal (robust) but asynchronous clock genes, and (3) a group of synchronized clock genes with normal amplitudes but variations in mean expression. For the three groups, the expressions of 9 representative diurnal genes over a time course of 24 hours are simulated using the following sine function:

$$y = A \sin\left(B(x + C)\right) + D \tag{3.1}$$

where A is the amplitude, C is the phase shift, D is the vertical shift, the period is $2\pi/B$, and x is a sequence of integers from 0 to 23. We set B to be 24, such that the period is $2\pi/24$, and D to be a value big enough to ensure possitive gene expression values. We used $D = 25$.

We used JTK_Cycle [88] to identify periodic genes, and its output contains inferred amplitudes and phase shifts for each gene. As inputs for our simulated datasets, we select the inferred amplitude and phase shift values for core clock genes *Bmal1*, *Dbp*, *Nr1d1*, *Nr1d2*, *Per1*, *Per2*, *Per3*, *Cry1*, and *Cry2* from [187]. Then, for each dataset in Group 1, we simulate the expression of gene i as follows:

$$y_i = (A_i \times R_i) \sin\left(B(x + C_i)\right) + D \tag{3.2}$$

where R_i is one draw from a Beta$(1, 2)$ distribution and all other parameters are as previously stated. Similarly, for each dataset in Group 2, we simulate the expression of gene i as follows:

$$y_i = A_i \sin\left(B(x + C_i + R_i)\right) + D \tag{3.3}$$

where R_i is one draw from a Normal$(0, 12)$ distribution and all other parameters are as previously stated. For each dataset in Group 3, we simulate the expression of gene i as follows:

$$y_i = A_i \sin\left(B(x + C_i)\right) + D + R_i \tag{3.4}$$

where R_i is one draw from a Normal$(0, 1)$ distribution and all other parameters are as previously stated. We generated 100 datasets for each group, which can be thought of as the simulated expression of 9 genes for 100 single cells over 24 hours. According to the simulations, only Group 1 and Group 2 scenarios can lead to dampened amplitudes at the

pseudobulk level. Group 3 scenario is not considered as a possible cause of the dampened pseudobulk expression (Figure 3.5c, d).

We randomly select 6 time points without replacement over the course of the 24 hours to investigate circadian phase heterogeneity in the simulated data. At each time point, we randomly select 20% of the simulated single cells without replacement and sum their expression to obtain a pseudobulk dataset. We repeat this procedure 500 times for each of Group 1 and Group 2, generating 500 pseudobulk datasets per group. Then we used tauFisher to predict circadian time labels for the resulting pseudobulk datasets.

3.4.5 Statistics for circular data

The circular R package was used to perform statistical calculations and tests, including calculation of the mean and standard deviation, as well as the Rao's Tests for Homogeneity and the Wallraff Test of Angular Distances, for the circadian time prediction output in the Results section.

3.5 Data Availability

The time series of scRNAseq data from mouse dermal skin collected in this study are available in the GEO database under GSE223109.

3.6 Code Availability

tauFisher is available as an R package at https://github.com/micnngo/tauFisher [129].

3.7 Acknowledgements

This project is supported by an award entitled "Skin Biology Resource-Based Center at UCI - Systems Biology Core" from the Center of Complex Biological Systems funded by NIH/-NIAMS P30-AR075047 (J.D. and M.N.); National Institute of Health grants R01AR056439 and P30AR075047 (B.A.); NSF grant DMS1763272 and a grant from the Simons Foundation (594598) (J.D., M.N., J.L. and B.A.); National Institute of General Medical Sciences, National Research Service Award GM136624 (J.D.); NSF grant DMS1936833 (M.N. and B.S.); the California Institute for Regenerative Medicine Training Program Award EDUC4-12822 (S.S.K.); and Chan Zuckerberg Initiative grant DAF2022-239946 (B.A., J.G., and L.C.T.).

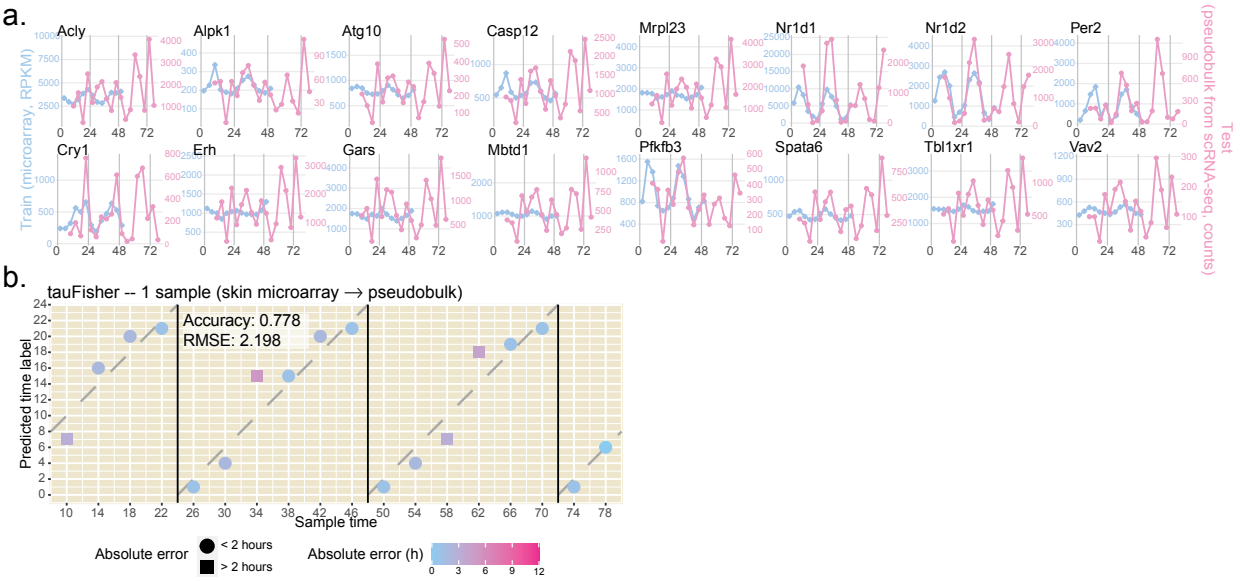

Figure 3.1: **tauFisher trained on mouse skin microarray data can predict circadian time of pseudobulk data generated from dermis scRNAseq data.** **a** Overlay of the predictor gene expression in GSE38622 (training) and GSE223109 (test). **b** Prediction outcomes from tauFisher. **b** The dashed lines mark where predictions equal truth. RMSE: root mean square error.

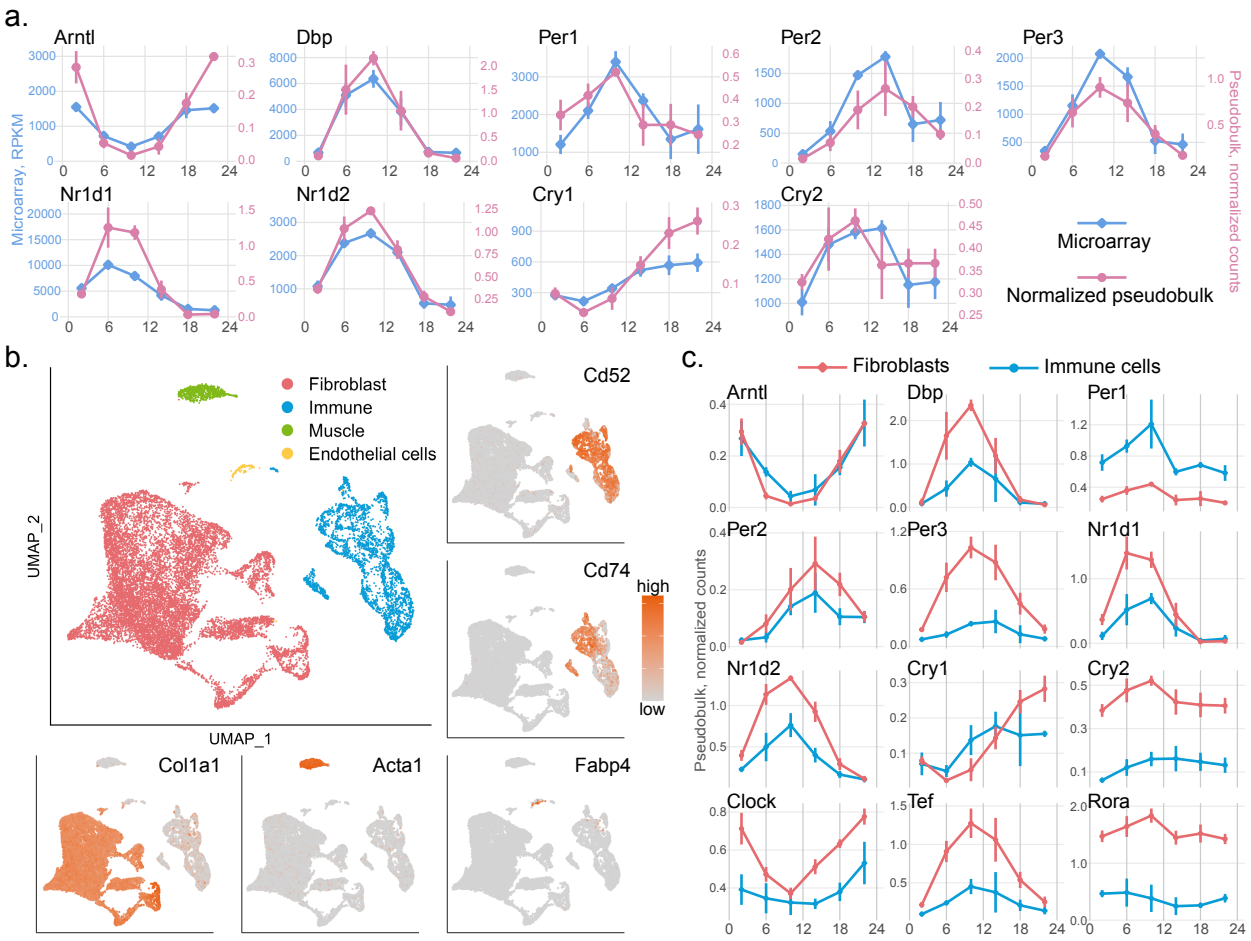

Figure 3.2: **The circadian clock is present in mouse dermal fibroblasts and immune cells.** **a** The normalized pseudobulk expression of the core clock genes generated from scRNAseq data (pink, n = 3 biologically independent samples per circadian time point) is consistent with their expression in the published microarray data (blue, n = 2 biologically independent samples per circadian time point, except that n = 3 at ZT2). Data are presented as mean values +/- SD. **b** Four major cell types, fibroblasts (red), immune cells (blue), muscle cells (green) and endothelial cells (yellow) were identified using canonical marker genes. Feature plots of the representative marker genes are shown (orange: high expression; grey: low expression); *Col1a1* for fibroblasts, *Acta1* for muscle cells, *Fabp4* for endothelial cells, *Cd52* and *Cd74* for immune cells. **c** At the pseudobulk-level, expression pattern of the core clock genes are similar in fibroblasts (red) and immune cells (blue), while the amplitudes of the oscillations are dampened in immune cells for most of the core clock genes. n = 3 biologically independent samples per circadian time point. Data are presented as mean values +/- SD.

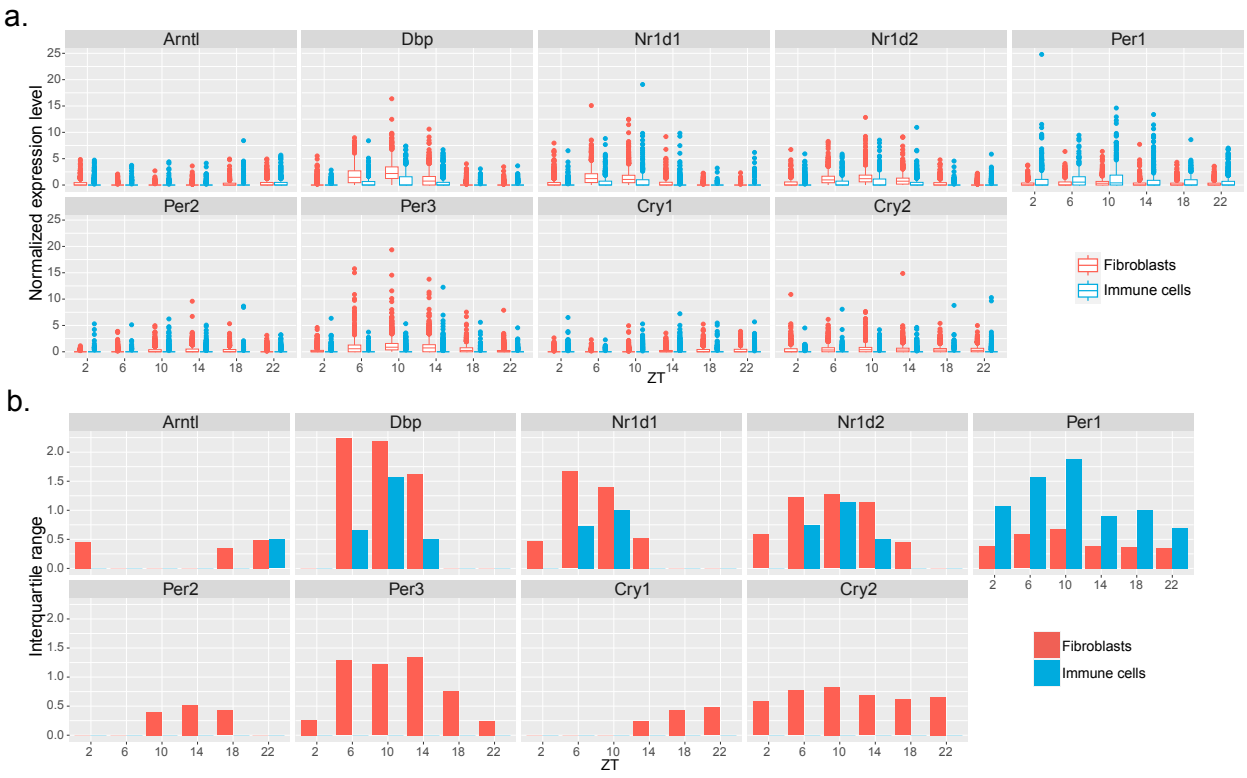

Figure 3.3: **The expression ranges of the core clock genes are similar in the dermal fibroblasts and immune cells.** **a** Box plots of expression levels of core clock genes in fibroblasts (red) and immune cells (blue). Expression value is normalized as transcript counts divided by total reads in each cell times 10000. The ranges of the expression levels of the core clock genes are similar in fibroblasts and immune cells. **b** Interquartile range of the expression of core clock genes in fibroblasts (red) and immune cells (blue). The measurements in fibroblasts are more variable than the measurements in immune cells in general.

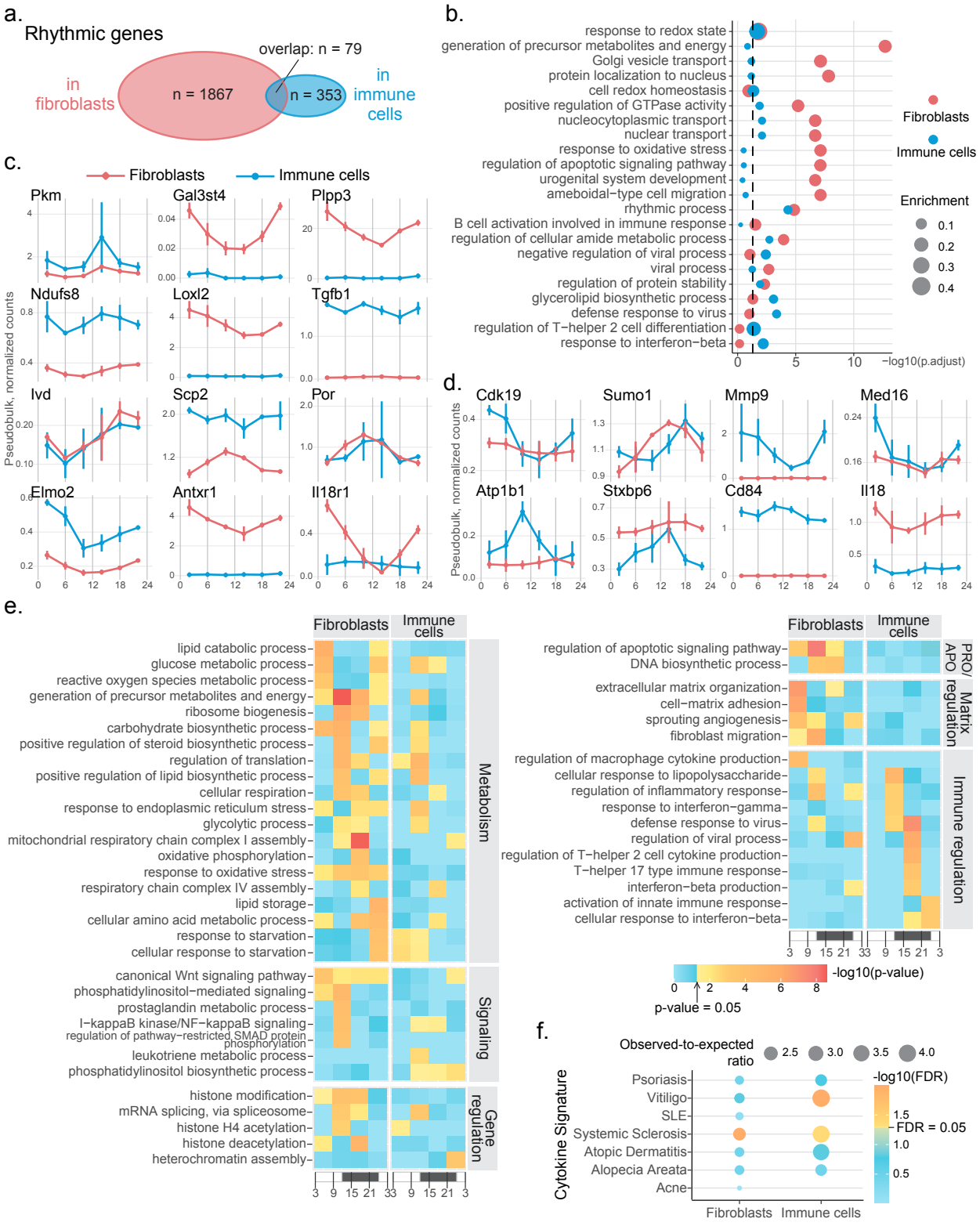

Figure 3.4: Legend on the next page.

Figure 3.4: **Different rhythmic processes are present in mouse dermal fibroblasts and immune cells. a** JTK_Cycle identified 1946 rhythmic genes in dermal fibroblasts (red) and 432 rhythmic genes in dermal immune cells (blue). Only 79 rhythmic genes are shared by the two cell types. **b** Gene Ontology analysis performed on rhythmic genes in fibroblasts (red) and immune cells (blue) reveals divergent biological processes being diurnally regulated in the two cell types. Dot size represents enrichment score. The vertical dashed line marks adjusted p-value = 0.05. P-values are determined using hypergeometric test and adjusted using Benjamini-Hochberg procedure. **c, d** Expression of some of the rhythmic genes found in fibroblasts (**c**), and immune cells (**d**). n = 3 biologically independent samples per circadian time point. Data are presented as mean values +/- SD. **e** A heatmap showing p-values for some of the biological processes enriched by rhythmic genes peaking during each quarter-day time range. Color represents p-value. Blue: insignificant; yellow to red: significant with red representing lower p-value. P-values are determined using hypergeometric test. x-axis represents time, with white being day and black being night. **f** Rhythmic genes in mouse dermal fibroblast and immune cells significantly enrich for genes within 200kb of the GWAS signals of immune-mediated skin conditions. Blue: insignificant; yellow to orange: significant with orange representing lower FDR; FDR: false discovery rate.

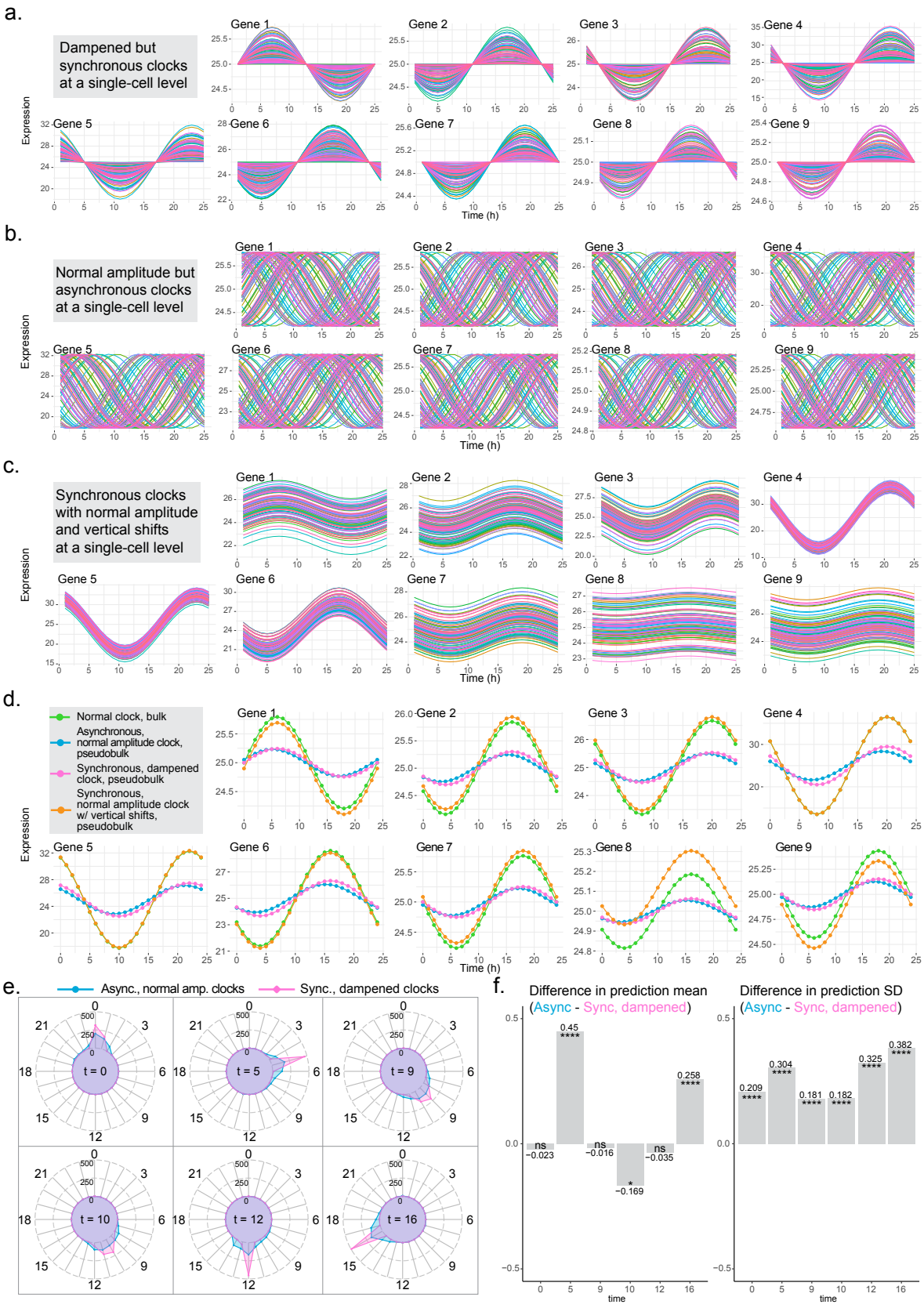

Figure 3.5: Legend on the next page.

Figure 3.5: **tauFisher can determine circadian phase heterogeneity in simulated data. a** Simulated expression of nine diurnal genes in 100 single cells that have synchronous circadian clocks with dampened amplitudes. **b** Simulated expression of nine diurnal genes in 100 single cells that have asynchronous circadian clocks but regular amplitudes. **c** Simulated expression of nine diurnal genes in 100 single cells that have synchronous circadian clocks with normal amplitudes but different mean expression level over time (vertical shifts). Because we needed to increase ranges of y-axis to plot all the curves, some curves may appear to be dampened (i.e. Gene 8). **a-c** Each line represents gene expression in a cell over time. **d** At the bulk level, scenarios in **a** and **b** generate similar patterns, which are oscillations with dampened amplitudes but similar peaking time when compared to a normal bulk-level clock. Scenario in **c** does not produce dampened amplitudes at the pseudobulk level. **e** We combined tauFisher with bootstrapping and randomly selected six time points to do the comparison. We generated 500 time labels predictions and plotted the distributions for the cells in **a** (pink) and **b**(blue). **f** Bar plots showing the differences between the prediction mean (left) and standard deviation (right) at each time point (cells in **b** - cells in **a**). ns: p-value > 0.05, $*$: p-value ≤ 0.05, $****$: p-value ≤ 0.0001.

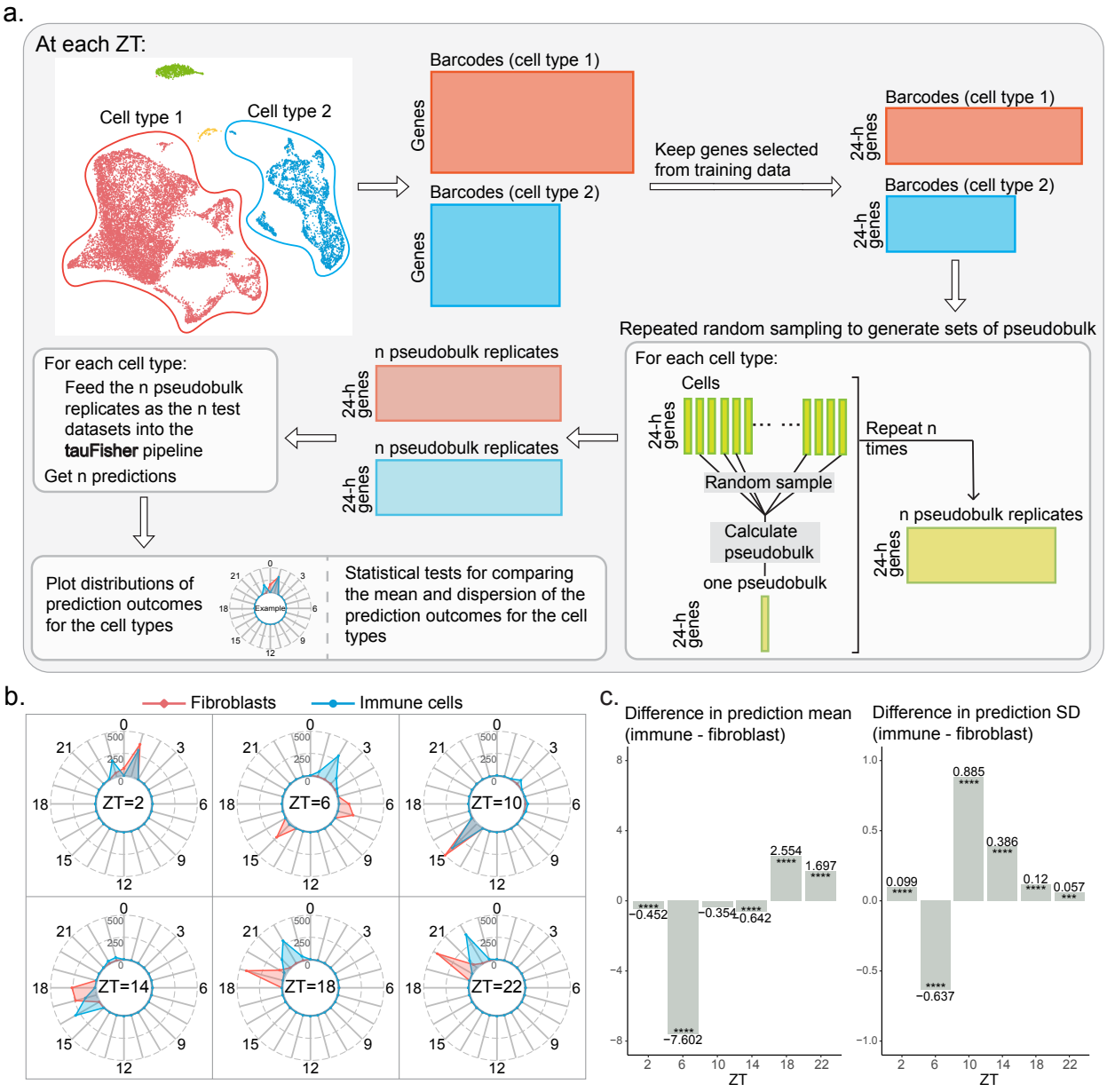

Figure 3.6: **tauFisher incorporated with bootstrapping suggests that the circadian phases in dermal immune cells are more heterogeneous than in dermal fibroblasts. a** A general overview of the pipeline that incorporates tauFisher with bootstrapping. **b** Radar plots showing the distribution of the prediction outcome for 500 pseudobulk replicates from dermal fibroblasts (red) and immune cells (blue). **c** Bar plots showing the differences between the prediction mean (left) and standard deviation (right) at each ZT (immune cells - fibroblasts). $****$: p-value ≤ 0.0001. P-values are determined using Rao's Tests for Homogeneity and the Wallraff Test of Angular Distances.

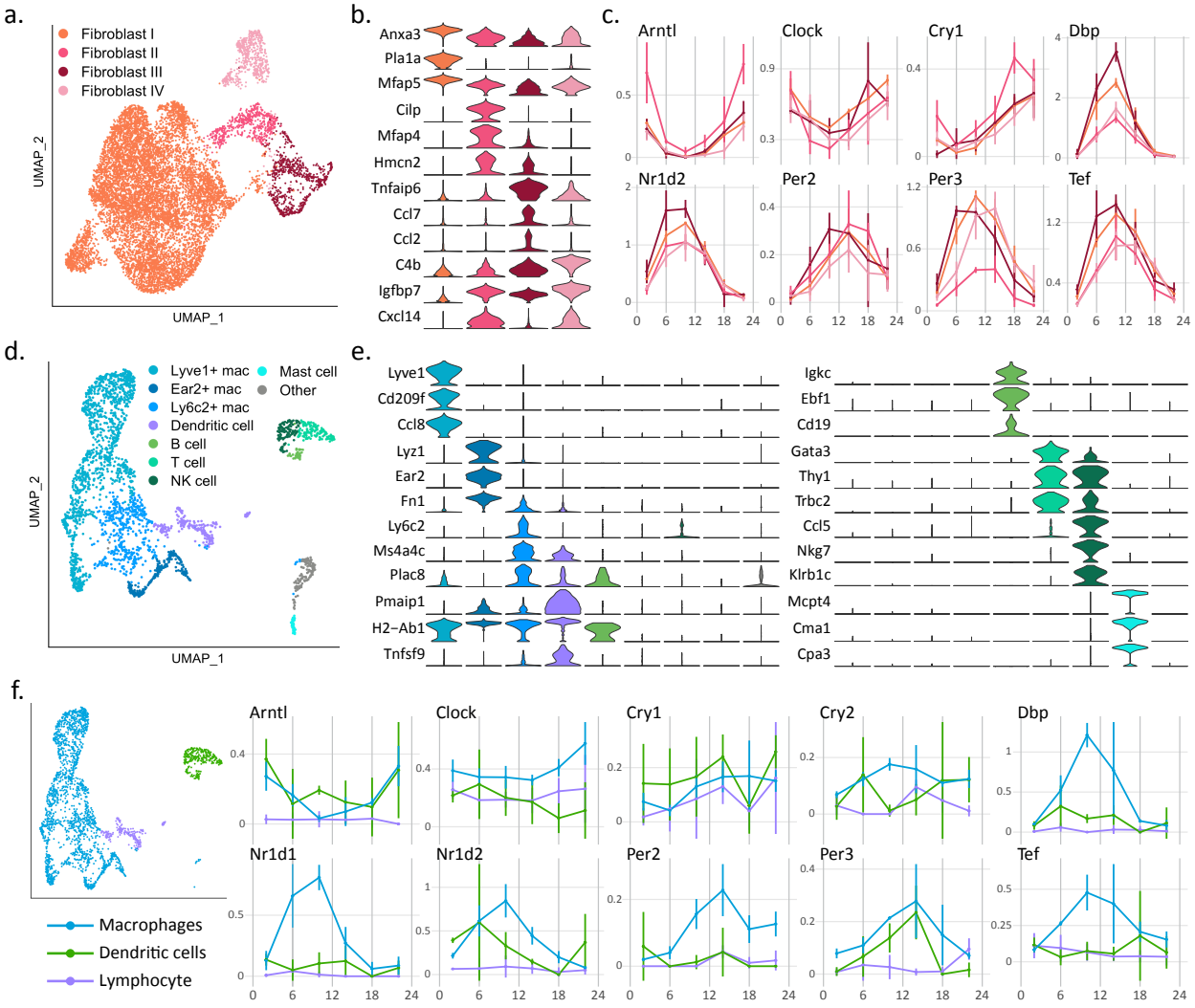

Figure 3.7: **Sub-populations of dermal fibroblasts and immune cells were identified.** **a** Four subclusters were identified for the dermal fibroblasts. **b** Violin plots show expression of marker genes for each fibroblast subcluster. **c** Core clock gene expression for the four fibroblast subclusters show similar rhythmic pattern. **d** Eight immune subclusters including both myeloid cells and lymphoid cells were identified. **e** Violin plots show expression of marker genes for each immune subcluster. **f** Due to low cell counts for some time points, we combined the eight subclusters of immune cells to form three major clusters. The core clock gene expression over time is plotted for the three major clusters. With the great variability present in the data, probably contributed by low cell counts, the core clock genes do not show robust rhythms.

Bibliography

[1] F. Abdallah, L. Mijouin, and C. Pichon. Skin immune landscape: Inside and outside the organism. *Mediators of inflammation*, 2017:5095293–5095293, 2017. 29180836[pmid].

[2] F. Agostinelli, N. Ceglia, B. Shahbaba, P. Sassone-Corsi, and P. Baldi. What time is it? deep learning approaches for circadian rhythms. *Bioinformatics*, 32(12):i8–i17, jun 2016.

[3] I. Aiello, M. L. M. Fedele, F. Román, L. Marpegan, C. Caldart, J. J. Chiesa, D. A. Golombek, C. V. Finkielstein, and N. Paladino. Circadian disruption promotes tumor-immune microenvironment remodeling favoring tumor cell proliferation. *Science advances*, 6(42):eaaz4530, Oct 2020. 33055171[pmid].

[4] M. Akashi, H. Soma, T. Yamamoto, A. Tsugitomi, S. Yamashita, T. Yamamoto, E. Nishida, A. Yasuda, J. K. Liao, and K. Node. Noninvasive method for assessing the human circadian clock using hair follicle cells. *Proceedings of the National Academy of Sciences*, 107(35):15643–15648, aug 2010.

[5] Y. Al-Nuaimi, J. A. Hardman, T. Bíró, I. S. Haslam, M. P. Philpott, B. I. Tóth, N. Farjo, B. Farjo, G. Baier, R. E. Watson, B. Grimaldi, J. E. Kloepper, and R. Paus. A meeting of two chronobiological systems: Circadian proteins period1 and BMAL1 modulate the human hair cycle clock. *Journal of Investigative Dermatology*, 134(3):610–619, mar 2014.

[6] H. Al-Waeli, B. Nicolau, L. Stone, L. Abu Nada, Q. Gao, M. N. Abdallah, E. Abdulkader, M. Suzuki, A. Mansour, A. Al Subaie, and F. Tamimi. Chronotherapy of non-steroidal anti-inflammatory drugs may enhance postoperative recovery. *Scientific Reports*, 10(1):468, Jan 2020.

[7] R. K. Alexander, Y.-H. Liou, N. H. Knudsen, K. A. Starost, C. Xu, A. L. Hyde, S. Liu, D. Jacobi, N.-S. Liao, and C.-H. Lee. Bmal1 integrates mitochondrial metabolism and macrophage activation. *eLife*, 9, may 2020.

[8] M. Ali, M. Zare, P. Zarrintaj, E. Alizadeh, E. Taghiabadi, M. Heidari-Kharaji, M. A. Amirkhani, M. R. Saeb, and M. Mozafari. Engineering the niche for hair regeneration — a critical review. *Nanomedicine: Nanotechnology, Biology and Medicine*, 15(1):70–85, jan 2019.

[9] R. C. Anafi, L. J. Francey, J. B. Hogenesch, and J. Kim. CYCLOPS reveals human transcriptional rhythms in health and disease. *Proceedings of the National Academy of Sciences*, 114(20):5312–5317, apr 2017.

[10] B. Andersen, J. Duan, and S. S. Karri. How and why the circadian clock regulates proliferation of adult epithelial stem cells. *Stem Cells*, Feburary 2023.

[11] N. Ando, Y. Nakamura, R. Aoki, K. Ishimaru, H. Ogawa, K. Okumura, S. Shibata, S. Shimada, and A. Nakao. Circadian gene clock regulates psoriasis-like skin inflammation in mice. *The Journal of investigative dermatology*, 135(12):3001–3008, Dec 2015. 26291684[pmid].

[12] E. S. Arnardottir, E. V. Nikonova, K. R. Shockley, A. A. Podtelezhnikov, R. C. Anafi, K. Q. Tanis, G. Maislin, D. J. Stone, J. J. Renger, C. J. Winrow, and A. I. Pack. Blood-gene expression reveals reduced circadian rhythmicity in individuals resistant to sleep deprivation. *Sleep*, 37:1589–1600, 10 2014.

[13] P. V. Ashok Kumar, P. P. Dakup, S. Sarkar, J. B. Modasia, M. S. Motzner, and S. Gaddameedhi. It's about time: Advances in understanding the circadian regulation of dna damage and repair in carcinogenesis and cancer treatment outcomes. *The Yale journal of biology and medicine*, 92(2):305–316, Jun 2019. 31249491[pmid].

[14] B. J. Auerbach, G. A. FitzGerald, and M. Li. Tempo: an unsupervised bayesian algorithm for circadian phase inference in single-cell transcriptomics. *Nature Communications*, 13(1), nov 2022.

[15] J. Bass. Circadian topology of metabolism. *Nature*, 491:348–356, 11 2012.

[16] A. Baumann, S. Gönnenwein, S. C. Bischoff, H. Sherman, N. Chapnik, O. Froy, and A. Lorentz. The circadian clock is functional in eosinophils and mast cells. *Immunology*, 140(4):465–474, Dec 2013.

[17] M. M. Bellet, E. Deriu, J. Z. Liu, B. Grimaldi, C. Blaschitz, M. Zeller, R. A. Edwards, S. Sahar, S. Dandekar, P. Baldi, M. D. George, M. Raffatellu, and P. Sassone-Corsi. Circadian clock regulates the host response to salmonella. *Proceedings of the National Academy of Sciences of the United States of America*, 110(24):9897–9902, Jun 2013. 23716692[pmid].

[18] S. A. Benitah and P.-S. Welz. Circadian regulation of adult stem cell homeostasis and aging. *Cell Stem Cell*, 26(6):817–831, jun 2020.

[19] J. Bentham, D. L. Morris, D. S. C. Graham, C. L. Pinder, P. Tombleson, T. W. Behrens, J. Martín, B. P. Fairfax, J. C. Knight, L. Chen, J. Replogle, A.-C. Syvänen, L. Rönnblom, R. R. Graham, J. E. Wither, J. D. Rioux, M. E. Alarcón-Riquelme, and T. J. Vyse. Genetic association analyses implicate aberrant regulation of innate and adaptive immunity genes in the pathogenesis of systemic lupus erythematosus. *Nature Genetics*, 47(12):1457–1464, oct 2015.

[20] R. C. Betz, L. Petukhova, S. Ripke, H. Huang, A. Menelaou, S. Redler, T. Becker, S. Heilmann, T. Yamany, M. Duvic, M. Hordinsky, D. Norris, V. H. Price, J. Mackay-Wiggan, A. de Jong, G. M. DeStefano, S. Moebus, M. Böhm, U. Blume-Peytavi, H. Wolff, G. Lutz, R. Kruse, L. Bian, C. I. Amos, A. Lee, P. K. Gregersen, B. Blaumeiser, D. Altshuler, R. Clynes, P. I. W. de Bakker, M. M. Nöthen, M. J. Daly, and A. M. Christiano. Genome-wide meta-analysis in alopecia areata resolves HLA associations and reveals two new susceptibility loci. *Nature Communications*, 6(1), jan 2015.

[21] B. Bilska, A. Zegar, A. T. Slominski, K. Kleszczyński, J. Cichy, and E. Pyza. Expression of antimicrobial peptide genes oscillates along day/night rhythm protecting mice skin from bacteria. *Experimental Dermatology*, n/a(n/a), Oct 2020.

[22] J. Blackwood, M. Malakhov, J. Duan, J. Pellett, I. Phadke, S. Lenhart, C. Sims, and K. Shea. Governance structure affects transboundary disease management under alternative objectives. *BMC Public Health*, 21, October 2021.

[23] F. Bonté, D. Girard, J.-C. Archambault, and A. Desmoulière. Skin changes during ageing. In *Subcellular Biochemistry*, pages 249–280. Springer Singapore, 2019.

[24] M. Bracci, V. Ciarapica, A. Copertaro, M. Barbaresi, N. Manzella, M. Tomasetti, S. Gaetani, F. Monaco, M. Amati, M. Valentino, V. Rapisarda, and L. Santarelli. Peripheral skin temperature and circadian biological clock in shift nurses after a day off. *International Journal of Molecular Sciences*, 17(5):623, apr 2016.

[25] N. L. Bragazzi, M. Sellami, I. Salem, R. Conic, M. Kimak, P. D. M. Pigatto, and G. Damiani. Fasting and its impact on skin anatomy, physiology, and physiopathology: A comprehensive review of the literature. *Nutrients*, 11(2):249, Jan 2019. 30678053[pmid].

[26] N. L. Bragazzi, K. Trabelsi, S. Garbarino, A. Ammar, H. Chtourou, A. Pacifico, P. Malagoli, H. Kocic, R. R. Z. Conic, K. Kridin, P. D. M. Pigatto, and G. D. and. Can intermittent, time-restricted circadian fasting modulate cutaneous severity of dermatological disorders? insights from a multicenter, observational, prospective study. *Dermatologic Therapy*, 34(3), mar 2021.

[27] R. Braun, W. L. Kath, M. Iwanaszko, E. Kula-Eversole, S. M. Abbott, K. J. Reid, P. C. Zee, and R. Allada. Universal method for robust detection of circadian state from gene expression. *Proceedings of the National Academy of Sciences*, 115(39):E9247–E9256, 2018.

[28] M. Budkowska, A. Lebiecka, Z. Marcinowska, J. Woźniak, M. Jastrzębska, and B. Dołęgowska. The circadian rhythm of selected parameters of the hemostasis system in healthy people. *Thrombosis Research*, 182:79–88, Oct 2019.

[29] E. D. Buhr and J. S. Takahashi. Molecular components of the mammalian circadian clock. In *Circadian Clocks*, pages 3–27. Springer Berlin Heidelberg, 2013.

[30] E. D. Buhr, S. Vemaraju, N. Diaz, R. A. Lang, and R. N. V. Gelder. Neuropsin (OPN5) mediates local light-dependent induction of circadian clock genes and circadian photoentrainment in exposed murine skin. *Current Biology*, 29(20):3478–3487.e4, oct 2019.

[31] E. D. Buhr, S.-H. Yoo, and J. S. Takahashi. Temperature as a universal resetting cue for mammalian circadian oscillators. *Science*, 330(6002):379–385, 2010.

[32] M. R. Buijink, A. H. O. O. Engberink, C. B. Wit, A. Almog, J. H. Meijer, J. H. T. Rohling, and S. Michel. Aging affects the capacity of photoperiodic adaptation downstream from the central molecular clock. *Journal of Biological Rhythms*, 35(2):167–179, jan 2020.

[33] E. J. Cable, K. G. Onishi, and B. J. Prendergast. Circadian rhythms accelerate wound healing in female siberian hamsters. *Physiology & behavior*, 171:165–174, Mar 2017. 27998755[pmid].

[34] K. V. Carias, M. Zoeteman, A. Seewald, M. R. Sanderson, J. M. Bischof, and R. Wevrick. A MAGEL2-deubiquitinase complex modulates the ubiquitination of circadian rhythm protein CRY1. *PLOS ONE*, 15(4):e0230874, apr 2020.

[35] Y.-S. Chang and B.-L. Chiang. Mechanism of sleep disturbance in children with atopic dermatitis and the role of the circadian rhythm and melatonin. *International Journal of Molecular Sciences*, 17(4):462, mar 2016.

[36] Y.-S. Chang, Y.-T. Chou, J.-H. Lee, P.-L. Lee, Y.-S. Dai, C. Sun, Y.-T. Lin, L.-C. Wang, H.-H. Yu, Y.-H. Yang, C.-A. Chen, K.-S. Wan, and B.-L. Chiang. Atopic dermatitis, melatonin, and sleep disturbance. *PEDIATRICS*, 134(2):e397–e405, jul 2014.

[37] L. Chen, S. Li, J. Nie, J. Zhao, S. Yu, Y. Li, and J. Peng. Bmal1 regulates coagulation factor biosynthesis in mouse liver in streptococcus oralis infection. *Frontiers in cellular and infection microbiology*, 10:530190–530190, Sep 2020. 33042871[pmid].

[38] K. H. Cox and J. S. Takahashi. Circadian clock genes and the transcriptional architecture of the clock mechanism. *Journal of molecular endocrinology*, 63(4):R93–R102, Nov 2019. 31557726[pmid].

[39] S. Crnko, B. C. Du Pré, J. P. G. Sluijter, and L. W. Van Laake. Circadian rhythms and the molecular clock in cardiovascular biology and disease. *Nature Reviews Cardiology*, 16(7):437–447, Jul 2019.

[40] P. Crosby, R. Hamnett, M. Putker, N. P. Hoyle, M. Reed, C. J. Karam, E. S. Maywood, A. Stangherlin, J. E. Chesham, E. A. Hayter, L. Rosenbrier-Ribeiro, P. Newham, H. Clevers, D. A. Bechtold, and J. S. O'Neill. Insulin/igf-1 drives period synthesis to entrain circadian rhythms with feeding time. *Cell*, 177(4):896–909.e20, May 2019. 31030999[pmid].

[41] P. Dakup and S. Gaddameedhi. Impact of the circadian clock on uv-induced dna damage response and photocarcinogenesis. *Photochemistry and photobiology*, 93(1):296–303, Jan 2017. 27861965[pmid].

[42] P. P. Dakup, K. I. Porter, and S. Gaddameedhi. The circadian clock protects against acute radiation-induced dermatitis. *Toxicology and Applied Pharmacology*, 399:115040, jul 2020.

[43] P. P. Dakup, K. I. Porter, A. A. Little, R. P. Gajula, H. Zhang, E. Skornyakov, M. G. Kemp, H. P. A. Van Dongen, and S. Gaddameedhi. The circadian clock regulates cisplatin-induced toxicity and tumor regression in melanoma mouse and human models. *Oncotarget*, 9(18):14524–14538, Feb 2018. PMC5865687[pmcid].

[44] G. Damiani, A. Watad, C. Bridgewood, P. Pigatto, A. Pacifico, P. Malagoli, N. Bragazzi, and M. Adawi. The impact of ramadan fasting on the reduction of PASI score, in moderate-to-severe psoriatic patients: A real-life multicenter study. *Nutrients*, 11(2):277, jan 2019.

[45] K. Davis, L. C. Roden, V. D. Leaner, and P. J. van der Watt. The tumour suppressing role of the circadian clock. *IUBMB Life*, 71(7):771–780, jan 2019.

[46] L. V. M. de Assis, G. S. Kinker, M. N. Moraes, R. P. Markus, P. A. Fernandes, and A. M. d. L. Castrucci. Expression of the circadian clock gene bmal1 positively correlates with antitumor immunity and patient survival in metastatic melanoma. *Frontiers in oncology*, 8:185–185, Jun 2018. 29946530[pmid].

[47] L. V. M. de Assis, M. N. Moraes, K. K. Magalhães-Marques, G. S. Kinker, S. da Silveira Cruz-Machado, and A. M. d. L. Castrucci. Non-metastatic cutaneous melanoma induces chronodisruption in central and peripheral circadian clocks. *International journal of molecular sciences*, 19(4):1065, Apr 2018. 29614021[pmid].

[48] L. V. M. de Assis, P. N. Tonolli, M. N. Moraes, M. S. Baptista, and A. M. de Lauro Castrucci. How does the skin sense sun light? an integrative view of light sensing molecules. *Journal of Photochemistry and Photobiology C: Photochemistry Reviews*, 47:100403, jun 2021.

[49] L. C. J. de Bree, V. P. Mourits, V. A. Koeken, S. J. Moorlag, R. Janssen, L. Folkman, D. Barreca, T. Krausgruber, V. Fife-Gernedl, B. Novakovic, R. J. Arts, H. Dijkstra, H. Lemmers, C. Bock, L. A. Joosten, R. van Crevel, C. S. Benn, and M. G. Netea. Circadian rhythm influences induction of trained immunity by bcg vaccination. *The Journal of clinical investigation*, 130(10):5603–5617, Oct 2020. 32692732[pmid].

[50] S. Deota and S. Panda. New horizons: Circadian control of metabolism offers novel insight into the cause and treatment of metabolic diseases. *The Journal of Clinical Endocrinology & Metabolism*, 106(3):e1488–e1493, Mar 2021.

[51] P. Di Meglio, G. K. Perera, and F. O. Nestle. The multitasking organ: Recent insights into skin immune function. *Immunity*, 35(6):857–869, Dec 2011.

[52] B. A. Dickerman, S. C. Markt, M. Koskenvuo, C. Hublin, E. Pukkala, L. A. Mucci, and J. Kaprio. Sleep disruption, chronotype, shift work, and prostate cancer risk and mortality: a 30-year prospective cohort study of finnish twins. *Cancer Causes & Control*, 27(11):1361–1370, oct 2016.

[53] K. Dong, E. Goyarts, A. Rella, E. Pelle, Y. H. Wong, and N. Pernodet. Age associated decrease of mt-1 melatonin receptor in human dermal skin fibroblasts impairs protection against uv-induced dna damage. *International journal of molecular sciences*, 21(1):326, Jan 2020. 31947744[pmid].

[54] J. Duan, C. Grando, S. Liu, A. Chernyavsky, J. K. Chen, B. Andersen, and S. A. Grando. The M3 muscarinic acetylcholine receptor promotes epidermal differentiation. *Journal of Investigative Dermatology*, July 2022.

[55] J. Duan, E. N. Greenberg, S. S. Karri, and B. Andersen. The circadian clock and diseases of the skin. *FEBS Letters*, 595(19):2413–2436, Sept. 2021.

[56] J. Duan, M. Malakhov, J. Pellett, I. Phadke, J. Barber, and J. Blackwood. Management efficacy in a metapopulation model of white-nose syndrome. *Natural Resource Modeling*, 34, August 2021.

[57] J. Duan, M. N. Ngo, S. S. Karri, L. C. Tsoi, J. E. Gudjonsson, B. Shahbaba, J. Lowengrub, and B. Andersen. taufisher predicts circadian time from a single sample of bulk and single-cell pseudobulk transcriptomic data. *Nature Communications*, 15(1), May 2024.

[58] Y. V. Dubrovsky, W. E. Samsa, and R. V. Kondratov. Deficiency of circadian protein clock reduces lifespan and increases age-related cataract development in mice. *Aging*, 2(12):936–944, Dec 2010. 21149897[pmid].

[59] S. Durinck, Y. Moreau, A. Kasprzyk, S. Davis, B. D. Moor, A. Brazma, and W. Huber. Biomart and bioconductor: a powerful link between biological databases and microarray data analysis. *Bioinformatics*, 21:3439–3440, 8 2005.

[60] S. Durinck, P. T. Spellman, E. Birney, and W. Huber. Mapping identifiers for the integration of genomic datasets with the r/bioconductor package biomart. *Nature Protocols 2009 4:8*, 4:1184–1191, 7 2009.

[61] R. S. Edgar, A. Stangherlin, A. D. Nagy, M. P. Nicoll, S. Efstathiou, J. S. O'Neill, and A. B. Reddy. Cell autonomous regulation of herpes and influenza virus infection by the circadian clock. *Proceedings of the National Academy of Sciences*, 113(36):10085, Sep 2016.

[62] A. Ehlers, W. Xie, E. Agapov, S. Brown, D. Steinberg, R. Tidwell, G. Sajol, R. Schutz, R. Weaver, H. Yu, M. Castro, L. B. Bacharier, X. Wang, M. J. Holtzman, and J. A. Haspel. Bmal1 links the circadian clock to viral airway pathology and asthma phenotypes. *Mucosal immunology*, 11(1):97–111, Jan 2018. 28401936[pmid].

[63] F. Ferguson, G. Lada, H. Hunter, C. Bundy, A. Henry, C. Griffiths, and C. Kleyn. Diurnal and seasonal variation in psoriasis symptoms. *Journal of the European Academy of Dermatology and Venereology*, 35(1), aug 2020.

[64] F. J. Ferguson, G. Lada, H. J. A. Hunter, C. Bundy, A. L. Henry, C. E. M. Griffiths, and C. E. Kleyn. Diurnal and seasonal variation in psoriasis symptoms. *Journal of the European Academy of Dermatology and Venereology*, 35(1):e45–e47, Jan 2021.

[65] M. F. Forni, J. Peloggia, T. T. Braga, J. E. O. Chinchilla, J. Shinohara, C. A. Navas, N. O. S. Camara, and A. J. Kowaltowski. Caloric restriction promotes structural and metabolic changes in the skin. *Cell Reports*, 20(11):2678–2692, sep 2017.

[66] A. Franzoni, E. Markova-Car, S. Dević-Pavlić, D. Jurišić, C. Puppin, C. Mio, M. D. Luca, G. Petruz, G. Damante, and S. K. Pavelić. A polymorphic GGC repeat in the NPAS2 gene and its association with melanoma. *Experimental Biology and Medicine*, 242(15):1553–1558, aug 2017.

[67] O. Froy and M. Garaulet. The circadian clock in white and brown adipose tissue: Mechanistic, endocrine, and clinical aspects. *Endocrine reviews*, 39(3):261–273, Jun 2018. 29490014[pmid].

[68] S. Gaddameedhi, C. P. Selby, W. K. Kaufmann, R. C. Smart, and A. Sancar. Control of skin cancer by the circadian rhythm. *Proceedings of the National Academy of Sciences of the United States of America*, 108(46):18790–18795, Nov 2011. 22025708[pmid].

[69] S. Gaddameedhi, C. P. Selby, M. G. Kemp, R. Ye, and A. Sancar. The circadian clock controls sunburn apoptosis and erythema in mouse skin. *The Journal of investigative dermatology*, 135(4):1119–1127, Apr 2015. 25431853[pmid].

[70] K. L. Gamble, R. Berry, S. J. Frank, and M. E. Young. Circadian clock control of endocrine factors. *Nature Reviews Endocrinology*, 10(8):466–475, may 2014.

[71] M. Geyfman and B. Andersen. Clock genes, hair growth and aging. *Aging*, 2(3):122–128, mar 2010.

[72] M. Geyfman, V. Kumar, Q. Liu, R. Ruiz, W. Gordon, F. Espitia, E. Cam, S. E. Millar, P. Smyth, A. Ihler, J. S. Takahashi, and B. Andersen. Brain and muscle arnt-like protein-1 (bmal1) controls circadian cell proliferation and susceptibility to uvb-induced dna damage in the epidermis. *Proceedings of the National Academy of Sciences*, 109(29):11758–11763, 2012.

[73] M. Geyfman, M. V. Plikus, E. Treffeisen, B. Andersen, and R. Paus. Resting no more: re-defining telogen, the maintenance stage of the hair growth cycle. *Biological reviews of the Cambridge Philosophical Society*, 90(4):1179–1196, Nov 2015. 25410793[pmid].

[74] E. F. Glynn, J. Chen, and A. R. Mushegian. Detecting periodic patterns in unevenly spaced gene expression time series using lomb–scargle periodograms. *Bioinformatics*, 22:310–316, 2 2006.

[75] E. N. Greenberg, M. E. Marshall, S. Jin, S. Venkatesh, M. Dragan, L. C. Tsoi, J. E. Gudjonsson, Q. Nie, J. S. Takahashi, and B. Andersen. Circadian control of interferon-sensitive gene expression in murine skin. *Proceedings of the National Academy of Sciences of the United States of America*, 117(11):5761–5771, Mar 2020. 32132203[pmid].

[76] D. Gutierrez and J. Arbesman. Circadian dysrhythmias, physiological aberrations, and the link to skin cancer. *International Journal of Molecular Sciences*, 17(5):621, apr 2016.

[77] J. Hansen. Night shift work and risk of breast cancer. *Current Environmental Health Reports*, 4(3):325–339, aug 2017.

[78] J. A. Hardman, I. S. Haslam, N. Farjo, B. Farjo, and R. Paus. Thyroxine differentially modulates the peripheral clock: Lessons from the human hair follicle. *PLOS ONE*, 10(3):e0121878, mar 2015.

[79] M. H. Hastings, E. S. Maywood, and M. Brancaccio. Generation of circadian rhythms in the suprachiasmatic nucleus. *Nature Reviews Neuroscience*, 19(8):453–469, Aug 2018.

[80] M. Hattammaru, Y. Tahara, T. Kikuchi, K. Okajima, K. Konishi, S. Nakajima, K. Sato, K. Otsuka, H. Sakura, S. Shibata, and T. Nakaoka. The effect of night shift work on the expression of clock genes in beard hair follicle cells. *Sleep Medicine*, 56:164–170, apr 2019.

[81] E. Healy, N. J. Reynolds, M. D. Smith, C. Campbell, P. M. Farr, and J. L. Rees. Dissociation of erythema and p53 protein expression in human skin following uvb irradiation, and induction of p53 protein and mrna following application of skin irritants. *Journal of Investigative Dermatology*, 103(4):493–499, 1994.

[82] K. Hiramoto, K. Orita, Y. Yamate, E. Kasahara, S. Yokoyama, and E. F. Sato. The clock genes are involved in the deterioration of atopic dermatitis after day-and-night reversed physical stress in nc/nga mice. *The open biochemistry journal*, 12:87–102, Jun 2018. 30069250[pmid].

[83] S. J. Holtkamp, L. M. Ince, C. Barnoud, M. T. Schmitt, F. Sinturel, V. Pilorz, R. Pick, S. Jemelin, M. Mühlstädt, W.-H. Boehncke, J. Weber, D. Laubender, J. Philippou-Massier, C.-S. Chen, L. Holtermann, D. Vestweber, M. Sperandio, B. U. Schraml, C. Halin, C. Dibner, H. Oster, J. Renkawitz, and C. Scheiermann. Circadian clocks guide dendritic cells into skin lymphatics. *Nature Immunology*, 22(11):1375–1381, Oct. 2021.

[84] S. Hood and S. Amir. The aging clock: circadian rhythms and later life. *Journal of Clinical Investigation*, 127(2):437–446, feb 2017.

[85] N. P. Hoyle, E. Seinkmane, M. Putker, K. A. Feeney, T. P. Krogager, J. E. Chesham, L. K. Bray, J. M. Thomas, K. Dunn, J. Blaikley, and J. S. O'Neill. Circadian actin dynamics drive rhythmic fibroblast mobilization during wound healing. *Science translational medicine*, 9(415):eaal2774, Nov 2017. 29118260[pmid].

[86] C.-M. Hsu, S.-F. Lin, C.-T. Lu, P.-M. Lin, and M.-Y. Yang. Altered expression of circadian clock genes in head and neck squamous cell carcinoma. *Tumor Biology*, 33(1):149–155, nov 2011.

[87] Y. Huang and R. Braun. Platform-independent estimation of human physiological time from single blood samples. *Proceedings of the National Academy of Sciences*, 121(3), Jan. 2024.

[88] M. E. Hughes, J. B. Hogenesch, and K. Kornacker. Jtk_cycle: an efficient non-parametric algorithm for detecting rhythmic components in genome-scale datasets. *Journal of biological rhythms*, 25:372, 10 2010.

[89] J. J. Hughey, T. Hastie, and A. J. Butte. Zeitzeiger: Supervised learning for high-dimensional data from an oscillatory system. *Nucleic Acids Research*, 44:e80, 5 2016.

[90] I. Iurisci, E. Filipski, J. Reinhardt, S. Bach, A. Gianella-Borradori, S. Iacobelli, L. Meijer, and F. Levi. Improved tumor control through circadian clock induction by seliciclib, a cyclin-dependent kinase inhibitor. *Cancer Research*, 66(22):10720–10728, nov 2006.

[91] H. Jacob, A. M. Curtis, and C. J. Kearney. Therapeutics on the clock: Circadian medicine in the treatment of chronic inflammatory diseases. *Biochemical Pharmacology*, 182:114254, Dec 2020.

[92] P. Janich, G. Pascual, A. Merlos-Suárez, E. Batlle, J. Ripperger, U. Albrecht, H.-Y. M. Cheng, K. Obrietan, L. D. Croce, and S. A. Benitah. The circadian molecular clock creates epidermal stem cell heterogeneity. *Nature*, 480(7376):209–214, nov 2011.

[93] Y. Jin, G. Andersen, D. Yorgov, T. M. Ferrara, S. Ben, K. M. Brownson, P. J. Holland, S. A. Birlea, J. Siebert, A. Hartmann, A. Lienert, N. van Geel, J. Lambert, R. M. Luiten, A. Wolkerstorfer, J. P. W. van der Veen, D. C. Bennett, A. Taïeb, K. Ezzedine, E. H. Kemp, D. J. Gawkrodger, A. P. Weetman, S. Kõks, E. Prans, K. Kingo, M. Karelson, M. R. Wallace, W. T. McCormack, A. Overbeck, S. Moretti, R. Colucci, M. Picardo, N. B. Silverberg, M. Olsson, Y. Valle, I. Korobko, M. Böhm, H. W. Lim, I. Hamzavi, L. Zhou, Q.-S. Mi, P. R. Fain, S. A. Santorico, and R. A. Spritz. Genome-wide association studies of autoimmune vitiligo identify 23 new risk loci and highlight key pathways and regulatory variants. *Nature Genetics*, 48(11):1418–1424, oct 2016.

[94] J. Kajimoto, R. Matsumura, K. Node, and M. Akashi. Potential role of the pancreatic hormone insulin in resetting human peripheral clocks. *Genes to Cells*, 23(5):393–399, 2018.

[95] D. J. Kennaway. A critical review of melatonin assays: Past and present. *Journal of Pineal Research*, 67(1):e12572, Aug 2019.

[96] N. M. Kettner, H. Voicu, M. J. Finegold, C. Coarfa, A. Sreekumar, N. Putluri, C. A. Katchy, C. Lee, D. D. Moore, and L. Fu. Circadian homeostasis of liver metabolism suppresses hepatocarcinogenesis. *Cancer Cell*, 30(6):909–924, dec 2016.

[97] R. V. Khapre, A. A. Kondratova, O. Susova, and R. V. Kondratov. Circadian clock protein BMAL1 regulates cellular senescence in vivo. *Cell Cycle*, 10(23):4162–4169, dec 2011.

[98] M. Khosravipour, P. Khanlari, S. Khazaie, H. Khosravipour, and H. Khazaie. A systematic review and meta-analysis of the association between shift work and metabolic syndrome: The roles of sleep, gender, and type of shift work. *Sleep Medicine Reviews*, 57:101427, jun 2021.

[99] M. Khosravipour, M. Shahmohammadi, and H. V. Athar. The effects of rotating and extended night shift work on the prevalence of metabolic syndrome and its components. *Diabetes & Metabolic Syndrome: Clinical Research & Reviews*, 13(6):3085–3089, nov 2019.

[100] S. Kiessling, L. Beaulieu-Laroche, I. D. Blum, D. Landgraf, D. K. Welsh, K.-F. Storch, N. Labrecque, and N. Cermakian. Enhancing circadian clock function in cancer cells inhibits tumor growth. *BMC Biology*, 15(1):13, Feb 2017.

[101] S. Kiessling, G. Dubeau-Laramée, H. Ohm, N. Labrecque, M. Olivier, and N. Cermakian. The circadian clock in immune cells controls the magnitude of leishmania parasite infection. *Scientific Reports*, 7(1):10892, Sep 2017.

[102] R. V. Kondratov, A. A. Kondratova, V. Y. Gorbacheva, O. V. Vykhovanets, and M. P. Antoch. Early aging and age-related pathologies in mice deficient in bmal1, the core componentof the circadian clock. *Genes & development*, 20(14):1868–1873, Jul 2006. 16847346[pmid].

[103] S. Koren, E. B. Whorton Jr., and W. R. Fleischmann Jr. Circadian dependence of interferon antitumor activity in mice. *JNCI: Journal of the National Cancer Institute*, 85(23):1927–1932, Dec 1993.

[104] K. B. Koronowski, K. Kinouchi, P.-S. Welz, J. G. Smith, V. M. Zinna, J. Shi, M. Samad, S. Chen, C. N. Magnan, J. M. Kinchen, W. Li, P. Baldi, S. A. Benitah, and P. Sassone-Corsi. Defining the independence of the liver circadian clock. *Cell*, 177(6):1448–1462.e14, may 2019.

[105] E. Kowalska, J. A. Ripperger, D. C. Hoegger, P. Bruegger, T. Buch, T. Birchler, A. Mueller, U. Albrecht, C. Contaldo, and S. A. Brown. Nono couples the circadian clock to the cell cycle. *Proceedings of the National Academy of Sciences of the United States of America*, 110(5):1592–1599, Jan 2012. 23267082[pmid].

[106] N. Labrecque and N. Cermakian. Circadian clocks in the immune system. *Journal of Biological Rhythms*, 30(4):277–290, Aug 2015.

[107] E. E. Laing, C. S. Möller-Levet, N. Poh, N. Santhi, S. N. Archer, and D. J. Dijk. Blood transcriptome based biomarkers for human circadian phase. *Elife*, 6, 02 2017.

[108] K. A. Lamia, S. J. Papp, R. T. Yu, G. D. Barish, N. H. Uhlenhaut, J. W. Jonker, M. Downes, and R. M. Evans. Cryptochromes mediate rhythmic repression of the glucocorticoid receptor. *Nature*, 480(7378):552–556, Dec 2011. 22170608[pmid].

[109] V. Lang, S. Ferencik, B. Ananthasubramaniam, A. Kramer, and B. Maier. Susceptibility rhythm to bacterial endotoxin in myeloid clock-knockout mice. *eLife*, 10:e62469, oct 2021.

[110] D. Lekkas and G. K. Paschos. The circadian clock control of adipose tissue physiology and metabolism. *Autonomic Neuroscience: Basic and Clinical*, 219:66–70, Jul 2019.

[111] W.-Q. Li, A. A. Qureshi, E. S. Schernhammer, and J. Han. Rotating night-shift work and risk of psoriasis in us women. *The Journal of investigative dermatology*, 133(2):565–567, Feb 2013. 22931920[pmid].

[112] X. Liang and G. A. FitzGerald. Timing the microbes: The circadian rhythm of the gut microbiome. *Journal of Biological Rhythms*, 32(6):505–515, Dec 2017.

[113] K. K. Lin, V. Kumar, M. Geyfman, D. Chudova, A. T. Ihler, P. Smyth, R. Paus, J. S. Takahashi, and B. Andersen. Circadian clock genes contribute to the regulation of hair follicle cycling. *PLoS Genetics*, 5(7):e1000573, jul 2009.

[114] J. E. Long, M. T. Drayson, A. E. Taylor, K. M. Toellner, J. M. Lord, and A. C. Phillips. Morning vaccination enhances antibody response over afternoon vaccination: A cluster-randomised trial. *Vaccine*, 34(24):2679–2685, May 2016. 27129425[pmid].

[115] E. López-Isac, M. Acosta-Herrera, M. Kerick, S. Assassi, A. T. Satpathy, J. Granja, M. R. Mumbach, L. Beretta, C. P. Simeón, P. Carreira, N. Ortego-Centeno, I. Castellvi, L. Bossini-Castillo, F. D. Carmona, G. Orozco, N. Hunzelmann, J. H. W. Distler, A. Franke, C. Lunardi, G. Moroncini, A. Gabrielli, J. de Vries-Bouwstra, C. Wijmenga, B. P. C. Koeleman, A. Nordin, L. Padyukov, A.-M. Hoffmann-Vold, B. Lie, R. Ríos, J. L. Callejas, J. A. Vargas-Hitos, R. García-Portales, M. T. Camps, A. Fernández-Nebro, M. F. González-Escribano, F. J. García-Hernández, M. J. Castillo, M. A. Aguirre, I. Gómez-Gracia, B. Fernández-Gutiérrez, L. Rodríguez-Rodríguez, P. G. de la Peña, E. Vicente, J. L. Andreu, M. F. de Castro, F. J. López-Longo, L. Martínez, Fonollosa, A. Guillén, G. Espinosa, C. Tolosa, A. Pros, M. Rodríguez-Carballeira, F. J. Narváez, M. Rubio-Rivas, Ortiz-Santamaría, A. B. M. nero, M. A. González-Gay, B. Díaz, L. Trapiella, A. Sousa, M. V. Egurbide, P. Fanlo-Mateo, L. Sáez-Comet, F. Díaz, Hernández, E. Beltrán, J. A. Román-Ivorra, E. Grau, J. J. Alegre-Sancho, M. Freire, F. J. Blanco-García, N. Oreiro, T. Witte, A. Kreuter, G. Riemekasten, P. Airó, C. Magro, A. E. Voskuyl, M. C. Vonk, R. Hesselstrand, S. Proudman, W. Stevens, M. Nikpour, J. Zochling, J. Sahhar, J. Roddy, P. Nash, K. Tymms, M. Rischmueller, S. Lester, T. Vyse, A. L. Herrick, J. Worthington, C. P. Denton, Y. Allanore, M. A. Brown, T. R. D. J. Radstake, C. Fonseca, H. Y. Chang, M. D. Mayes, J. Martin, and and. GWAS for systemic sclerosis identifies multiple risk loci and highlights fibrotic and vasculopathy pathways. *Nature Communications*, 10(1), oct 2019.

[116] F. Lu, A. Suggs, H. H. Ezaldein, J. Ya, P. Fu, J. Jamora, V. Verallo-Rowel, and E. D. Baron. The effect of shift work and poor sleep on self-reported skin conditions: A survey of call center agents in the philippines. *Clocks & sleep*, 1(2):273–279, May 2019. 33089169[pmid].

[117] J. Lubov, W. Cvammen, and M. Kemp. The impact of the circadian clock on skin physiology and cancer development. *International Journal of Molecular Sciences*, 22(11):6112, jun 2021.

[118] P. Martin and R. Nunan. Cellular and molecular mechanisms of repair in acute and chronic wound healing. *British Journal of Dermatology*, 173(2):370–378, jul 2015.

[119] S. Masri, K. Kinouchi, and P. Sassone-Corsi. Circadian clocks, epigenetics, and cancer. *Current Opinion in Oncology*, 27(1):50–56, jan 2015.

[120] R. Matsumura, K. Node, and M. Akashi. Estimation methods for human circadian phase by use of peripheral tissues. *Hypertension Research*, 39(9):623–627, Sep 2016.

[121] N. Matsunaga, K. Itcho, K. Hamamura, E. Ikeda, H. Ikeyama, Y. Furuichi, M. Watanabe, S. Koyanagi, and S. Ohdo. 24-hour rhythm of aquaporin-3 function in the epidermis is regulated by molecular clocks. *Journal of Investigative Dermatology*, 134(6):1636–1644, jun 2014.

[122] B. L. Mitchell, J. R. Saklatvala, N. Dand, F. A. Hagenbeek, X. Li, J. L. Min, L. Thomas, M. Bartels, J. J. Hottenga, M. K. Lupton, D. I. Boomsma, X. Dong, K. Hveem, M. Løset, N. G. Martin, J. N. Barker, J. Han, C. H. Smith, M. E. Rentería, and M. A. Simpson. Genome-wide association meta-analysis identifies 29 new acne susceptibility loci. *Nature Communications*, 13(1), feb 2022.

[123] H. Mizutani, R. Tamagawa-Mineoka, Y. Minami, K. Yagita, and N. Katoh. Constant light exposure impairs immune tolerance development in mice. *Journal of Dermatological Science*, 86(1):63–70, Apr 2017.

[124] D. Montaigne, X. Marechal, T. Modine, A. Coisne, S. Mouton, G. Fayad, S. Ninni, C. Klein, S. Ortmans, C. Seunes, C. Potelle, A. Berthier, C. Gheeraert, C. Piveteau, R. Deprez, J. Eeckhoute, H. Duez, D. Lacroix, B. Deprez, B. Jegou, M. Koussa, J.-L. Edme, P. Lefebvre, and B. Staels. Daytime variation of perioperative myocardial injury in cardiac surgery and its prevention by rev-erbα antagonism: a single-centre propensity-matched cohort study and a randomised study. *The Lancet*, 391(10115):59–69, jan 2018.

[125] B. A. Morgan. The dermal papilla: an instructive niche for epithelial stem and progenitor cells in development and regeneration of the hair follicle. *Cold Spring Harbor perspectives in medicine*, 4(7):a015180–a015180, Jul 2014. 24985131[pmid].

[126] H. Morinaga, Y. Mohri, M. Grachtchouk, K. Asakawa, H. Matsumura, M. Oshima, N. Takayama, T. Kato, Y. Nishimori, Y. Sorimachi, K. Takubo, T. Suganami, A. Iwama, Y. Iwakura, A. A. Dlugosz, and E. K. Nishimura. Obesity accelerates

hair thinning by stem cell-centric converging mechanisms. *Nature*, 595(7866):266–271, jun 2021.

[127] C. J. Morris, T. E. Purvis, K. Hu, and F. A. J. L. Scheer. Circadian misalignment increases cardiovascular disease risk factors in humans. *Proceedings of the National Academy of Sciences*, 113(10), feb 2016.

[128] Y. Nakamura, N. Nakano, K. Ishimaru, M. Hara, T. Ikegami, Y. Tahara, R. Katoh, H. Ogawa, K. Okumura, S. Shibata, C. Nishiyama, and A. Nakao. Circadian regulation of allergic reactions by the mast cell clock in mice. *Journal of Allergy and Clinical Immunology*, 133(2):568–575.e12, Feb 2014.

[129] M. N. Ngo and J. Duan. micnngo/taufisher: Issue doi. Mar. 2024.

[130] A. V. Nguyen and A. M. Soulika. The dynamics of the skin's immune system. *International journal of molecular sciences*, 20(8):1811, Apr 2019.

[131] N. T. Nguyen and D. E. Fisher. Mitf and uv responses in skin: From pigmentation to addiction. *Pigment cell & melanoma research*, 32(2):224–236, Mar 2019.

[132] V. Nikkola, M. Grönroos, R. Huotari-Orava, H. Kautiainen, L. Ylianttila, T. Karppinen, T. Partonen, and E. Snellman. Circadian time effects on nb-uvb-induced erythema in human skin in vivo. *Journal of Investigative Dermatology*, 138(2):464–467, Feb 2018.

[133] J. Nowowiejska, A. Baran, and I. Flisiak. Aberrations in lipid expression and metabolism in psoriasis. *International Journal of Molecular Sciences*, 22(12):6561, jun 2021.

[134] S. Panda. Circadian physiology of metabolism. *Science*, 354(6315):1008–1015, nov 2016.

[135] M. Pasparakis, I. Haase, and F. O. Nestle. Mechanisms regulating skin immunity and inflammation. *Nature Reviews Immunology*, 14(5):289–301, May 2014.

[136] L. Paternoster, 10.1038/s41467-019-12760-yMarie Standl, and S. J. Brown. Multiancestry genome-wide association study of 21,000 cases and 95,000 controls identifies new risk loci for atopic dermatitis. *Nature Genetics*, 47(12):1449–1456, oct 2015.

[137] M. T. Patrick, P. E. Stuart, K. Raja, J. E. Gudjonsson, T. Tejasvi, J. Yang, V. Chandran, S. Das, K. Callis-Duffin, E. Ellinghaus, C. Enerbäck, T. onu Esko, A. Franke, H. M. Kang, G. G. Krueger, H. W. Lim, P. Rahman, C. F. Rosen, S. Weidinger, M. Weichenthal, X. Wen, J. J. Voorhees, G. R. Abecasis, D. D. Gladman, R. P. Nair, J. T. Elder, and L. C. Tsoi. Genetic signature to provide robust risk assessment of psoriatic arthritis development in psoriasis patients. *Nature Communications*, 9(1), oct 2018.

[138] M. V. Plikus and B. Andersen. Skin as a window to body-clock time. *Proceedings of the National Academy of Sciences*, 115(48):12095–12097, nov 2018.

[139] M. V. Plikus, E. N. Van Spyk, K. Pham, M. Geyfman, V. Kumar, J. S. Takahashi, and B. Andersen. The circadian clock in skin: implications for adult stem cells, tissue regeneration, cancer, aging, and immunity. *Journal of biological rhythms*, 30(3):163–182, Jun 2015. 25589491[pmid].

[140] M. V. Plikus, C. Vollmers, D. de la Cruz, A. Chaix, R. Ramos, S. Panda, and C.-M. Chuong. Local circadian clock gates cell cycle progression of transient amplifying cells during regenerative hair cycling. *Proceedings of the National Academy of Sciences*, 110(23):E2106–E2115, may 2013.

[141] M. V. Plikus, C. Vollmers, D. de la Cruz, A. Chaix, R. Ramos, S. Panda, and C.-M. Chuong. Local circadian clock gates cell cycle progression of transient amplifying cells during regenerative hair cycling. *Proceedings of the National Academy of Sciences*, 110(23), may 2013.

[142] E. Poggiogalle, H. Jamshed, and C. M. Peterson. Circadian regulation of glucose, lipid, and energy metabolism in humans. *Metabolism*, 84:11–27, jul 2018.

[143] M. Ramos-e Silva, M. Chaves Azevedo-e Silva, and S. C. Carneiro. Hair, nail, and pigment changes in major systemic disease. *Clinics in Dermatology*, 26(3):296–305, May 2008.

[144] A. Relógio, P. Thomas, P. Medina-Pérez, S. Reischl, S. Bervoets, E. Gloc, P. Riemer, S. Mang-Fatehi, B. Maier, R. Schäfer, U. Leser, H. Herzel, A. Kramer, and C. Sers. Ras-mediated deregulation of the circadian clock in cancer. *PLoS Genetics*, 10(5):e1004338, may 2014.

[145] A. L. Rippa, E. P. Kalabusheva, and E. A. Vorotelyak. Regeneration of dermis: Scarring and cells involved. *Cells*, 8(6):607, June 2019.

[146] V. P. Roche, A. Mohamad-Djafari, P. F. Innominato, A. Karaboué, A. Gorbach, and F. A. Lévi. Thoracic surface temperature rhythms as circadian biomarkers for cancer chronotherapy. *Chronobiology international*, 31(3):409–420, Apr 2014. 24397341[pmid].

[147] G. D. Rodrigues, E. M. Fiorelli, L. Furlan, N. Montano, and E. Tobaldini. Obesity and sleep disturbances: The "chicken or the egg" question. *European Journal of Internal Medicine*, may 2021.

[148] M. Rodrigues, N. Kosaric, C. A. Bonham, and G. C. Gurtner. Wound healing: A cellular perspective. *Physiological reviews*, 99(1):665–706, Jan 2019. 30475656[pmid].

[149] A. Sancar, L. A. Lindsey-Boltz, T.-H. Kang, J. T. Reardon, J. H. Lee, and N. Ozturk. Circadian clock control of the cellular response to dna damage. *FEBS letters*, 584(12):2618–2625, Jun 2010. 20227409[pmid].

[150] A. Sancar and R. N. Van Gelder. Clocks, cancer, and chronochemotherapy. *Science*, 371(6524), 2021.

[151] C. Sandu, T. Liu, A. Malan, E. Challet, P. Pévet, and M.-P. Felder-Schmittbuhl. Circadian clocks in rat skin and dermal fibroblasts: differential effects of aging, temperature and melatonin. *Cellular and Molecular Life Sciences*, 72(11):2237–2248, Jun 2015.

[152] R. Santoro, F. Mori, M. Marani, G. Grasso, M. A. Cambria, G. Blandino, P. Muti, and S. Strano. Blockage of melatonin receptors impairs p53-mediated prevention of dna damage accumulation. *Carcinogenesis*, 34(5):1051–1061, May 2013.

[153] A. Sarkar, M. N. Kuehl, A. C. Alman, and B. R. Burkhardt. Linking the oral microbiome and salivary cytokine abundance to circadian oscillations. *Scientific Reports*, 11(1):2658, Jan 2021.

[154] S. Sarkar and S. Gaddameedhi. Solar ultraviolet-induced DNA damage response: Melanocytes story in transformation to environmental melanomagenesis. *Environmental and Molecular Mutagenesis*, 61(7):736–751, may 2020.

[155] S. Sarkar, K. I. Porter, P. P. Dakup, R. P. Gajula, B. S. C. Koritala, R. Hylton, M. G. Kemp, K. Wakamatsu, and S. Gaddameedhi. Circadian clock protein BMAL1 regulates melanogenesis through MITF in melanoma cells. *Pigment Cell & Melanoma Research*, jul 2021.

[156] H. Sasaki, A. Hokugo, L. Wang, K. Morinaga, J. T. Ngo, H. Okawa, and I. Nishimura. Neuronal pas domain 2 (npas2)-deficient fibroblasts accelerate skin wound healing and dermal collagen reconstruction. *The Anatomical Record*, 303(6):1630–1641, Mar. 2019.

[157] S. Sato, T. Sakurai, J. Ogasawara, M. Takahashi, T. Izawa, K. Imaizumi, N. Taniguchi, H. Ohno, and T. Kizaki. A circadian clock gene, rev-erbα, modulates the inflammatory function of macrophages through the negative regulation of ccl2 expression. *The Journal of Immunology*, 192(1):407, Jan 2014.

[158] Y. Sawada, N. Saito-Sasaki, E. Mashima, and M. Nakamura. Daily lifestyle and inflammatory skin diseases. *International journal of molecular sciences*, 22(10):5204, May 2021. 34069063[pmid].

[159] J. Schauber and R. L. Gallo. Antimicrobial peptides and the skin immune defense system. *The Journal of allergy and clinical immunology*, 122(2):261–266, Aug 2008. 18439663[pmid].

[160] C. Scheiermann, Y. Kunisaki, and P. S. Frenette. Circadian control of the immune system. *Nature reviews. Immunology*, 13(3):190–198, Mar 2013. 23391992[pmid].

[161] E. S. Schernhammer, F. Laden, F. E. Speizer, W. C. Willett, D. J. Hunter, I. Kawachi, and G. A. Colditz. Rotating night shifts and risk of breast cancer in women participating in the nurses' health study. *JNCI Journal of the National Cancer Institute*, 93(20):1563–1568, oct 2001.

[162] M. R. Schneider, R. Schmidt-Ullrich, and R. Paus. The hair follicle as a dynamic miniorgan. *Current Biology*, 19(3):R132–R142, feb 2009.

[163] L. Segalla, S. Chirumbolo, and A. Sbarbati. Dermal white adipose tissue: Much more than a metabolic, lipid-storage organ? *Tissue and Cell*, 71:101583, aug 2021.

[164] S. Sengupta, S. Y. Tang, J. C. Devine, S. T. Anderson, S. Nayak, S. L. Zhang, A. Valenzuela, D. G. Fisher, G. R. Grant, C. B. López, and G. A. FitzGerald. Circadian control of lung inflammation in influenza infection. *Nature communications*, 10(1):4107–4107, Sep 2019. 31511530[pmid].

[165] A. A. Shafi and K. E. Knudsen. Cancer and the circadian clock. *Cancer Research*, 79(15):3806–3814, aug 2019.

[166] Y. Shan, J. H. Abel, Y. Li, M. Izumo, K. H. Cox, B. Jeong, S.-H. Yoo, D. P. Olson, F. J. Doyle, and J. S. Takahashi. Dual-color single-cell imaging of the suprachiasmatic nucleus reveals a circadian role in network synchrony. *Neuron*, 108(1):164–179.e7, oct 2020.

[167] D. D. Shuboni-Mulligan, G. Breton, D. Smart, M. Gilbert, and T. S. Armstrong. Radiation chronotherapy-clinical impact of treatment time-of-day: a systematic review. *Journal of neuro-oncology*, 145(3):415–427, Dec 2019. 31729636[pmid].

[168] M. Simões, J. Sousa, and A. Pais. Skin cancer and new treatment perspectives: A review. *Cancer Letters*, 357(1):8–42, feb 2015.

[169] F. Sinturel, P. Gos, V. Petrenko, C. Hagedorn, F. Kreppel, K.-F. Storch, D. Knutti, A. Liani, C. Weitz, Y. Emmenegger, P. Franken, L. Bonacina, C. Dibner, and U. Schibler. Circadian hepatocyte clocks keep synchrony in the absence of a master pacemaker in the suprachiasmatic nucleus or other extrahepatic clocks. *Genes & Development*, 35(5-6):329–334, feb 2021.

[170] A. T. Slominski, R. Hardeland, M. A. Zmijewski, R. M. Slominski, R. J. Reiter, and R. Paus. Melatonin: A cutaneous perspective on its production, metabolism, and functions. *Journal of Investigative Dermatology*, 138(3):490–499, mar 2018.

[171] G. Solanas, F. O. Peixoto, E. Perdiguero, M. Jardí, V. Ruiz-Bonilla, D. Datta, A. Symeonidi, A. Castellanos, P.-S. Welz, J. M. Caballero, P. Sassone-Corsi, P. Muñoz-Cánoves, and S. A. Benitah. Aged stem cells reprogram their daily rhythmic functions to adapt to stress. *Cell*, 170(4):678–692.e20, Aug 2017.

[172] M. E. Straat, R. Hogenboom, M. R. Boon, P. C. Rensen, and S. Kooijman. Circadian control of brown adipose tissue. *Biochimica et Biophysica Acta (BBA) - Molecular and Cell Biology of Lipids*, 1866(8):158961, aug 2021.

[173] C. Stringari, H. Wang, M. Geyfman, V. Crosignani, V. Kumar, J. Takahashi, B. Andersen, and E. Gratton. In vivo single-cell detection of metabolic oscillations in stem cells. *Cell Reports*, 10(1):1–7, Jan 2015.

[174] S. Suh, E. H. Choi, and N. A. Mesinkovska. The expression of opsins in the human skin and its implications for photobiomodulation: A systematic review. *Photodermatology, Photoimmunology & Photomedicine*, 36(5):329–338, jun 2020.

[175] G. Sulli, M. T. Y. Lam, and S. Panda. Interplay between circadian clock and cancer: New frontiers for cancer treatment. *Trends in cancer*, 5(8):475–494, Aug 2019. 31421905[pmid].

[176] G. Sulli, E. N. C. Manoogian, P. R. Taub, and S. Panda. Training the circadian clock, clocking the drugs, and drugging the clock to prevent, manage, and treat chronic diseases. *Trends in pharmacological sciences*, 39(9):812–827, Sep 2018.

[177] G. Sulli, A. Rommel, X. Wang, M. J. Kolar, F. Puca, A. Saghatelian, M. V. Plikus, I. M. Verma, and S. Panda. Pharmacological activation of REV-ERBs is lethal in cancer and oncogene-induced senescence. *Nature*, 553(7688):351–355, jan 2018.

[178] I. K. Sundar, H. Yao, M. T. Sellix, and I. Rahman. Circadian molecular clock in lung pathophysiology. *American journal of physiology. Lung cellular and molecular physiology*, 309(10):L1056–L1075, Nov 2015. 26361874[pmid].

[179] Y. Tahara, Y. Takatsu, T. Shiraishi, Y. Kikuchi, M. Yamazaki, H. Motohashi, A. Muto, H. Sasaki, A. Haraguchi, D. Kuriki, T. J. Nakamura, and S. Shibata. Age-related circadian disorganization caused by sympathetic dysfunction in peripheral clock regulation. *npj Aging and Mechanisms of Disease*, 3(1), jan 2017.

[180] J. S. Takahashi. Transcriptional architecture of the mammalian circadian clock. *Nature Reviews Genetics*, 18(3):164–179, Dec 2016.

[181] J. S. Takahashi. Transcriptional architecture of the mammalian circadian clock. *Nature reviews. Genetics*, 18(3):164–179, Mar 2017.

[182] E. Takita, S. Yokota, Y. Tahara, A. Hirao, N. Aoki, Y. Nakamura, A. Nakao, and S. Shibata. Biological clock dysfunction exacerbates contact hypersensitivity in mice. *British Journal of Dermatology*, 168(1):39–46, Jan 2013.

[183] M. Tanioka, H. Yamada, M. Doi, H. Bando, Y. Yamaguchi, C. Nishigori, and H. Okamura. Molecular clocks in mouse skin. *Journal of Investigative Dermatology*, 129(5):1225–1231, May 2009.

[184] B. Tas and V. Kabeloglu. Prevalence of metabolic syndrome and its parameters and their correlations with psoriasis duration, severity, and sleep quality in psoriasis patients: A cross-sectional study. *Dermatology Practical & Conceptual*, page 2021049, may 2021.

[185] **J, Duan**, E. N. Greenberg, S. S. Karri, and B. Andersen. The circadian clock and diseases of the skin. *FEBS Letters*, 595(19):2413–2436, Sept. 2021.

[186] **J. Duan**, M. N. Ngo, S. S. Karri, L. C. Tsoi, J. E. Gudjonsson, B. Shahbaba, J. Lowengrub, and B. Andersen. taufisher predicts circadian time from a single sample of bulk and single-cell pseudobulk transcriptomic data. *Nature Communications*, 15(1), May 2024.

[187] P. Tognini, M. Samad, K. Kinouchi, Y. Liu, J.-C. Helbling, M.-P. Moisan, K. L. Eckel-Mahan, P. Baldi, and P. Sassone-Corsi. Reshaping circadian metabolism in the suprachiasmatic nucleus and prefrontal cortex by nutritional challenge. *Proceedings of the National Academy of Sciences*, 117:29904–29913, 11 2020.

[188] S. Upasham and S. Prasad. Slock (sensor for circadian clock): passive sweat-based chronobiology tracker. *Lab Chip*, 20:1947–1960, 2020.

[189] J. C. Vary. Selected disorders of skin appendages—acne, alopecia, hyperhidrosis. *Medical Clinics of North America*, 99(6):1195–1211, nov 2015.

[190] A. R. Vaughn, A. K. Clark, R. K. Sivamani, and V. Y. Shi. Circadian rhythm in atopic dermatitis—pathophysiology and implications for chronotherapy. *Pediatric Dermatology*, 35(1):152–157, Jan 2018.

[191] C. Vetter, H. S. Dashti, J. M. Lane, S. G. Anderson, E. S. Schernhammer, M. K. Rutter, R. Saxena, and F. A. Scheer. Night shift work, genetic risk, and type 2 diabetes in the UK biobank. *Diabetes Care*, 41(4):762–769, feb 2018.

[192] R. M. Voigt, C. B. Forsyth, S. J. Green, P. A. Engen, and A. Keshavarzian. *Chapter Nine - Circadian Rhythm and the Gut Microbiome*, volume 131 of *Gut Microbiome and Behavior*, pages 193–205. Academic Press, Jan 2016.

[193] n. Walker, William H, O. H. Meléndez-Fernández, and R. J. Nelson. Prior exposure to dim light at night impairs dermal wound healing in female c57bl/6 mice. *Archives of dermatological research*, 311(7):573–576, Sep 2019. 31144020[pmid].

[194] W. H. Walker, J. C. Walton, A. C. DeVries, and R. J. Nelson. Circadian rhythm disruption and mental health. *Translational Psychiatry*, 10(1), jan 2020.

[195] H. Wang, E. van Spyk, Q. Liu, M. Geyfman, M. L. Salmans, V. Kumar, A. Ihler, N. Li, J. S. Takahashi, and B. Andersen. Time-restricted feeding shifts the skin circadian clock and alters uvb-induced dna damage. *Cell reports*, 20(5):1061–1072, Aug 2017. 28768192[pmid].

[196] X. Wang, J. Tang, L. Xing, G. Shi, H. Ruan, X. Gu, Z. Liu, X. Wu, X. Gao, and Y. Xu. Interaction of MAGED1 with nuclear receptors affects circadian clock function. *The EMBO Journal*, 29(8):1389–1400, mar 2010.

[197] M. Watanabe, A. Hida, S. Kitamura, M. Enomoto, Y. Ohsawa, Y. Katayose, K. Nozaki, Y. Moriguchi, S. Aritake, S. Higuchi, M. Tamura, M. Kato, and K. Mishima. Rhythmic expression of circadian clock genes in human leukocytes and beard hair follicle cells. *Biochemical and Biophysical Research Communications*, 425(4):902–907, sep 2012.

[198] P.-S. Welz, V. M. Zinna, A. Symeonidi, K. B. Koronowski, K. Kinouchi, J. G. Smith, I. M. Guillén, A. Castellanos, S. Furrow, F. Aragón, G. Crainiciuc, N. Prats, J. M. Caballero, A. Hidalgo, P. Sassone-Corsi, and S. A. Benitah. BMAL1-driven tissue clocks respond independently to light to maintain homeostasis. *Cell*, 177(6):1436–1447.e12, may 2019.

[199] S. Wen, D. Ma, M. Zhao, L. Xie, Q. Wu, L. Gou, C. Zhu, Y. Fan, H. Wang, and J. Yan. Spatiotemporal single-cell analysis of gene expression in the mouse suprachiasmatic nucleus. *Nature Neuroscience*, 2020.

[200] M. G. Wendeu-Foyet and F. Menegaux. Circadian disruption and prostate cancer risk: An updated review of epidemiological evidences. *Cancer Epidemiology, Biomarkers & Prevention*, 26(7):985–991, jul 2017.

[201] D. Wilkins, X. Tong, M. H. Y. Leung, C. E. Mason, and P. K. H. Lee. Diurnal variation in the human skin microbiome affects accuracy of forensic microbiome matching. *Microbiome*, 9(1):129, Jun 2021.

[202] M. Wilkinson, R. Maidstone, A. Loudon, J. Blaikley, I. R. White, D. Singh, D. W. Ray, R. Goodacre, S. J. Fowler, and H. J. Durrington. Circadian rhythm of exhaled biomarkers in health and asthma. *The European respiratory journal*, 54(4):1901068, Oct 2019. 31221808[pmid].

[203] N. Wittenbrink, B. Ananthasubramaniam, M. Münch, B. Koller, B. Maier, C. Weschke, F. Bes, J. de Zeeuw, C. Nowozin, A. Wahnschaffe, S. Wisniewski, M. Zaleska, O. Bartok, R. Ashwal-Fluss, H. Lammert, H. Herzel, M. Hummel, S. Kadener, D. Kunz, and A. Kramer. High-accuracy determination of internal circadian time from a single blood sample. *The Journal of clinical investigation*, 128(9):3826–3839, Aug 2018. 29953415[pmid].

[204] R. Wong, S. Geyer, W. Weninger, J.-C. Guimberteau, and J. K. Wong. The dynamic anatomy and patterning of skin. *Experimental Dermatology*, 25(2):92–98, 2016.

[205] R. Wong, V. Tran, V. Morhenn, S. pin Hung, B. Andersen, E. Ito, G. W. Hatfield, and N. R. Benson. Use of RT-PCR and DNA microarrays to characterize RNA recovered by non-invasive tape harvesting of normal and inflamed skin. *Journal of Investigative Dermatology*, 123(1):159–167, jul 2004.

[206] G. Wu, R. C. Anafi, M. E. Hughes, K. Kornacker, and J. B. Hogenesch. Metacycle: an integrated r package to evaluate periodicity in large scale data. *Bioinformatics*, 32:3351–3353, 11 2016.

[207] G. Wu, M. D. Ruben, L. J. Francey, D. F. Smith, J. D. Sherrill, J. E. Oblong, K. J. Mills, and J. B. Hogenesch. A population-based gene expression signature of molecular clock phase from a single epidermal sample. *Genome Medicine*, 12(1):73, Aug 2020.

[208] G. Wu, M. D. Ruben, R. E. Schmidt, L. J. Francey, D. F. Smith, R. C. Anafi, J. J. Hughey, R. Tasseff, J. D. Sherrill, J. E. Oblong, K. J. Mills, and J. B. Hogenesch. Population-level rhythms in human skin with implications for circadian medicine. *Proceedings of the National Academy of Sciences*, 115(48):12313–12318, 2018.

[209] Y. Ye, Y. Xiang, F. M. Ozguc, Y. Kim, C.-J. Liu, P. K. Park, Q. Hu, L. Diao, Y. Lou, C. Lin, A.-Y. Guo, B. Zhou, L. Wang, Z. Chen, J. S. Takahashi, G. B. Mills, S.-H. Yoo, and L. Han. The genomic landscape and pharmacogenomic interactions of clock genes in cancer chronotherapy. *Cell Systems*, 6(3):314–328.e2, mar 2018.

[210] D. Yoshioka, H. Ando, K. Ushijima, M. Kumazaki, and A. Fujimura. Chronotherapy of maxacalcitol on skin inflammation induced by topical 12-o-tetradecanoylphorbol-13-acetate in mice. *Chronobiology International*, 35(9):1269–1280, Sep 2018.

[211] G. Yosipovitch, A. T. J. Goon, J. Wee, Y. H. Chan, I. Zucker, and C. L. Goh. Itch characteristics in chinese patients with atopic dermatitis using a new questionnaire for the assessment of pruritus. *International Journal of Dermatology*, 41(4):212–216, Apr 2002.

[212] E. Yousef, N. Mitwally, N. Noufal, and M. R. Tahir. Shift work and risk of skin cancer: A systematic review and meta-analysis. *Scientific Reports*, 10(1), feb 2020.

[213] S. H. Yu, H. Attarian, P. Zee, and J. I. Silverberg. Burden of sleep and fatigue in US adults with atopic dermatitis. *Dermatitis*, 27(2):50–58, mar 2016.

[214] Y. Yu, X. Zhang, F. Liu, P. Zhu, L. Zhang, Y. Peng, X. Yan, Y. Li, P. Hua, C. Liu, Q. Li, and L. Zhang. A stress-induced mir-31–clock–erk pathway is a key driver and therapeutic target for skin aging. *Nature Aging*, Aug 2021.

[215] Z. Yu, Y. Gong, L. Cui, Y. Hu, Q. Zhou, Z. Chen, Y. Yu, Y. Chen, P. Xu, X. Zhang, C. Guo, and Y. Shi. High-throughput transcriptome and pathogenesis analysis of clinical psoriasis. *Journal of Dermatological Science*, 98(2):109–118, may 2020.

[216] V. Q. Yujra, E. J. d. Silveira, D. A. Ribeiro, R. M. Castilho, and C. H. Squarize. Clock gene per2 modulates epidermal tissue repair in vivo. *Journal of Cellular Biochemistry*, 125(2), Jan. 2024.

[217] C. Zagni, L. O. Almeida, T. Balan, M. T. Martins, L. K. Rosselli-Murai, P. Papagerakis, R. M. Castilho, and C. H. Squarize. Pten mediates activation of core clock protein bmal1 and accumulation of epidermal stem cells. *Stem cell reports*, 9(1):304–314, Jul 2017. 28602615[pmid].

[218] A. Zarrinpar, A. Chaix, S. Yooseph, and S. Panda. Diet and feeding pattern affect the diurnal dynamics of the gut microbiome. *Cell metabolism*, 20(6):1006–1017, Dec 2014. 25470548[pmid].

[219] H. Zhang, Y. Liu, D. Liu, Q. Zeng, L. Li, Q. Zhou, M. Li, J. Mei, N. Yang, S. Mo, Q. Liu, M. Liu, S. Peng, and H. Xiao. Time of day influences immune response to an inactivated vaccine against SARS-CoV-2. *Cell Research*, aug 2021.

[220] R. Zhang, N. F. Lahens, H. I. Ballance, M. E. Hughes, and J. B. Hogenesch. A circadian gene expression atlas in mammals: Implications for biology and medicine. *Proceedings of the National Academy of Sciences*, 111(45):16219–16224, 2014.

[221] D. Zheng, K. Ratiner, and E. Elinav. Circadian influences of diet on the microbiome and immunity. *Trends in Immunology*, 41(6):512–530, Jun 2020.

[222] X. Zhuang, S. B. Rambhatla, A. G. Lai, and J. A. McKeating. Interplay between circadian clock and viral infection. *Journal of molecular medicine (Berlin, Germany)*, 95(12):1283–1289, Dec 2017. 28963570[pmid].

[223] C. C. Zouboulis. The skin as an endocrine organ. *Dermato-endocrinology*, 1(5):250–252, Sep 2009. 20808511[pmid].